

Biogeochemistry of Marine Dissolved Organic Matter

Third Edition

Edited by
Dennis A. Hansell
Craig A. Carlson



BIOGEOCHEMISTRY OF MARINE DISSOLVED ORGANIC MATTER

THIRD EDITION

Edited by

DENNIS A. HANSELL

Department of Ocean Sciences, University of Miami, Coral Gables, FL, United States

CRAIG A. CARLSON

*Department of Ecology, Evolution and Marine Biology & The Marine Science Institute,
University of California, Santa Barbara, CA, United States*



ACADEMIC PRESS

An imprint of Elsevier

Academic Press is an imprint of Elsevier
125 London Wall, London EC2Y 5AS, United Kingdom
525 B Street, Suite 1650, San Diego, CA 92101, United States
50 Hampshire Street, 5th Floor, Cambridge, MA 02139, United States

Copyright © 2024 Elsevier Inc. All rights are reserved, including those for text and data mining, AI training, and similar technologies.

Publisher's note: Elsevier takes a neutral position with respect to territorial disputes or jurisdictional claims in its published content, including in maps and institutional affiliations.

No part of this publication may be reproduced or transmitted in any form or by any means, electronic or mechanical, including photocopying, recording, or any information storage and retrieval system, without permission in writing from the publisher. Details on how to seek permission, further information about the Publisher's permissions policies and our arrangements with organizations such as the Copyright Clearance Center and the Copyright Licensing Agency, can be found at our website: www.elsevier.com/permissions.

This book and the individual contributions contained in it are protected under copyright by the Publisher (other than as may be noted herein).

Notices

Knowledge and best practice in this field are constantly changing. As new research and experience broaden our understanding, changes in research methods, professional practices, or medical treatment may become necessary.

Practitioners and researchers must always rely on their own experience and knowledge in evaluating and using any information, methods, compounds, or experiments described herein. In using such information or methods they should be mindful of their own safety and the safety of others, including parties for whom they have a professional responsibility.

To the fullest extent of the law, neither the Publisher nor the authors, contributors, or editors, assume any liability for any injury and/or damage to persons or property as a matter of products liability, negligence or otherwise, or from any use or operation of any methods, products, instructions, or ideas contained in the material herein.

ISBN 978-0-443-13858-4

For information on all Academic Press publications
visit our website at <https://www.elsevier.com/books-and-journals>

Publisher: Candice Janco
Acquisitions Editor: Maria Elekidou
Editorial Project Manager: Sara Valentino
Production Project Manager: Kumar Anbazhagan
Cover Designer: Matthew Limbert

Typeset by STRAIVE, India



Working together
to grow libraries in
developing countries

www.elsevier.com • www.bookaid.org

Marine photochemistry of organic matter: Processes and impacts

David J. Kieber^a, Leanne C. Powers^a, Aron Stubbins^{b,c,d},
and William L. Miller^e

^aDepartment of Chemistry, State University of New York, College of Environmental Science and Forestry, Syracuse, NY, United States ^bDepartment of Marine and Environmental Sciences, Northeastern University, Boston, MA, United States ^cDepartment of Chemistry and Chemical Biology, Northeastern University, Boston, MA, United States ^dDepartment of Civil and Environmental Engineering, Northeastern University, Boston, MA, United States ^eDepartment of Marine Sciences, University of Georgia, Athens, GA, United States

O U T L I N E

11.1 Introduction	509	<i>11.4.2 Fate of terrigenous DOM in the oceans</i>	528
11.2 Caveats and cautionary notes	511	11.5 Photochemical environments, intermediates, and reactions	532
11.2.1 Photochemistry	511	11.5.1 Radicals and redox transitions	532
11.2.2 Relevance to seawater	513	11.5.2 Particles, photoflocculation, and photodissolution	540
11.2.3 Analytical procedures	514	11.5.3 VOC photoproduction	541
11.3 Impact of photochemistry on elemental cycles	515	11.5.4 Fate of compounds of concern and plastics	542
11.3.1 Carbon	515	11.5.5 Sea-surface microlayer	550
11.3.2 Sulfur	519		
11.3.3 Nitrogen and phosphorus	524		
11.4 DOM photolability spectrum and fate of terrigenous DOM in the ocean	526	11.6 Modeling photochemical rates	553
11.4.1 Photolability spectrum	526	11.6.1 Fundamental approaches	553

11.6.2 Scaling to oceans	556	Acknowledgments	562
11.7 Future directions	560	References	562

List of acronyms

<i>a</i>	Naperian absorption coefficient (m^{-1})
AQYs	apparent quantum yields
BATS	Bermuda Atlantic Time-series Study
BLP	biolabile photoproducts
CDOM	chromophoric dissolved organic matter
DBC	dissolved black carbon
$\delta^{13}\text{C}$	carbon isotopic signature, measured as the ratio of ^{13}C to ^{12}C (‰)
DIC	dissolved inorganic carbon
DIN	dissolved inorganic nitrogen
DIP	dissolved inorganic phosphorus
DMS	dimethylsulfide
DMSO	dimethylsulfoxide
DMSP	dimethylsulfoniopropionate
DOC	dissolved organic carbon
$^3\text{DOM}^*$	triplet excited state DOM
DON	dissolved organic nitrogen
DOP	dissolved organic phosphorus
DOS	dissolved organic sulfur
E_o	solar irradiance at the sea surface
EEM-PARAFAC	excitation-emission matrix-parallel factor analysis
EPS	expanded polystyrene
ESI	electrospray ionization
FDOM	fluorescent dissolved organic matter
FT-ICR MS	Fourier Transform-Ion Cyclotron Resonance Mass Spectrometry
GC	gas chromatography
HAB	harmful algal bloom
HRMS	high-resolution mass spectrometry
IHSS	International Humic Substances Society
k_p	photolysis rate constant
K_{dUV}	downward irradiance attenuation coefficient in the UV
λ	wavelength
LED	light emitting diode
MoDIE	moderate dissolved inorganic carbon isotope enrichment
MS	mass spectrometry
MSA	methanesulfonic acid
MSIA	methanesulfinic acid
NADW	North Atlantic Deep Water
NMR	nuclear magnetic resonance
OERs	one-electron reductants
PAHs	polycyclic aromatic hydrocarbons
PE	polyethylene
PFAS	poly- and perfluoroalkyl substances
PFOA	perfluorooctanoate

PLFA	Pony Lake Fulvic Acid
POC	particulate organic carbon
POM	particulate organic matter
PP	polypropylene
Q_a	photon absorption rate
R_{tot}	photochemical loss or production ration
ϕ	quantum yield
RHS	reactive halogen species
RI	reactive intermediate
ROS	reactive oxygen species
R_{tot}	total measured production or loss rate
SOD	superoxide dismutase
SPE	solid phase extraction
SRFA	Suwannee River fulvic acid
SRHA	Suwannee River humic acid
SRNOM	Suwannee River natural organic matter
tDOM	terrigenous DOM
UV	ultraviolet radiation
UV-A	UV radiation from 320 to 400 nm
UV-B	UV radiation from 280 to 320 nm
UHPLC	ultrahigh performance liquid chromatography

11.1 Introduction

Photochemistry has been a fundamental component of chemistry since the early days of discovery in the mid-1800s (Kemsley, 2015). However, it was not until the early to mid-1970s, through pioneering work by the “three Zs,” Oliver Zafiriou, Richard Zepp, and Rod Zika, as outlined in two reviews (Zafiriou, 1977; Zika, 1981), that photochemistry took hold as a field of study in oceanography. The main driver for environmental photochemistry is the absorption of ultraviolet (UV) and visible solar radiation by organic and inorganic matter in the oceans resulting in a cascade of photophysical and photochemical processes. These include the loss of absorption by chromophoric dissolved organic matter (CDOM) across the entire absorption spectrum, photomineralization of dissolved organic matter (DOM) [to form dissolved inorganic carbon (DIC), carbon monoxide (CO), and nutrients (e.g., nitrate)], photoreduction of trace metals, photodissolution of particulate organic matter (POM) including plastics, photoflocculation, production of volatile organic matter, and photoproduction of a suite of low molecular weight products and reactive oxygen species (ROS). These transformations, and many others not listed here, have broad-ranging impacts on the redox state of metals in the sea, photic-zone marine ecology, as well as atmospheric chemistry and climate through the photochemical production of trace gases and modification of gas exchange rates at the sea surface via, for example, the photoproduction or photolysis of surfactants.

From its early development in the 1970s, marine photochemistry remained a peripheral field in oceanography for the next 10 years, despite advances, until it was proposed that sunlight could transform biologically recalcitrant dissolved organic carbon (DOC) into substrates used by marine heterotrophs for energy and growth. This process was proposed to remove “old” DOC from the sea directly through the photochemical mineralization of DOM to CO and DIC and indirectly through a coupled photochemical-biological pathway via the

photoproduction of organic substrates and their microbial consumption (Kieber et al., 1989; Mopper et al., 1991). These studies resulted in an upsurge in research investigating the links between sunlight, organic matter, the carbon cycle, and heterotrophic activity in the oceans, as reviewed by Mopper and Kieber (2002) and Mopper et al. (2015).

Although many details are not yet understood, the importance of sunlight-driven photochemical transformations in the field of oceanography is well established. One obstacle to advancing the field of marine photochemistry has been the lack of knowledge regarding the composition of DOM, with many compounds that comprise the bulk of DOM unknown (see Chapter 2). This lack of knowledge limits discussions of quantum yields, photosensitizers, and precursors to varying degrees of uncertainty depending on the process. However, advances in instrumentation now allow the examination of photochemical transformations of uncharacterized DOM by probing changes in molecular composition, greatly improving our ability to study marine photochemical processes. Future advances are needed to probe the transient radicals proposed to form in seawater, as only a few have been studied and quantified in detail. The ability to model photochemical processes has also progressed dramatically, providing improved estimates of photochemical rates to gauge their importance on regional and global scales.

Building on the large body of prior work, new questions and areas of study have emerged. For example, there is increasing interest in the role photochemistry plays in modifying the sea-surface microlayer and on the role of photochemistry in plastic cycling in the oceans. Are photochemical reactions at the sea surface fundamentally different from those in the underlying seawater? Is trace gas production in the sea-surface microlayer important? What are the best experimental approaches to study the photochemistry of POM or sea-surface microlayer photochemistry? How important is plastic photochemistry in the removal of plastics from surface waters and the production of new DOM, volatile gases, and toxicants? Does this new DOM contribute to the radiocarbon signal in the oceans, and if so, is this important? What are the consequences of these processes on the cycling of organic matter in the sea? These and many other questions need to be addressed to further understand the role photochemistry plays in marine biogeochemical cycles.

To help determine research priorities and important questions related to marine photochemistry, the reader is referred to several reviews (Barrios et al., 2021; Carpenter and Nightingale, 2015; Hu et al., 2022a; Gligorovski et al., 2015; McNeill and Canonica, 2016; McKay, 2020; Rose, 2016; Sulzberger and Arey, 2016; Sulzberger et al., 2019) and the 2021 U.S. SOLAS Science Plan (Stanley et al., 2021). Additionally, several publications highlight fundamental principles of electromagnetic radiation and photochemistry, including, for example, the two laws of photochemistry (Bunsen-Roscoe Law of Reciprocity, Beer-Lambert law), the Jablonski diagram, quantum yields, quenching, triplet excited state, irradiation sources, solar radiation, optical screening, and actinometry (Braslavsky, 2007; Calvert and Pitts, 1966; Caukins, 1982; Hu et al., 2002; Rabek, 1982a, b; Kirk, 1994; Kuhn et al., 2004; Leifer, 1988; Mobley, 2022; Montalti et al., 2006). These books and reviews will provide the reader with the necessary background and context to better understand the subject matter covered in this chapter.

Since the first edition of this chapter in 2002, there have been significant advances in marine DOM photochemistry. However, much of what was presented in the past two editions is still relevant, particularly concerning the fundamental role of photochemistry in elemental cycles; the technical details of the methods employed; and the changes, products, and transients

produced during DOM photochemistry (Mopper and Kieber, 2002; Mopper et al., 2015). Our review will focus on the marine photochemistry of organic carbon, sulfur, nitrogen, and phosphorus, highlighting and evaluating advances, new and emerging areas of study, and areas for future work. Recommendations for continued advancement of marine photochemistry and elemental cycles are presented in Section 11.7. While Mopper et al. (2015) reviewed sea-ice photochemistry and natural product photochemistry, these topics are not covered here because very few advances have been made since 2015, except for the photochemistry of toxins (Section 11.5.4.1). Likewise, photochemical oxygen consumption will not be examined here, as little work has been done since the Mopper et al. (2015) review except for a few noteworthy studies (Gieskes et al., 2015; Sutherland et al., 2020; Ward and Cory, 2020). Photochemical reactions also significantly impact trace metal cycling in seawater; however, this topic is discussed in detail elsewhere (e.g., Butler et al., 2021; Lueder et al., 2020; Morel and Price, 2003; Rose, 2016; Sunda, 2012) and will not be reviewed here beyond their impact on organic matter photochemical transformations. Likewise, marine optics and photoinhibition, although important topics, are beyond the scope and focus of our review.

Unless stated otherwise, for studies discussed in this chapter, the source of radiation used for photochemical experiments is either natural sunlight or various artificial light sources (e.g., xenon arc, low-pressure Hg, fluorescent bulbs) with optical filters used to remove radiation below ~ 290 nm, the approximate solar cutoff at the Earth's surface; the reader is referred to the original publications for experimental details. Throughout this chapter, dissolved, as in DOM or DIC, refers to seawater components that pass through a filter with a well-defined (e.g., Nylon) or nominal pore size (e.g., glass fiber filter) ranging from 0.2 to $1.2\text{ }\mu\text{m}$; particulate components are those retained by the filter. Hereafter, marine waters that are optically clear with an absorption coefficient at 300 nm, a_{300} , less than 0.2 m^{-1} , and nutrient impoverished (\sim low nmol L^{-1} concentrations of macronutrients) will be referred to as either oligotrophic, blue, or open ocean waters. The acronyms used in this chapter are given in the “List of acronyms.”

Even though the emphasis of this chapter is on marine photochemistry, in several cases the findings and conclusions from freshwater and DOM-amended laboratory water studies are discussed. Although not necessarily applicable to marine waters except perhaps terrestrially impacted coastal and inland (e.g., estuarine) waters, these studies will be mentioned and discussed where there are limited results in seawater for a given photochemical process.

11.2 Caveats and cautionary notes

11.2.1 Photochemistry

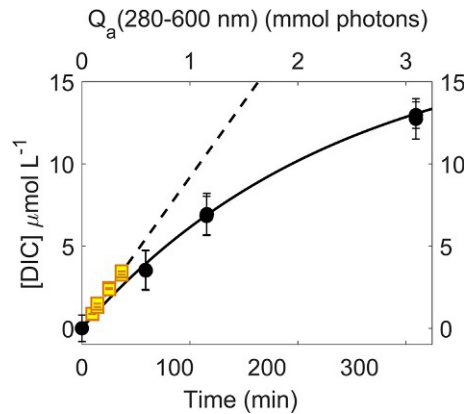
Throughout this chapter, it will be evident that different studies are oftentimes not comparable or in agreement. A noteworthy example is the large range of differences obtained when evaluating the photoproduction of biolabile photoproducts (BLP) and their role in DOM remineralization. BLP determination is not a trivial task; experiments typically involve exposure of filtered or unfiltered samples to solar radiation, followed by dark incubations after the addition of unfiltered water, and a final assessment of O_2 loss, DOC loss, or CO_2 production postincubation (see Mopper et al., 2015). To date, BLP photoproduction

studies generally have used vastly different irradiation parameters, incubation times, and treatment conditions; consequently, direct comparisons between studies are problematic. Because some photoproducts are both biolabile and photolabile, the photon exposure (i.e., time-integrated irradiance) should be taken into consideration for any study aimed at understanding DOM turnover and BLP cycling (Reader and Miller, 2014).

More generally, differences in photochemical results can be due to differences in experimental design, particularly the light source and photon exposure. For example, comparing results from short photon exposures to long exposures is problematic if the condition of reciprocity is not met (Powers et al., 2017; Zhu et al., 2022). In other words, results between studies should only be compared if time-dependent photochemical responses are similar or linear functions of the cumulative irradiance dose (i.e., photon exposure). Nonlinearity can occur at some photon exposure threshold for all photochemical processes for several reasons that include, for example, the loss of precursors or sensitizers or competing pathways with different nonreciprocity thresholds (Fig. 11.1). Since all photochemical processes, with DOC loss being a good example, eventually become nonlinear with photon exposure, it is important to determine that reciprocity is met before conducting “long-term” irradiations (Koehler et al., 2022). This condition is required to allow for comparison of results from different studies, to accurately determine apparent quantum yields (AQYs), and to model photochemical processes. Rates determined using long-exposure experiments with constant high photon flux and strong CDOM fading are likely not representative of environmental photochemistry, even though long irradiations are sometimes needed to see measurable photochemical changes (e.g., DOC loss, 28 d experiment; Stubbins et al., 2012). This limitation is further exacerbated when determining AQYs for these photoprocesses since the act of parsing the light by wavelength can reduce rates beyond the limits of quantification. A complicating factor is that some photoprocesses may never meet the condition of reciprocity, as has been observed for selected plastic photodegradation processes (Section 11.5.4.4).

Natural-water photochemical studies are also replete with issues regarding accurate determination of the photon exposure (Almulhtaram et al., 2021), uncertainties associated with long exposure times, and self-shading effects. So-called screening, self-shading, or inner filter effects must be quantified and documented in any photochemical experiment where samples

FIG. 11.1 Measured [DIC] ($\mu\text{mol L}^{-1}$) versus irradiation time and photon exposure, Q_a (280–600 nm), during irradiation of St. Mary’s River water. The solid line is a model fit using the following equation $A_0*(1 - \exp(-k*Q_{a,int}))$ where k is the observed first-order rate constant and $Q_{a,int}$ is the absorbed photon dose from 280 to 600 nm. Also shown is the DIC measured using the MoDIE method over a much shorter irradiation period (yellow squares). The initial rate (<1 h irradiation) determined using data from MoDIE (dashed black line, $3.99 \pm 0.08 \mu\text{mol L}^{-1} \text{ h}^{-1}$) is in good agreement with that predicted from the initial rate fit from the longer time-series experiment (solid black line, $4.02 \mu\text{mol L}^{-1} \text{ h}^{-1}$). Figure adapted from Powers et al. (2017).



are not optically thin (Hu et al., 2002). Actinometry should be used to quantify the photon exposure in reaction vessels for all photochemical studies, including studies conducted both in the lab where different irradiation systems are used, and in the field where photon exposure variations can result from differences in environmental conditions (e.g., cloudy vs. sunny day, winter vs. summer) rather than from chemical differences inherent in the samples. Equally important, an optically thin actinometer should be used to quantify the photon exposure over the radiation wavelength interval that drives the marine photochemistry of interest in waters that are also optically thin, and in the same container used for sample irradiations in photochemical or photobiological studies (Kuhn et al., 2004; Kieber et al., 2007; Rabani et al., 2021). By using an appropriate actinometer, results from different studies can be directly compared.

One final precaution to consider is that commercial-grade gases such as Ar or He are not O₂ free; they generally contain ppm levels of O₂ and bubbling samples with Ar or He will not produce anoxic conditions. Therefore an in-line oxygen scrubber is recommended to remove residual oxygen from these gases for mechanistic photochemical studies.

11.2.2 Relevance to seawater

Throughout this chapter, studies are discussed that use standard reference materials or extracts to study photochemical processes, but extrapolation of these results to marine DOM can be highly uncertain. Many studies also use high concentrations of organic matter to see a clear photochemical signal, a condition rarely relevant in marine systems considering the much lower concentrations of organic matter in seawater. Additionally, the process of extracting organic matter from seawater or other natural water using solid-phase extraction (SPE) may change the physical and chemical properties of the extracted organic matter through chemical reactions on the sorbent surface (e.g., aldol reaction, Michael addition), but this outcome has not been explicitly tested. Moreover, samples with high DOM concentrations are more likely to require inner-filter effect optical corrections, which often are not reported or perhaps not considered. While many of these studies are nonetheless discussed herein, the reader should keep in mind that much of the work using these reference materials or extracts should only be considered proof-of-concept.

Another important issue is the difficulty of quantifying photochemical changes in low-DOM open-ocean waters. It can be tempting to extrapolate rates and AQYs to open-ocean waters from reference materials or extracts, or even terrestrially influenced coastal waters, where it is much easier to generate photochemical data in the laboratory. However, rate constants or AQYs for the photochemical production or loss of specific compounds can show a nonlinear decrease, a nonlinear increase, or no apparent pattern at all when moving from estuarine waters to the open ocean (Galí et al., 2016; Li et al., 2020; Powers and Miller, 2015a, b; Uher et al., 2017). Likewise, a photochemical process may be important when compounds and precursors are added to seawater at $\mu\text{mol L}^{-1}$ concentrations, but the same process may not be important at ambient pmol L^{-1} to nmol L^{-1} concentrations (e.g., acrylate photolysis, Xue and Kieber, 2021; methane photoproduction from dimethylsulfide (DMS), Zhang and Xie, 2015), especially if that compound is photoproduced or photolyzed via competing pathways or a secondary photochemical pathway involving photosensitizers or ROS.

11.2.3 Analytical procedures

High-resolution mass spectrometry (HRMS), such as Fourier Transform-Ion Cyclotron Resonance Mass Spectrometry (FT-ICR MS) with negative mode electrospray ionization (ESI), is often used to investigate changes in DOM molecular composition, but this methodology comes with limitations (see [Chapter 2](#), Section 2.4.3). HRMS analysis requires desalting seawater samples, which is typically done by SPE using hydrophobic sorbents such as silica-bonded octadecyl particles (C18). However, SPE does not quantitatively extract DOM from seawater. DOC extraction efficiencies are ~40%–50% for marine samples ([Dittmar et al., 2008](#)), and SPE may have lower recoveries for dissolved organic nitrogen (DON) than for DOC, e.g., 22% and 42% DON and DOC recoveries have been reported, respectively ([Ksionzek et al., 2016](#)). In addition, dissolved organic sulfur (DOS) and phosphorus (DOP) extraction efficiencies have yet to be reported. Given these findings and uncertainties, are SPE extracts representative of the original samples in terms of their photochemical and optical properties? Since extracted CDOM responded similarly to borohydride reduction as it did in unfiltered water samples, [Andrew et al. \(2016\)](#) concluded changes in spectral slopes postextraction did not impact CDOM’s chemical properties, suggesting that SPE extracts adequately represent the CDOM in the original sample. Other studies have reported somewhat low CDOM extraction efficiencies that are comparable to bulk DOC extraction efficiencies ([Jerusalén-Lléo et al., 2023](#); [Wünsch et al., 2018](#)), but results cannot be compared given differences in seawater volumes loaded onto cartridges, methanol elution volumes, and sample matrices for dissolved extracts in these studies (e.g., high-purity laboratory water vs. seawater). SPE is also often performed before and after samples are irradiated, but this may bias results since low molecular weight polar photoproducts might be involved in the photoreaction of interest but are not extracted using SPE.

Only compounds that strongly ionize will survive or be “visible” and detected by FT-ICR MS. Often strong ionizers suppress the response of weak ionizers thereby making the weak ionizers “invisible” during analysis. Thus it is not possible to completely distinguish molecular signatures among irradiated samples and dark controls in a photochemical experiment, since all samples will contain both strong and weak ionizers, and the composition of ionizers will change when samples are irradiated. Despite these caveats, HRMS has been extremely useful as a tool to study marine DOM photoreactivity by revealing changes in bulk extractable DOM composition, which is discussed in detail in [Section 11.4](#).

Complicating issues arise in quantifying photochemical production rates of reactive intermediates (RIs) that are not stable in solution. One measurement technique is to use probe molecules that “trap” RIs as they are formed, giving information about initial reaction rates but no information about subsequent pathways ([Zafiriou et al., 1990](#)). Two questions are inherent in this approach: (1) do probes generate unintended chemistry in the sample and (2) do the probes access all chemical environments? For example, measurements of triplet excited state DOM (${}^3\text{DOM}^*$) and singlet oxygen (${}^1\text{O}_2$) typically rely on probe compounds, such as furfuryl alcohol (FFA) for ${}^1\text{O}_2$. Reevaluation of the rate constant between FFA and ${}^1\text{O}_2$ using time-resolved phosphorescence showed a lower rate constant than previously reported, having both a temperature and ionic strength dependence ([Appiani et al., 2017](#)). These considerations will be important for the study of these RIs in seawater, which to date have been rare.

Furthermore, when using probes (or scavengers) to study transient species, as was done in several studies discussed throughout this chapter (e.g., [Parker and Mitch, 2016](#); [Timko et al., 2014](#); [Yang et al., 2021](#)), one potential issue is that production of a radical or transient excited state species can occur intramolecularly within the DOM phase and not in the bulk solution, leading to photochemical transformations that may proceed even in the presence of the probe or scavenger, both of which may not be accessible to the DOM “phase” ([Burns et al., 1997](#); [Grandbois et al., 2008](#); [Hassett, 2006](#); [Latch and McNeill, 2006](#)). [Cheng et al. \(2023\)](#) irradiated solutions containing aquatic and soil DOM isolates with FFA’s structural analog, furfuryl amine, which is protonated below pH 9 and was therefore expected to have enhanced concentrations near the DOM “phase.” While $^1\text{O}_2$ concentrations were higher near or within the DOM microenvironment, in agreement with prior work ([Latch and McNeill, 2006](#)), increasing ionic strength generally decreased $^1\text{O}_2$ measured by furfuryl amine. The authors proposed that the shielding effect of salts decreased the interaction between furfuryl amine and DOM ([Cheng et al., 2023](#)), leaving the importance of ROS reactions within the marine DOM microenvironment an open question.

Another method to quantify RIs involves measuring dark decay rates postirradiation, assuming steady-state concentrations measured in the light result from a balance between photochemical production and dark decay (e.g., superoxide, Fe(II)). This steady-state approach will not detect short-lived transient RIs that persist only when the sun is shining. Consequently, daytime decay rates could be different from dark decay rates when examining radical and redox photochemistry. Lastly, the photochemical electron redistribution that leads to RIs steady-state conditions generates both reduced and oxidized transients. Most studies focus on either one or several of the radical products and ignore the rest, whereas redox conditions in the sunlit ocean are influenced by the entirety of the RI pool. Extrapolation of RI results from these studies to critical biogeochemical processes like Fe-aerosol solubility, Mn and Cu redox cycling, and ligand distributions is tenuous.

11.3 Impact of photochemistry on elemental cycles

11.3.1 Carbon

Carbon on Earth occurs in organic and inorganic forms. Sunlight can aid in the conversion between these two classes of carbon. The photochemical power of the sun is harnessed to convert inorganic carbon to organic carbon through photosynthesis, and this photoreaction gives rise to most of the biogenic organic carbon on Earth ([Field et al., 1998](#)). In the oceans, most DOC is marigenous, being produced *in situ* by marine phytoplankton ([Moran et al., 2016](#)). Although most marine DOC is converted back to DIC via microbial respiration ([Robinson and Williams, 2005](#)), some DOC is lost via photochemical transformations. Exposure to sunlight converts DOC to DIC via two main pathways: (1) direct photochemical mineralization of DOC to DIC and CO and (2) photochemical transformation of DOC to organic molecules consumed by microbes and respired to DIC. These pathways will be discussed in the ensuing sections.

11.3.1.1 Direct photoproduction of dissolved inorganic carbon

DIC is an important terminal product of DOC photolysis that is measured by the increase in DIC concentration or the loss of DOC (Mopper et al., 2015). In low DIC freshwaters, measuring DIC production against the low background provides a more sensitive measure of DOC photooxidation than quantifying DOC losses. Further, in freshwaters, AQYs and rates of DOC loss and DIC production are high enough to be relatively easy to measure in short-term irradiation experiments. By contrast, in marine systems, photochemical rates are much lower. Experimental rates of DIC photoproduction in coastal waters are approximately $25\text{--}200\text{ nmol L}^{-1}\text{ h}^{-1}$ (Powers and Miller, 2015a; Wang et al., 2009; White et al., 2008) and lower still in the open ocean ($\sim 3\text{--}6\text{ nmol L}^{-1}\text{ h}^{-1}$, White et al., 2008). These low rates combined with high background DIC ($\sim 2\text{ mM}$ or $2,000,000\text{ nmol L}^{-1}$) make measuring marine DIC photoproduction challenging.

Even though measurements are easier, freshwater measurements of DIC AQYs have proven highly uncertain. For eight separate inland lakes and freshwaters collected in Sweden, Finland, and Alaska, AQYs determined by four independent laboratories varied by as much as $\sim 40\%$ for any given lake, which was almost as large as the interlake variability of $\sim 60\%$ (Koehler et al., 2022). Perhaps this result is not surprising given the differences among the laboratories in methodologies used to prepare and irradiate samples. This uncertainty is quite large given that the AQYs spectrum is a core parameter in environmental photochemical models (Section 11.6). The Koehler et al. (2022) intercomparison study, albeit for freshwaters, nonetheless highlights the potentially large uncertainties associated with DIC AQYs.

Three methods are used to quantify marine DIC photoproduction. In the first, seawater samples are acidified and sparged with CO_2 -free air to remove DIC, then the pH is readjusted to the original pH of the sample. Sparged samples are transferred to quartz tubes or cells pneumatically and exposed to solar radiation with all steps done in a system closed to the atmosphere (Miller and Zepp, 1995; White et al., 2008). This approach requires an experienced analyst to maintain low blanks and excellent precision. One drawback with this technique is the potential effect of the pH cycling of samples on DOM chemistry and DIC photoproduction rates. However, this concern may not be an issue based on results from an intercomparison study using the pH-cycling/purging method and the pool isotope exchange (PIE) method to study DIC photoproduction in coastal seawater (White et al., 2008; Wang et al., 2009). The PIE method replaces nearly all the sample's DI^{12}C with DI^{13}C . This method was modified to a moderate DI^{13}C isotope enrichment method (MoDIE), wherein a small quantity of DI^{13}C (as $\text{NaH}^{13}\text{CO}_3$) is added to enrich a sample's DI^{13}C without altering the pH (Powers et al., 2017). These methods provide the analytical precision to measure sub- $\mu\text{mol L}^{-1}$ changes in DIC against the seawater background (Powers et al., 2017). Although there are several avenues for improvement of the MoDIE method, including partially stripping DIC from the samples, it will remain extremely difficult to measure total DIC photoproduction below $1\text{ }\mu\text{mol L}^{-1}$ with $\sim 2000\text{ }\mu\text{mol L}^{-1}$ background DIC, even with intense ^{13}C enrichment, unless procedural and analytical errors can be reduced (Lu and Beaupré, 2021). This analytical limitation may restrict MoDIE's use to inshore and coastal waters since production rates in oligotrophic seawater samples are expected to be too low.

AQY values for DIC photoproduction vary nearly two orders of magnitude in marine waters, but AQY measurements have been largely limited to relatively high DOM riverine, estuarine, or coastal waters (Mopper et al., 2015). The only blue water AQY spectra were reported by Johannessen and Miller (2001) using Gulf Stream seawater. In addition, current methodological limitations often require long irradiation times to produce quantifiable DIC photoproduction, even in coastal seawater, which may mean that these experiments do not capture initial AQYs or meet the condition of reciprocity (Fig. 11.1). For example, Powers and Miller (2015a) found nonlinear DIC photoproduction rates in riverine and coastal waters during prolonged irradiation experiments that were not the result of CDOM fading. Nonlinearity was also observed using the MoDIE method to quantify DIC photoproduction in a St. Mary's River, Georgia, USA sample (Fig. 11.1). Additional methodological differences among laboratories may also contribute to variability in marine DIC AQY spectra (Koehler et al., 2022). With so few data and current variability of reported AQY spectra for DIC photoproduction, it is not surprising that there is no obvious relationship between AQYs and DOM type (e.g., fresh vs. inshore vs. coastal), CDOM absorbance, temperature, or salinity (Reader and Miller, 2012; White et al., 2010). Therefore quantitative global marine DIC photoproduction models (Section 11.6) will remain highly uncertain until more AQY and chemical data provide improved insight on the underlying processes that allow models to capture such variability with any confidence.

Given the challenges of measuring DIC photoproduction in blue waters, DIC photoproduction rates have been estimated from measured DIC/CO photoproduction ratios in samples where both were quantified. This approach was used with CO models to determine global blue-water DIC photoproduction rates that ranged from 0.05 to 0.11 Pmol Cyr⁻¹ (Stubbins et al., 2006; Zafiriou et al., 2003). These rates are modest compared to the net photosynthetic production of organic carbon by phytoplankton (\sim 4 Pmol Cyr⁻¹, Field et al., 1998) and would account for the oxidation of 2.9%–6.5% of DOC produced in the ocean (\sim 1.7 Pmol Cyr⁻¹, Moran et al., 2016). Rates of DIC photoproduction are of more significance when compared to the input of riverine DOC to the sea (\sim 0.02 Pmol Cyr⁻¹; see Chapter 14), the accumulation of organic carbon in deep-ocean sediments (\sim 0.017 Pmol Cyr⁻¹) (Canadell et al., 2021), the production of blue carbon in coastal ecosystems (\sim 0.010 Pmol Cyr⁻¹) (Alongi, 2018), or annual input of organic carbon in inland water sediments (0.013 Pmol Cyr⁻¹) (Canadell et al., 2021).

CO has been used as a DIC photoproduction proxy because its photoproduction rates are relatively easy to measure in oceanic waters. CO has been used not only as a proxy for harder-to-quantify photoreactions, including DIC photoproduction (Stubbins et al., 2006; Powers and Miller, 2015a), but also as a tracer for testing and tuning models of mixed layer processes (Doney et al., 1995; Kettle, 2005; Najjar et al., 1995) and as a tool to reveal photochemical mechanisms (e.g., Stubbins et al., 2008; Ossola et al., 2022; Zafiriou et al., 2024). However, one implicit assumption for using CO photoproduction as a proxy for DIC photoproduction is that the DIC/CO photoproduction ratio is relatively constant spatially and seasonally in the oceans. Unfortunately, other work has shown that this ratio varies widely from 2 to >60 (Powers and Miller, 2015a; Reader and Miller, 2012; White et al., 2010) in estuarine and coastal waters. Intriguingly, H₂O₂, and therefore superoxide (Section 11.5.1.1), may be a useful proxy for DOM photomineralization. Using a small sample set from inshore to offshore waters in the South Atlantic Bight (SAB), the ratio between DIC photoproduction and H₂O₂

photoproduction fell in a narrow range (3.6–9.5) and averaged 6.6 ± 1.8 across samples and irradiation times (Powers and Miller, 2015b). Superoxide (O_2^-) and DIC photoproduction rates were similar for a tidal creek sample, implying O_2^- may be a better proxy for DIC photoproduction compared to H_2O_2 . Whether or not DIC, O_2^- , and H_2O_2 arise from similar mechanisms remains unknown, but it is clear CO is not a good proxy for DIC photochemistry in seawater. When more data on open-ocean DIC AQY spectra become available, it may be valuable to investigate alternative proxies for photoproduced DIC.

Since Miller and Zepp (1995) first reported photochemical production rates of DIC in high DOC inland and riverine waters that were 15–20× higher than those for CO, it has been assumed that DIC is the main carbon product formed from the photolysis of DOC in the oceans. However, direct evidence to support this assumption is lacking in the open ocean. While DIC remains the presumptive main photochemical carbon product formed from the photolysis of marine DOC, we know very little about how production rates vary spatiotemporally in the oceans. Moreover, it is often assumed that CO is the second most abundant product of DOC photooxidation (Miller and Zepp, 1995), but this assumption has not been tested in blue waters. Indeed, the low production rates of DIC modeled and measured in the Gulf Stream, 3 and 6 nmol L⁻¹ h⁻¹ (White et al., 2008), call into question this long-held assumption. If DIC photoproduction rates in Gulf Stream waters are characteristic of the open ocean, then other photochemical products, such as formaldehyde or acet-aldehyde whose rates are in the low nmol L⁻¹ h⁻¹ range, may be equally important (Zhu and Kieber, 2020).

Given these combined uncertainties, it is not surprising that the impact of DIC photoproduction in marine surface waters is not explicitly represented either as an average global value or with regional and temporal resolution in global climate models. It will be important to refine predictions of DIC photoproduction for proper accounting within the global carbon cycle and assess the role of photochemistry in altering regional and seasonal CO₂ fluxes.

11.3.1.2 Coupled photochemical-microbial DOC degradation

Photochemical transformations of DOM create biolabile DOC and alter microbial activity through the photoproduction of inorganic nutrients and biolabile DON and DOP, as discussed in Section 11.3.3. Since this topic was reviewed by Mopper et al. (2015), there have been numerous studies continuing this line of research (e.g., Amado et al., 2015; Antony et al., 2018; Blanchet et al., 2018; Bowen et al., 2020a; Fitch et al., 2018; Harriman et al., 2017; Hu et al., 2022b; Lønborg et al., 2016; Madsen-Østerbye et al., 2018; Mazoyer et al., 2022; Mostovaya et al., 2016; Nalven et al., 2022; Neilen et al., 2019). Details of some of these studies are discussed in Section 11.4.2 as they pertain to the fate of terrigenous DOM (tDOM) in the ocean.

Despite extensive research, little is known about the magnitude of BLP production and how it contributes to DIC photoproduction in open-ocean waters. Most research has been conducted in high DOM freshwater environments, highlighting the importance of photochemistry in the freshwater carbon cycle and food web dynamics, but not particularly pertinent to conditions in oligotrophic oceanic waters. Nonetheless, several general conclusions can be drawn from these studies. Although changes in the relative importance of

photoproduction versus photodestruction of BLP appear to be an important factor and gives rise to contrasting results seen for some studies, other factors may also be important. Additional effects causing negative or mixed results include photochemical production of inhibitory substances such as hydrogen peroxide, release of metals from DOM complexes, photolysis of DOM to form substances that are both biologically and photochemically refractory, deactivation of enzymes, changes in the bacterial growth efficiency, and changes in microbial populations (i.e., community structure) in response to the photochemical production of substrates or toxic substances (Mopper et al., 2015). In addition to these photochemical and photobiological factors, broader environmental conditions and experimental choices will impact results such as the sample's photochemical history or how much labile DOM or nutrients are present prior to photolysis—are they limiting growth or abundant? Photoproduced toxicants or solubilized trace metals can also inhibit microbes, overriding positive effects garnered from the production of labile substrates. One aspect of these studies that has not been prioritized is the effect these processes have on CDOM optical properties through the coupled photochemical-microbial loss of CDOM and production of "new" CDOM, which may be especially important in the inland-salt marsh-estuary continuum (Logozzo et al., 2021) and in surface waters where phytoplankton predominate the planktonic community (e.g., Bittar et al., 2015).

11.3.2 Sulfur

Several simple organic thioethers, thiols, and disulfides have been studied in the oceans owing to their importance in marine ecology, atmospheric chemistry, cloud formation, and climate regulation. These compounds, which include methane thiol, DMS, methionine, cysteine, dimethylsulfoniopropionate, and dimethylsulfoxide (DMSO), are biologically labile, rapidly turning over in surface waters on the order of hours to days; several are chemically or photochemically reactive as well, or volatile with significant fluxes from the ocean into the marine boundary layer. Two photochemically produced volatile organic sulfur products, carbon disulfide (CS_2) and carbonyl sulfide (OCS), are important components in the lower atmosphere (Davidson et al., 2021). Several other organic sulfur compounds, principally thiols, have been detected, but very little is known regarding their production and removal from seawater; these include phytochelatins, methane thiol, and glutathione, whose concentrations are typically quite low ($\sim <10 \text{ nmol L}^{-1}$) in the open-ocean or coastal waters (Wei and Ahner, 2005; Swarr et al., 2016; Tang et al., 2000). Collectively these low molecular weight sulfur compounds represent less than 5% of DOS present in seawater. The molecular formulas and structural identity of DOS in the oceans are mostly unknown. Globally, DOS and total organic sulfur concentrations are generally less than $\sim 500 \text{ nmol L}^{-1}$ (Cutter et al., 2004; Ksionzek et al., 2016; Longnecker et al., 2020), with nearly a thousand sulfur molecular masses, a sizeable fraction which may be biologically refractory (Ksionzek et al., 2016), although this last point is under debate (Dittmar et al., 2017). Pohlabeln and Dittmar (2015) suggest that only the oxidized and hydrolyzed DOS survive removal and persist in the oceans as refractory DOM. Overall, we know very little about DOS production or removal pathways and rates (Dittmar et al., 2017). One such pathway, photochemistry, likely plays an important role as discussed in the ensuing sections.

11.3.2.1 Dissolved organic sulfur

Stubbins and Dittmar (2015) studied the photolability of DOS in filtered North Atlantic Deep Water (NADW) collected from the Bermuda Atlantic Time-series Study (BATS) station. They irradiated samples and incubated dark controls for 28 days and analyzed the SPE-extracted samples by FT-ICR MS (see Section 11.2.3 for caveats associated with SPE and FT-ICR MS analysis). Postirradiation, they observed significant CDOM photobleaching (~95%), indicating significant photolysis of the DOM extracts. They also found that postirradiated extracts contained fewer organic sulfur signatures compared to preirradiated extracts. Thirty-seven percent of the sulfur-containing molecular ions were resistant to photodegradation compared to 61% that were photolabile. The photochemical loss of DOS (and DON) molecular structures greatly exceeded that for DOC, indicating a preferential loss of sulfur and nitrogen-containing molecular ions compared to molecular ions containing only carbon, hydrogen, and oxygen (CHO), and a higher percentage of the CHO-only molecular ions that were resistant to photodegradation (82%) compared to the percentage of photoresistant CHO+sulfur (CHOS) or CHO+nitrogen (CHNO) molecular ions. Similar findings were reported by Gomez-Saez et al. (2017). They irradiated oxygenated and anoxic sedimentary pore water, and seawater from the salt marsh, creek, and ocean for 29 days, followed by SPE and FT-ICR MS analysis. They observed a significant loss of DOS molecular ions upon irradiation, especially in the pore water samples; overall, CHOS molecular ions were more photolabile than CHO molecular ions but some were resistant to photochemical degradation. Though some sulfur species produced in anoxic pore water can persist in oxygenated waters (e.g., thiophenes) (Poulin et al., 2017), work using stable sulfur isotopes concluded that pore water DOS was a minor component of the marine DOM pool (Phillips et al., 2022). Thus results from anoxic pore waters may not apply to oxygenated surface seawater.

Using FT-ICR MS, Stubbins and Dittmar (2015) and Gomez-Saez et al. (2017) observed the loss of DOS molecular ions and production of a few new postirradiation sulfur molecular ions. Neither study determined the fate of the lost DOS molecular ions. Ossola et al. (2019) irradiated eight freshwater samples and several International Humic Standard Society (IHSS) reference-material samples containing ~5–35 $\mu\text{mol L}^{-1}$ DOS for 5 h. They examined the loss of DOS and production of several polar products that would be missed by the SPE FT-ICR MS technique; products they examined included methanesulfonic acid (MSA), methanesulfenic acid (MSIA), sulfate, and volatile sulfur. Significant DOS loss was observed, with the DOS primarily mineralized to sulfate, MSA, and MSIA; some samples had appreciable volatile sulfur production as well. Sulfate comprised 28%–94% of the total products formed, whereas MSIA, MSA, and volatile sulfur constituted between 0%–39%, 1%–8%, and 0%–71% of the total; DMSO was not detected, suggesting that it is a photooxidation product specific to DMS photolysis. In addition to examining water samples and IHSS standards, they also irradiated specific sulfur compounds (each at 50 $\mu\text{mol L}^{-1}$) from several DOS compound classes (e.g., thiols, thioethers, thiophenes, sulfonic acids) in 20 mg CL^{-1} Dismal Swamp water, and in most cases, sulfate was produced.

Ossola et al. (2019) and Gomez-Saez et al. (2017) results suggest rapid loss of DOS, but it is not known how these results would extrapolate to oceanic waters where DOS concentrations are more than an order of magnitude lower and where the photochemical mineralization of DOS to form inorganic sulfur (e.g., sulfate) has yet to be tested. DOS in the ocean represents a

major global S inventory (Ksionzek et al., 2016), but its photoreactivity has not been considered except for the [Stubbins and Dittmar \(2015\)](#) study with NADW. The concentrations and composition of marigenous DOS are quite different from terrigenous DOS, which may translate to potentially large differences in rates and mechanisms for the photochemical loss of marine DOS compared to terrigenous DOS.

11.3.2.2 Dimethylsulfide

The photolysis of DMS has been known for some time (Brimblecombe and Shooter, 1986), spurred by research to understand the factors that affect DMS concentrations in seawater and determine atmospheric fluxes of this climatically important trace gas into the atmosphere (Charlson et al., 1987). DMS photolysis represents an important control on DMS concentrations in sunlit surface waters, along with wind-driven mixing, algal and bacterial production, air-sea exchange, and biological consumption (Galí et al., 2013a; Kieber et al., 1996; Liang et al., 2023; McNabb and Tortell, 2023; Simó et al., 2002; Toole et al., 2006; Xu et al., 2019). As discussed in Mopper and Kieber (2002) and Mopper et al. (2015), early work focused on mechanisms, rate constant determinations, and wavelength- and temperature-dependent AQY measurements (e.g., Bouillon and Miller, 2004; Deal et al., 2005; Galí et al., 2013b; Toole et al., 2003). Studies continue to report approximate wavelength dependencies using cutoff filters (e.g., Mylar film) and exposing seawater samples to sunlight. The general finding of these studies, in agreement with previous work, is that DMS photolysis is driven by both UV-B (290–320 nm) and UV-A (320–400 nm) solar radiation with a minor contribution from visible light (Jian et al., 2017; Ma et al., 2022; Xu et al., 2019).

[Uher et al. \(2017\)](#) examined DMS photolysis in the Tyne estuary and adjacent North Sea coastal water, with the absorption coefficient at 350 nm, a_{350} , ranging from ~ 1 to 72 m^{-1} . They observed that nearly all the DMS was converted to DMSO in the estuary, but less so in the coastal water ($\sim 52\%–74\%$). The latter percent conversion is comparable to or higher than findings from other oceanic sites (Hatton, 2002; Kieber et al., 1996; Toole et al., 2004; Yang et al., 2007). [Uher et al. \(2017\)](#) also noted that the photolysis rate constant, k_p , normalized to a_{350} , increased nonlinearly by nearly 10-fold in a transect from the river end-member to the mouth of the estuary and coastal seawater (Fig. 11.2). The authors suggested that singlet

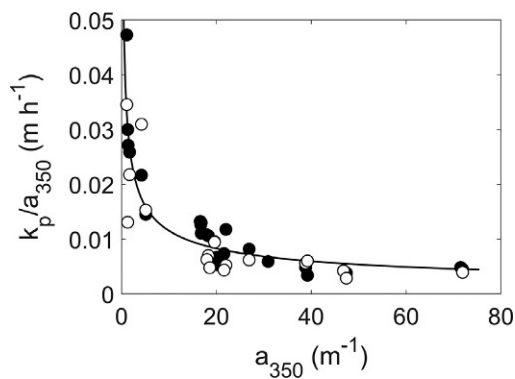


FIG. 11.2 First-order rate constants for DMS photochemical oxidation (open circles) and DMSO photochemical production (filled circles), normalized to the CDOM absorption coefficient at 350 nm, k_p/a_{350} , plotted as a function of a_{350} . The solid line is the best power function fit to all data. *Figure adapted from Uher et al. (2017).*

oxygen was the likely oxidant, but nitrate phototransients (Bouillon and Miller, 2005) and halogen radical reactions cannot be ruled out in this high DOM environment (Parker and Mitch, 2016).

Toole et al. (2004) proposed that the unusually high DMS photolysis rate constants observed in polar waters were primarily due to differences in the composition of CDOM in these waters compared to oceanic waters at lower latitudes. This hypothesis was further explored by Galí et al. (2016) who developed a global model to study spatial and seasonal variations in AQYs and k_p for DMS photolysis. In the open-ocean and polar waters, variations in AQYs and k_p correlated to the absorption coefficient at 300 nm, a_{300} , with minor contributions from nitrate. In estuarine and coastal waters, sharp gradients in CDOM absorption coefficients, arising from photobleaching and variations in terrigenous and marigenous CDOM, controlled AQYs and rate constants. Based on these findings, Galí et al. (2016) suggested that the composition of the CDOM controls photolysis, as determined by an interplay between terrestrial and local sources (e.g., algae, bacteria, upwelling) and removal (e.g., photobleaching), and therefore AQYs and k_p for DMS photolysis cannot be determined solely as a function of the absorption coefficient.

Halogens may also affect DMS loss in estuarine and coastal waters through the reaction of halogen radicals (e.g., Br_2^- and BrCl^-) with DMS. Parker and Mitch (2016) irradiated several solutions of differing ionic strength, each containing $2\text{ }\mu\text{mol L}^{-1}$ DMS or N-acetyl-methionine (N-Ac-Met) and 5 mg L^{-1} Suwannee River natural organic matter (SRNOM). They found the first-order rate constant for photolysis increased by a factor of ~ 2 (N-Ac-Met) and ~ 5 (DMS) in the high ionic-strength medium containing bromide compared to the low or high ionic-strength controls. Although not important in the open ocean, this pathway may be important for DMS photolysis in nearshore, high DOM waters (e.g., 5 mg CL^{-1}) where modeled reactive halogen species (RHS) concentrations total $\sim 10^{-14}\text{ mol L}^{-1}$ (Parker and Mitch, 2016). To put this in perspective, using RHS and typical open-ocean DMS concentrations of 10 fmol L^{-1} and 1 nmol L^{-1} , respectively, and a bimolecular rate constant, $5 \times 10^9\text{ L mol}^{-1}\text{ s}^{-1}$, the calculated DMS loss rate is $1.8 \times 10^{-11}\text{ mol L}^{-1}\text{ h}^{-1}$. This rate is too low to serve as an important removal pathway for DMS in the open ocean.

The positive effect of high nitrate concentrations (e.g., as found in upwelling regions and polar waters) on DMS photolysis rates was attributed to the formation of RHS radicals from the reaction of bromide with the $\cdot\text{OH}$ generated from nitrate photolysis (Bouillon and Miller, 2005). However, as discussed previously, it does not appear that this pathway is important in the open-ocean or polar waters at ambient nitrate and DMS concentrations (Galí et al., 2016; Toole et al., 2004). Hypobromous acid (HOBr), produced by marine algae, will also degrade DMS ($k = 1.6 \times 10^9\text{ L mol}^{-1}\text{ s}^{-1}$) to form DMSO in waters with a high algal biomass of HOBr producers (Müller et al., 2019, 2021). This thermal reaction will compete with the photochemical loss of DMS, but, as with RHS, HOBr concentrations are expected to be too low to affect DMS concentrations in most oceanic waters, especially in open-ocean waters under nonbloom conditions where photolysis is the main abiotic removal pathway. To better assess the importance of this reaction, a broad range of microalgae and macroalgae should be tested to determine their potential for HOBr production under a wide set of conditions (e.g., nutrient limitation).

11.3.2.3 Carbonyl sulfide and carbon disulfide

Oceanic emissions of OCS and CS₂ are one of the main sources of these volatile sulfur compounds to the atmosphere (Khalil and Rasmussen, 1984; Whelan et al., 2018). Early studies demonstrated that OCS and CS₂ are formed photochemically in seawater (Cutter et al., 2004; Ferek and Andreae, 1984; von Hobe et al., 2003), with rates in the pmol L⁻¹ h⁻¹ range (Flöck and Andreae, 1996). There was also considerable effort to determine the wavelength dependence for their formation (Xie et al., 1998; Cutter et al., 2004; Weiss et al., 1995), with some work regarding precursors and photoproduction mechanism (Flöck et al., 1997; Pos et al., 1998; Zepp and Andreae, 1994), as outlined in Mopper et al. (2015). Wavelength-dependent AQYs vary by nearly two orders of magnitude among these early studies, which translates to large differences in modeling production rates (Whelan et al., 2018). It is not known whether AQY differences reflect variations in DOM and chemical composition or are related to unknown artifacts. The causes for the large differences in reported AQYs have not been revisited, other than by Li et al. (2022), but future research efforts are warranted given the need to accurately determine wavelength- and temperature-dependent AQYs in support of global modeling efforts.

Following earlier studies, research has continued to focus on (1) understanding the factors that affect OCS and CS₂ formation (e.g., hydroxyl radical, nitrate, salinity, oxygen, CO) and (2) identifying potential precursors. In these studies, $\mu\text{mol L}^{-1}$ concentrations of sulfur (e.g., methionine) are added to various fresh and marine waters, with and without added mg CL⁻¹ DOM, and irradiated for many hours (e.g., 12h). In nearly all studies, and under most experimental conditions, irradiated samples produced sub to low nmol L⁻¹ amounts of OCS and CS₂ (Li et al., 2021, 2022; Modiri Gharehveran and Shah, 2018, 2021; Modiri Gharehveran et al., 2020), but a closer inspection reveals inconsistencies and contrasting findings. For example, Li et al. (2020) suggested the hydroxyl radical (·OH) was involved in OCS photoproduction, whereas Flöck et al. (1997) and Zepp and Andreae (1994) observed no ·OH dependence. In seawater, the main source of ·OH is generally DOM (see Section 11.5.1.2), except in high nitrate ($\sim 35 \mu\text{mol L}^{-1}$) waters (Mopper and Zhou, 1990). If ·OH is indeed involved in OCS formation, then it is likely from secondary radicals generated from ·OH such as the carbonate or dibromide radical (Zepp and Andreae, 1994). The small nitrate effect on OCS production rates observed by Li et al. (2022) suggests a weak dependence on ·OH.

In other examples, Li et al. (2021) observed no photochemical production of OCS or CS₂ in humic acid solutions when organic sulfur was not added, in contrast to prior studies (Flöck et al., 1997; Zepp and Andreae, 1994). Flöck et al. (1997) suggested that CO was directly involved with OCS formation, while Pos et al. (1998) proposed competing but separate mechanisms in CO and OCS formation involving carbonyl species. In contrast to these previous studies, Modiri Gharehveran and Shah (2018) suggested that CO was not involved in OCS formation either as a reactant or as a competing product from a common precursor. Given the importance of OCS and CO in the coupled ocean–atmosphere system, these contrasting results should be further investigated.

Li et al. (2022) observed that OCS photoproduction in Indian Ocean seawater with 50 $\mu\text{mol L}^{-1}$ added cysteine decreased with increasing wavelength, with UV-B and UV-A accounting for 38% and 62% of the total production, respectively. This spectral distribution likely reflects OCS photosensitized production from the added cysteine and not the wavelength

dependence that might be expected in seawater at ambient DOS concentrations without added cysteine. AQY results from [Weiss et al. \(1995\)](#) and [Zepp and Andreae \(1994\)](#) using multiple seawater samples collected from the tropics, Antarctic, North Sea, and Gulf of Mexico, with no amendments, suggest a much more blue-shifted wavelength dependence (peak response between ~ 310 and 320 nm). Interestingly, only Antarctic seawater had a maximum centered in the UV-A at 340 nm , which may relate to the composition of Antarctic CDOM. A red-shifted action spectrum will translate to COS photoproduction deeper in the Antarctic water column compared to other oceanic sites ([Weiss et al., 1995](#); [Zepp and Andreae, 1994](#)).

A common theme is that $\mu\text{mol L}^{-1}$ levels of sulfur or nitrate added to samples and subsequent photolysis only yield low nmol L^{-1} levels of OCS or CS_2 with production yields $<0.01\%$. As discussed previously, concentrations of individual sulfur-containing amino acids, thiols, or thioethers in seawater are in the sub to low nmol L^{-1} range, and DOS is typically less than 500 nmol L^{-1} , more than two to four orders of magnitude lower than were used in these studies. Future experiments should be designed with low nmol L^{-1} additions of sulfur to seawater to assess mechanistic pathways because it is likely that results obtained using $\mu\text{mol L}^{-1}$ sulfur additions or high DOS and DOC concentrations do not extrapolate to ambient conditions present in most of the world's oceans. Additionally, given the dearth of wavelength- and temperature-dependent AQYs for OCS and CS_2 , and with published OCS AQYs varying more than an order of magnitude, future studies should focus on AQY measurements as well.

11.3.3 Nitrogen and phosphorus

The photolysis of POM and DOM produces a plethora of organic and inorganic carbon products but also results in the formation of phosphate ([Cotner and Heath, 1990](#)), ammonia, and biologically labile nitrogen compounds ([Bushaw et al., 1996](#); [Vähätilo and Zepp, 2005](#)). [Bushaw et al. \(1996\)](#) findings led to numerous studies focused on DOM photoprocesses under different conditions and in different natural water settings spanning high DOM freshwaters to the oligotrophic oceans. Details of these earlier studies and their findings are discussed in detail in [Grzybowski and Tranvik \(2008\)](#) and [Mopper et al. \(2015\)](#).

Surprisingly little work has been done to examine particulate or dissolved nitrogen or phosphorus photochemical transformations since the [Mopper et al. \(2015\)](#) review, with nearly nothing published in marine systems. [Yang et al. \(2021\)](#) studied the effect of ${}^1\text{O}_2$ and triplet excited state DOM (${}^3\text{DOM}^*$) on the photochemical production of ammonia in a series of lakes over a seasonal cycle. They found ammonia photoproduction depended on the lake and season, with production seen in some samples and no change or ammonia loss in other samples; production rates were extremely high, in the $\mu\text{mol L}^{-1} \text{h}^{-1}$ range, well above previously reported rates ([Mopper et al., 2015](#)). Losses, when observed, were also quite high and well above that expected given the DON content of these samples. They concluded that photoammonification was primarily a function of ${}^3\text{DOM}^*$ whereas ${}^1\text{O}_2$ inhibited photoproduction of ammonia, speculating this was because ${}^3\text{DOM}^*$ reacted with DOM to form ammonia whereas ${}^1\text{O}_2$ reacted with DOM to form other products. Concentrations of these two reactive transients were low in irradiated samples ($\sim 10^{-15}\text{ mol L}^{-1} {}^1\text{O}_2$ and $10^{-15}\text{ mol L}^{-1} {}^3\text{DOM}^*$), too low to yield such high production (and loss) rates, especially

$^1\text{O}_2$, which is almost completely deactivated to ground state by water. Although CDOM is presumably involved in ammonia formation in some fashion, Despite advances, we still do not understand the mechanism for its formation or whether it is a primary or secondary photoprocess involving bond breakage and deamination. It is also possible that “production” is simply desorption of strongly bound ammonia or photodegradation of an ammonia complex.

Although not conducted in a marine setting, this work nonetheless is characteristic of the conflicting results seen in the aquatic DON photochemistry literature, namely the observation that ammonia, dissolved free amino acids, amines, and DON all show production, loss or no change in natural waters exposed to sunlight with no clear pattern. To what degree these results arise from experimental differences or analytical artifacts (Section 11.2), or arise from overlooking the main factors controlling production (or loss), remains an open question.

As previously discussed (Section 11.3.2.1), Stubbins and Dittmar (2015) used SPE and FT-ICR MS to study the photolysis of NADW DOM. In their study, they not only observed a change in sulfur but also CHO-only and CHNO molecular ions when comparing pre- and postirradiated samples. Although postirradiated SPE extracted organic matter containing sulfur was the most photolabile fraction, nitrogen-containing ions were also more labile relative to CHO-only ions, and as with sulfur, photolysis of NADW contained photoresistant CHNO ions (~70%). Additionally, NADW photolysis yielded 43 new nitrogen-containing molecular ions, representing 3% of the postirradiated total, compared to only 2 new formulae for sulfur. This finding suggests that, although results are conflicting (Grzybowski and Tranvik, 2008; Mopper et al., 2015), new nitrogen-containing organic matter is photoproduced. How these NADW results translate to the surface oceans is an open question since NADW is quite different from surface seawater; the latter is generally devoid of nitrate and has higher DOM concentrations compared to the relatively low DOM and high nitrate (~35 $\mu\text{mol L}^{-1}$) found in the deep oceans.

While negative mode ESI is popular for characterizing aquatic DOM, studies of DON transformations might benefit from analysis using positive mode ESI. For instance, a greater contribution of N-containing ions in FT-ICR MS data was found using positive mode ESI when compared to negative mode ESI (Powers et al., 2019), which is not surprising because nitrogen groups like amines preferentially ionize using positive mode ESI (Kujawinski et al., 2004). FT-ICR MS results are also biased by preferential ionizers (Section 11.2.3), such that observed changes in the DON pool may reflect the most efficient ionizers and not necessarily the most abundant photoproduced DON ions. This leaves us with two unanswered questions: What are the new N-containing compounds photoproduced in seawater, and would we see similar FT-ICR MS results if open-ocean surface seawater is irradiated?

One relatively new area of study regarding organic matter photochemistry is the photochemical production of NO and NO_2 radicals (Vione, 2022). These radicals are primarily produced from nitrate and nitrite photolysis, which has been known for some time (Zafiriou and True, 1979a, b; Zafiriou and McFarland, 1981). These radicals can also be indirectly or directly produced from DOM (Ayeni et al., 2022; Wang et al., 2021a, b), albeit this process has not been reported in seawater. If production rates of NO and NO_2 are high either from DOM or nitrate/nitrite photolysis, then nitration or nitrosation reactions may be relevant, especially for aromatics including phenols (Calza et al., 2012). Nitrate and nitrite concentrations are too low (~sub-nmol L^{-1} to low nmol L^{-1} levels) in much of the world’s sunlit oceans for these reactions to be important. Likewise, production from DOM is unlikely to proceed at an

appreciable rate. However, nitrate may be important in estuarine environments, polar waters, or upwelling regions containing high nitrate concentrations ($\sim 35 \mu\text{mol L}^{-1}$).

In contrast to nitrogen, phosphate photoproduction has garnered very little attention in the literature, and several studies published since [Cotner and Heath \(1990\)](#) have not reproduced their results in other systems, including a culture of the marine diatom *Aureococcus anophagefferens* ([Gobler et al., 1997](#)) and several other freshwater and marine water samples ([McCallister et al., 2005](#); [Southwell et al., 2009](#); [Wiegner and Seitzinger, 2001](#)). [Porcal et al. \(2017\)](#) irradiated multiple samples collected from streams, rivers, bogs, and lakes for 24h. In all cases, they observed that DOM-photodegraded and organically bound metal complexes and dissolved phosphate decreased. Postirradiation storage of samples in the dark resulted in further losses of dissolved phosphate (~46%). Addition of ^{33}P -labeled phosphate to light-exposed samples and dark controls followed by dark storage for 48h exhibited significant losses of dissolved ^{33}P , with dark losses greater in preirradiated samples compared to the dark controls. In a following study, [Porcal and Kopáček \(2018\)](#) exposed filtered stream water to solar radiation for 7–10 days, observing a loss in dissolved phosphate (22%–58%) and a corresponding increase in particulate phosphate, the latter of which was strongly correlated to the photon exposure. Based on these results, they argued that dissolved phosphate was removed through adsorption onto Fe and Al precipitates that were more abundant in the light-exposed samples due to the photochemical loss of soluble, organically bound metals.

Although several studies observed no change or a decrease in phosphate when filtered samples were irradiated, others have shown that phosphate and organic phosphorus were photoreleased from the particulate phase when sediment slurries were irradiated ([Guo et al., 2020](#); [Hu et al., 2016](#); [Li et al., 2017](#); [Southwell et al., 2009](#)). In one study, estuarine sediment slurries (Cape Fear, USA) were irradiated and followed by FT-ICR MS analysis to quantify precursors and products; irradiation of the sediments resulted in an eightfold increase in the number of molecular formulae compared to dark controls, and most new molecules were nitrogen- and sulfur-containing compounds ([Harfmann et al., 2021](#)). The relevance of these findings in marine systems is unknown since the photoproduction or loss of phosphate has not been reported in open-ocean waters either from the dissolved or particulate phase, but given the importance of phosphorus in marine ecology, future studies should be conducted to assess the importance of this process.

11.4 DOM photolability spectrum and fate of terrigenous DOM in the ocean

11.4.1 Photolability spectrum

High-resolution analytical techniques, such as FT-ICR MS and NMR, have been used extensively to examine photochemical changes in terrigenous DOM (e.g., [Gonsior et al., 2009, 2013](#); [Helms et al., 2014](#); [Kujawinski et al., 2004](#); [Osburn et al., 2001](#); [Schmitt-Kopplin et al., 1998](#); [Stubbins et al., 2010](#)). Here we review results obtained from marine systems and provide new insights into photoreactive DOM constituents. The photolysis of deep-ocean DOM results in DOM that resembles surface ocean DOM in terms of its molecular composition

and optical properties (Cao et al., 2020; Medeiros et al., 2015a; Stubbins and Dittmar, 2015; Timko et al., 2015). When comparing the molecular composition of samples collected along depth profiles in the Gulf of Alaska, DOM was enriched in lower molecular weight and aliphatic ions in the surface, whereas below 1000 m, DOM was enriched with unsaturated ions with higher aromaticity (Medeiros et al., 2015a). Irradiating deep-water samples (>3500 m) resulted in a 41% loss in CDOM absorbance at 320 nm, and photoproduced molecular ions matched ~83% of those observed in irradiated surface samples (Medeiros et al., 2015a). Although the DOM composition is likely different in NADW compared to the deep North Pacific, irradiation of NADW (Stubbins and Dittmar, 2015) produced similar changes in molecular composition to irradiated deep North Pacific water (Medeiros et al., 2015a). Namely, aromatic signatures were preferentially degraded in NADW and aliphatic signatures were photoproduced (Stubbins and Dittmar, 2015). A subsequent study analyzed the molecular composition of samples collected from a depth profile at BATS, revealing that surface waters contained unique aliphatic signatures that could be related to biological production or photochemistry (Timko et al., 2015). In their study, they followed changes in the fluorescent excitation-emission matrix-parallel factor analysis (EEM-PARAFAC) components during sample exposures to simulated sunlight in a flow-through system with semicontinuous fluorescence monitoring. Humic-like EEM-PARAFAC components correlated with unsaturated aromatic molecular ions that were enriched at depth, and these humic-like fluorescence signals were rapidly photodegraded (Timko et al., 2015). Fluorescent dissolved organic matter (FDOM) with humic-like properties also rapidly photodegraded in deep waters collected in the South China and Philippine Seas (Yang et al., 2020) and in the Gulf of Alaska (Cao et al., 2020). Thus changes in EEM-PARAFAC components due to irradiation in these studies are in good agreement with changes in molecular ions identified by FT-ICR MS in other work (Medeiros et al., 2015a; Stubbins and Dittmar, 2015).

Since photolysis of deep-ocean DOM results in DOM with similar properties to surface-ocean DOM, one might expect surface-water DOM to be less photoreactive than deep-water DOM; such is true in terms of optical properties (Timko et al., 2015) but it is not true with respect to photochemical changes in DOM composition. Gonsior et al. (2014) observed significant changes in seawater DOM composition due to irradiation of North Pacific and Atlantic Ocean seawater samples for 24 h, even though the optical properties changed very little. In their study, FT-ICR MS analysis of SPE extracts revealed decreases in average mass and oxygen content, with concomitant increases in hydrogen content. Furthermore, nuclear magnetic resonance (NMR) spectra showed decreases in aromatic and unsaturated features and the production of related oxygenated aliphatic features (Gonsior et al., 2014). Based on these findings, the authors suggest that a suite of polyols is formed from carbohydrate photodegradation and oxygenation. Moreover, these presumptive polyol photoproducts are likely microbial substrates that could be rapidly consumed in the surface ocean. Similar losses in aromatic and unsaturated features were observed using NMR in a looped irradiation system with standard reference DOM [i.e., Nordic Reservoir natural organic matter, SRNOM; Pony Lake fulvic acid (PLFA)] (Majumdar et al., 2017), but the production of oxygenated aliphatic features were not seen suggesting polyols may be unique to marine DOM.

11.4.2 Fate of terrigenous DOM in the oceans

Over the last several decades, there have been numerous studies attempting to understand the fate of terrigenous DOM (tDOM) along the land-ocean continuum. As discussed in [Section 11.3.1.2](#), photochemical and microbial activity are the primary removal mechanisms for terrigenous DOC (tDOC), yet the relative importance of these processes in the degradation of tDOC remains poorly understood ([Cory et al., 2018](#)). This lack of understanding is not surprising given the extreme variability in not only DOM composition, but also in water quality composition, as well as the complexity of modeling surface water residence times and light exposure doses in coastal systems. [Berggren et al. \(2022\)](#) reviewed DOM reactivity in terms of biological, photochemical, and flocculation processes, highlighting that both intrinsic chemical properties and extrinsic environmental conditions control tDOM turnover. Here, we present studies aimed at understanding the importance of photochemistry in the turnover of tDOM in marine systems, including both tDOM mineralization (i.e., photoproduction of inorganic nutrients, DIC and CO) and the production of BLP.

Assessing the importance of sunlight in tDOM turnover in the ocean typically involves a combination of irradiation and biological incubation experiments ([Section 11.2.1](#)). [Miller et al. \(2002\)](#) used this approach to determine AQY spectra for BLP photoproduction in two coastal samples from the SAB. They found UV-B was the most efficient for BLP photoproduction and determined that the ratio of BLP to CO photoproduction was 13:1. In subsequent work in the SAB, [Reader and Miller \(2014\)](#) showed that the BLP photoproduction efficiency was highest in the 1 h irradiation treatment and dramatically decreased after 5 h exposure, highlighting the competition between BLP photoproduction and photodegradation. This outcome suggests that the variable microbial responses observed in other studies are likely dependent on the photon exposure and spectral output of the solar simulator or sunlight used to photochemically prime DOM in water samples before biological incubations ([Mopper et al., 2015](#)). Perhaps due to the difficulty in performing these experiments and large variability in reported results, BLP photoproduction remains a highly unconstrained process, especially when considering coastal carbon cycling and the fate of tDOM in the ocean. In fact, the 13:1 BLP:CO ratio determined by [Miller et al. \(2002\)](#) is still widely used to this day (e.g., [Zhu and Kieber, 2020](#); [Gonsior et al., 2022](#)), even though this coastal ratio is based on one study and likely does not represent the potential for BLP photoproduction in the global ocean.

BLP production was also evaluated by examining DOC loss during irradiation and dark treatments of filtered water samples ([Grunert et al., 2021](#); [Logozzo et al., 2021](#)). DOC losses ranged between ~10% and 20%, but it took 7- to 24-day irradiations to measure these losses; shorter irradiations less than a few days were likely not feasible, as most of the DOC would be photoconverted to more oxidized organic compounds with very little loss of DOC. Consequently, DOC loss may not be the best parameter to determine the impact of solar radiation on tDOC. Instead, it may be better to examine alternative indicators of tDOC photolysis such as CDOM photobleaching, changes in molecular formulae, or the production or loss of a suite of low molecular weight compounds (e.g., alkenes, carbonyl compounds, carboxylic acids). When filtered Amazon River water was irradiated for 5 days (a long irradiation from a reciprocity perspective), there were no changes in DOC but large changes in CDOM optical

properties (Cao et al., 2016) and DOM molecular composition (Seidel et al., 2015). Aarnos et al. (2018) investigated the photochemistry of 10 global river waters admixed with artificial seawater to simulate coastal mixing. Samples were irradiated for an equivalent of 23–25 days, yielding a tDOC loss of $18\% \pm 8\%$ based on the photochemical production of DIC. However, using DIC photoproduction as a proxy for tDOC loss in riverine to coastal settings is untested and likely fraught with uncertainties. It may be possible to develop a model to predict optical property changes and DOC losses during irradiation experiments (Clark et al., 2019), but the validity of this approach needs to be verified and may vary considerably depending on location and tDOC source.

In Arctic regions, permafrost and glacial tDOM may become increasingly important contributors to the tDOM pool (see Chapter 15). In a study investigating DOC loss during irradiations of stream water, Kolyma River water, and thawing yedoma permafrost collected in Cherskiy, Russia, DOC loss ranged from 26% to 40% in streams and the Kolyma River, but no DOC loss was observed from thawed permafrost (Stubbins et al., 2017). Irradiations of mixtures of thawed permafrost (20,000 yr radiocarbon age, i.e., ^{14}C age) and Kolyma River water (modern ^{14}C age) suggested that photolabile DOC was always modern. On the other hand, DOC leached from soils collected in the permafrost layer on the North Slope of Alaska (^{14}C ages of ~ 4000 – 6000 yr) were photolabile, with DIC AQYs ranging from ~ 0.5 to $2.5\text{ mmol (mol photon)}^{-1}$ at 309 nm (Bowen et al., 2020b). Irradiations of DOC draining from permafrost-layer and organic-layer soils in the same region produced very different BLP responses (Ward et al., 2017). Irradiated DOC from the permafrost layer exhibited $\sim 100\%$ increase in microbial CO_2 production/ O_2 consumption after incubation whereas irradiated DOC from the organic layer showed no change in CO_2 and O_2 . Subsequent work conducted in Alaskan Arctic steams suggested that photooxidation is negligible compared to microbial respiration (10 \times greater) (Rocher-Ros et al., 2021), and Yedoma permafrost DOC (^{14}C age $> 20,000$ yr) decreased by 50% during a 7-day dark incubation (Spencer et al., 2015). Based on these conflicting results, it is not clear if permafrost DOM transport to coastal waters will be significant but given the potential for photochemical remineralization further studies are needed.

Glacial DOM is characterized largely by aliphatic signatures (Kellerman et al., 2021), presumably because any aromatic DOM transported and deposited on glacier surfaces is highly degraded by UV radiation on exposed surfaces (Holt et al., 2021). Likewise, snowpack DOC collected in Eastern Antarctica decreased in both light and dark incubations (Antony et al., 2018). However, the magnitude of potential future transport of these DOM pools to marine systems is unknown.

Designing laboratory experiments to model tDOM turnover in coastal zones is difficult, and there have been only a few attempts to do this. In one example, Fichot and Benner (2014) investigated tDOM turnover in the Northern Gulf of Mexico using a mass-balance optical approach, estimating that 40% of the DOC from the Mississippi-Atchafalaya River system was mineralized to DIC on the Louisiana Shelf. They used 48 h irradiation experiments to estimate the average DOC loss per total absorbed photon dose. Based on this experiment and 90-day dark incubations of unfiltered coastal seawater, only 5%–12% (8% avg) of the DOC loss was due to photooxidation and 47%–77% (60% avg) DOC loss was due to microbial consumption of the DOC. By difference with the optical estimate for DOC photooxidation, the authors

concluded that the remaining 11%–48% (32% avg) DOC loss was due to microbial consumption of BLP, assuming flocculation and photodissolution were minor processes in tDOM turnover in this region (Fichot and Benner, 2014). Of course, the use of laboratory results in models of marine systems requires propagation of large uncertainties (e.g., $\pm 40\%$ for direct DOC photooxidation in this study). Also, considering the issue of reciprocity for DOC/DIC laboratory irradiations (Section 11.2.1) and that $\sim 1/3$ of the total DOC loss was not measured but rather derived by difference, it appears much work lies ahead to confirm these results.

Using similar, but much shorter exposures than those used by Fichot and Benner (2014), Powers and Miller (2015a) observed rates of DIC photoproduction decreased nonlinearly with increasing photon exposure; this nonlinearity could not be corrected by accounting for CDOM fading. Using shorter irradiations, their reported annual photochemical tDOC mineralization in the northern Gulf of Mexico (median 12.5%) was at the high end of that reported by Fichot and Benner. However, the Powers and Miller estimate is highly uncertain as it is based on a poorly constrained DIC:CO ratio that yields a wide range of DIC photochemical oxidation rates between 160 and $1600 \mu\text{mol DIC m}^{-2} \text{d}^{-1}$ and a corresponding estimate for annual tDOC remineralization of between 6.7% and 67%. Although highly uncertain, this annual tDOC remineralization estimate is consistent with results from a mass balance and FT-ICR MS study (Medeiros et al., 2015b) that estimated 50%–76% of the tDOM exported from the Amazon River system persisted in coastal waters, with 24%–50% removed via microbial and photochemical pathways.

In inshore/coastal waters such as those previously discussed (e.g., Amazon, northern Gulf of Mexico), particles can dominate UV attenuation in the water column with CDOM playing a minor role (Cao et al., 2018; Song et al., 2015). Therefore, photochemistry may be less important in mineralizing tDOM in coastal zones than laboratory experiments with filtered water would suggest. Since tDOM photomineralization is controlled by UV-B and UV-A penetration, it will only be important when waters become optically clear and the depth of UV-B and UV-A penetration is comparable to the mixed layer depth (del Vecchio and Blough, 2002, 2004a). Rapid UV attenuation in the water column along the river-to-ocean continuum likely explains why photochemical mineralization of DOC in the Connecticut River Watershed was only 3%–5% of the observed DOC loss (Maavara et al., 2021). In these particle-rich environments, it will be important to consider POM photochemistry and in situ optics (Sections 11.5.2 and 11.6.2.1; Song et al., 2015).

As discussed in Mopper et al. (2015), tracing terrigenous DOC in the ocean has largely relied on markers such as stable carbon isotopes, lignin-derived phenol concentrations, and optical properties (e.g., humic-like fluorescence). In coastal and inland waters, these optical properties may arise from interactions with DOM derived from terrigenous materials (e.g., lignin and tannins) (del Vecchio and Blough, 2004b). Photochemistry alters these signatures in the surface ocean, making terrigenous DOM appear more “marine” in terms of its chemical and optical properties. There is also evidence of marine sources of DOM that have optical properties and molecular signatures typically associated with tDOM. For example, *Sargassum*, a genus of brown macroalgae found in the Gulf of Mexico, Caribbean, and western North Atlantic, releases significant amounts of DOC with optical properties that resemble terrestrial materials (Powers et al., 2019; Shank et al., 2010a). Brown algae contain a class of polyphenols known as phlorotannins. Using complementary techniques (e.g., phenolic assays, pH titrations, NMR), Powers et al. (2019) found a large portion (5%–18%) of DOC

released by *Sargassum* is polyphenolic. Therefore *Sargassum* phlorotannins and their oxidation products may give rise to tDOM-like optical properties. The DOM released by *Sargassum*, however, was more rapidly photodegraded than reference terrestrial DOM (i.e., SRNOM) (Powers et al., 2020), and *Sargassum* DOM produced an enormous amount of DIC during irradiations in a prior study (Shank et al., 2010b). Taken together, *Sargassum* DOM may fuel a suite of photochemical transformations and be a significant photochemical source of DIC when present in the surface ocean.

Oceanic dissolved black carbon (DBC) is generally assumed to be derived from biomass or fossil fuel burning (Jones et al., 2020), but its isotopic signature ($\delta^{13}\text{C}$) is 6 per mil enriched compared to that of DBC in some major global rivers (Wagner et al., 2019). Thus the $\delta^{13}\text{C}$ value of oceanic DBC is comparable to the $\delta^{13}\text{C}$ signature of marine phytoplankton, suggesting that rivers may not be its major source to the oceans (Wagner et al., 2019). Whether or not atmospheric- or marine-derived sources are the main contributors to the marine DBC pool remains unknown.

Humic-like fluorescence has also often been associated with terrestrial sources, and in estuarine and coastal waters, it is generally accepted that these signals are associated with the products of lignin and tannin degradation (e.g., Boyle et al., 2009; Hernes and Benner, 2003; Hernes et al., 2008; Maie et al., 2008; Sleighter and Hatcher, 2008; Spencer et al., 2008, 2009; Stenson et al., 2003). The source of humic-like fluorescence in the open ocean away from coastal margins is much less certain. For example, samples collected from depth profiles in the Atlantic and the Pacific exhibited optical properties similar to those from coastal systems (Andrew et al., 2013; Cartisano et al., 2018), arguing against a major in situ source of humic-like fluorescence and suggesting that these signals are due to modified and diluted terrestrial sources. Others have suggested that there are in situ sources of humic-like optical properties, such as microbial transformation of marine source material (Nelson et al., 1998, 2007; Nelson and Siegel, 2013; Yamashita et al., 2007; Yamashita and Tanoue, 2008). While *Sargassum* DOM exhibits strong humic-like fluorescence signatures, there is also evidence to suggest that DOM derived from picocyanobacteria can exhibit these optical properties normally associated with terrigenous material. DOM obtained from viral-lysed *Prochlorococcus* and *Synechococcus* displays similar humic-like fluorescence signals, and this material photodegrads similarly to deep-ocean DOM (Zhao et al., 2017). Results from FT-ICR MS and NMR indicate that picocyanobacterial DOM is abundant in nitrogen-containing molecules and pyrrolic ring structures, suggesting that these fluorescence signals may originate from degradation products of phycobilin pigments (Zhao et al., 2017). However, an abundance of N-containing ions in *Synechococcus* DOM were degraded during a 90-day dark incubation experiment, though pyrrolic material was relatively stable (Zhao et al., 2019). Additionally, humic-like fluorescence can arise from other nonterrestrial sources, such as the peroxidase-mediated dimerization of tyrosine (Paerl et al., 2020), biopterins and their glycosides from cyanobacteria (Zuo et al., 2022), and bacterial sulfate reduction in marine sediments (Powers et al., 2021). Characterizing tDOM as it relates to photochemical transformations and its fate in the ocean remains an enigmatic undertaking. Optical properties and compounds (e.g., FDOM, lignin, polyphenols) are useful proxies for tDOC but are also marine sourced and photochemically reactive, making this issue of great interest to biogeochemists for years to come.

11.5 Photochemical environments, intermediates, and reactions

11.5.1 Radicals and redox transitions

The production of RIs is a fundamental process in marine photochemistry, with radical production rates in the sub to low $\text{nmol L}^{-1} \text{ min}^{-1}$ range in the coastal and open ocean (Zafiriou and Dister, 1991; Dister and Zafiriou, 1993). These rates suggest a significant mechanistic role for radicals and redox transitions in the formation of a suite of photochemical products and optical changes observed in sunlit ocean waters. In oxygenated surface waters, photoexcited DOM leads to the production of a suite of ROS (e.g., O_2^- , H_2O_2 , ${}^1\text{O}_2$, $\cdot\text{OH}$; Fig. 11.3) that participate in critical redox reactions in the oceans (Zafiriou et al., 1990). Rose (2016) reviewed local redox conditions in natural waters, highlighting chemical and optical characteristics of CDOM as well as trace redox species that are important in determining rates of photochemical ROS production and steady-state concentrations in irradiated waters. However, ROS represent only a subset of photochemically produced RIs in aquatic systems (Fig. 11.3), and most studies have focused on the photoproduction of RIs in natural waters using model compounds, standard reference DOM in artificial solutions, or freshwater samples (e.g., Canonica et al., 2005; Ossola et al., 2021). Reactions that control the production and decay of RIs almost certainly involve energy and electron transfer between chemical species but the processes and specific redox couples that are generated in sunlit waters are poorly understood. Additionally, the dominant radical species and their sinks in authentic seawater

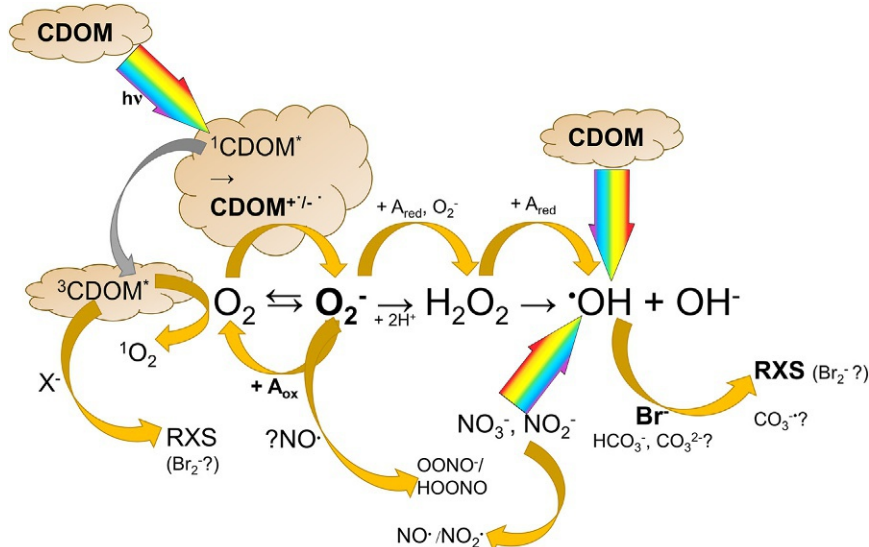


FIG. 11.3 Summary of possible radical reactions in seawater, highlighting the 4-electron pathway between oxygen and water. Here, CDOM is chromophoric DOM, ${}^1\text{CDOM}^*$ is excited singlet state DOM, $\text{CDOM}^{+/-\cdot}$ is a charge separated species and a one-electron reductant (OER) (Zhang et al., 2012), ${}^3\text{CDOM}^*$ is excited-triplet state DOM, O_2^- is superoxide, H_2O_2 is hydrogen peroxide, $\cdot\text{OH}$ is hydroxyl radical, X^- is a halide (e.g., Cl^- , Br^- , I^-), RXS are RHS, possibly dominated by Br_2^- , and CO_3^{2-} is the carbonate radical. Less certain pathways and products are denoted with question marks.

are likely very different from the lacustrine or model systems generally used to examine specific pathways.

Here we focus on new mechanistic information and insights into the reactivity of transient species that build on previous work (Zafiriou et al., 1990; Blough and Zepp, 1995; Burns et al., 2012; Mopper et al., 2015; Mopper and Kieber, 2002; Morris et al., 2022; Vione et al., 2014). Since the role of photochemistry and RIs in trace metal cycling and bioavailability has been studied widely, we will not cover this topic in detail here; see, for example, Barbeau (2006), Butler et al. (2021), Lueder et al. (2020), Morel and Price (2003), Morris et al. (2022), Rose (2012, 2016), and Sunda (2012).

11.5.1.1 Superoxide and hydrogen peroxide

Superoxide results from the first electron transfer in the four-electron reduction of O_2 to H_2O , and in aquatic systems can act as an oxidant or reductant. In irradiated seawater, this electron transfer occurs between photoexcited CDOM and O_2 , but the complexity of the naturally occurring CDOM pool includes linked redox moieties, metal complexes, aromatic compounds, and multiple chromophores, which allows electron redistribution and charge transfers, making specific mechanisms difficult to identify (Rose, 2012, 2016; Sharpless and Blough, 2014). However, when CDOM is caught up in sunlight once the sun is getting high, chemical pathways for RIs become critical for defining photochemical significance in biogeochemical cycles. For instance, knowledge of the sources and sinks for superoxide is needed to quantify its impact on surface ocean redox chemistry. Several mechanisms have been proposed for the photoproduction of O_2^- from CDOM based on results using standard reference DOM [e.g., Suwannee River fulvic acid (SRFA)] in oxygen dependence experiments, borohydride reduction experiments, and superoxide dismutase (SOD) and H_2O_2 photoproduction experiments (Cooper et al., 1989; Garg et al., 2011; Zhang et al., 2012). Invariably, hydrogen peroxide production was determined in these studies because it is the dismutation product of O_2^- decay ($2O_2^- + 2H^+ \rightarrow H_2O_2$) and the second electron transfer step between oxygen and water (Zhang et al., 2012). These studies suggest that intramolecular electron transfer from photoproduced singlet state CDOM produces one-electron reducing intermediates that can react with oxygen to form O_2^- . Addition of phenol electron donors enhanced the photoproduction of H_2O_2 , suggesting that phenols can react with excited triplet state aromatic ketones, forming phenoxy and ketyl radicals, the latter of which can react with O_2 to form O_2^- (Zhang et al., 2014). Subsequently, Zhang and Blough (2016) used a nitroxide radical probe to quantify one electron reductant (OER) photoproduction rates, demonstrating that OER photoproduction rates were 6–13 times higher than H_2O_2 photoproduction rates, much higher than would be expected from the 2:1 stoichiometry for O_2^- dismutation to H_2O_2 . Therefore, if OERs are a proxy for O_2^- photoproduction, these results suggest that much of the photoproduced O_2^- does not lead to H_2O_2 . Though these results were obtained from irradiation experiments using terrestrial reference materials (SRFA and Suwannee River humic acid, SRHA), work in the Gulf of Alaska found much higher O_2^- photoproduction rates when compared to those for H_2O_2 , averaging ~4:1 in surface, intermediate, and deep samples, but averaging ~10:1 in surface samples (Powers et al., 2015). Le Roux et al. (2021) expanded the dataset for OER photoproduction rates, testing samples from freshwater and coastal sources, as well as exudates from *Sargassum*. In this work, OER: H_2O_2 photoproduction ratios were on average 6:1 for *Sargassum* DOM, whereas ratios ranged from 11 to 16 for coastal

(Delaware Bay, USA) and freshwater samples from the Northeastern USA. OER, O_2^- , and H_2O_2 photoproduction rates were also determined for SRFA and SRNOM. Aqueous solutions of these reference materials had OER: O_2^- production ratios that ranged from ~1.5 to 2.0 (Le Roux et al., 2021); the $\sim 2\times$ lower O_2^- photoproduction rates may be because “net” O_2^- photoproduction rates were determined in Le Roux et al. (2021). Irradiated solutions of SRFA and SRNOM amended with superoxide exhibited superoxide decay rates that were much higher than in the dark (Le Roux et al., 2023). Thus it is likely that O_2^- photoproduction rate estimates based on net production in the early stages of irradiation or steady-state approximations using dark decay are underestimates.

Superoxide decay can result in either formation of H_2O_2 or reoxidation to molecular O_2 , depending on available redox-active compounds (Rose, 2012). The abiotic superoxide dismutation reaction plays only a minor role in superoxide decay in metal and DOM-rich coastal waters (Goldstone and Voelker, 2000). Other studies have found Cu, Mn, Fe, and DOM all contribute significantly to O_2^- decay depending on the oceanographic setting (Heller and Croot, 2010a, b, 2011; Heller et al., 2016; Rose and Waite, 2006; Voelker and Sulzberger, 1996; Wuttig et al., 2013a, b). One potential superoxide sink is phenoxy radicals (Le Roux et al., 2021; Zhang and Blough, 2016), albeit the phenolic content in marine DOM is low compared to freshwaters or standard reference materials (Takeda et al., 2013). Using competition kinetics between ascorbic acid and a chemiluminescent reagent for O_2^- , antioxidant activity for O_2^- has been detected in near-surface seawater during the day (King et al., 2016), consistent with a O_2^- sink derived from photochemical and/or photobiological reactions. Even in the absence of light, it was estimated that $\sim 60\%$ of O_2^- loss in the Mauritanian upwelling region was due to reactions with DOM (Heller et al., 2016). Additional sinks have been investigated such as reaction with photoproduced NO. The NO radical is a reactive species most often associated with anthropogenic air pollution, but NO can react with O_2^- at near-diffusion controlled rates to form peroxy nitrite/peroxy nitrous acid ($OONO^-/HOONO$) (Adesina et al., 2018, 2020; Huie and Padmaja, 1993). However, only 0.11%–0.17% of the photoproduced NO radical was predicted to react with O_2^- using coastal seawater, suggesting the reaction is not significant, and likely most NO is lost to the atmosphere (Adesina and Sakugawa, 2021). Thus further work is needed to better understand superoxide sinks, especially in sunlit waters.

Both Powers et al. (2015) and Fujii and Otani (2017) noted decreasing superoxide steady-state concentrations with prolonged irradiation of oligotrophic seawater and solutions with reference materials (e.g., SRFA, SRHA, PLFA). It is unclear if this trend represents a decrease of CDOM source material or the buildup of a transient oxidized reactant pool that increases O_2^- decay rates during irradiation. It is well known that continued irradiation bleaches CDOM, and therefore a decrease in source is likely during hours-long irradiations. However, as previously discussed, King et al. (2016) detected $nmol\ L^{-1}$ concentrations of ascorbic acid-equivalent antioxidants in the surface 25 m during the day, but never at night, supporting the idea that photoproduced transients may be a significant sink for O_2^- . Petasne and Zika (1987) measured H_2O_2 in samples irradiated in the presence and absence of SOD. Since SOD should force a 2:1 stoichiometry between O_2^- and H_2O_2 (Cudd and Fridovich, 1982), this approach allows examination of the relationship between O_2^- and H_2O_2 during irradiation (i.e., $\sim O_2^- = 2 \times H_2O_2$ in the presence of SOD). Based on their SOD experiments, Petasne and Zika (1987) reported that 21%–41% of the photoproduced O_2^- does not lead to H_2O_2 .

Subsequently, Powers and Miller (2016) used the SOD method and measured rates of H_2O_2 photoproduction in a series of samples along a transect from a river to offshore waters. They observed a trend of increasing oxidative O_2^- decay from riverine waters ($\sim 2:1 \text{ O}_2^-:\text{H}_2\text{O}_2$) to offshore waters near the Gulf Stream ($3.4:1 \text{ O}_2^-:\text{H}_2\text{O}_2$) in the SAB, although only a limited number of samples were examined. The wavelength dependence was also determined with and without SOD to generate AQY spectra for O_2^- ($2 \times \text{H}_2\text{O}_2$ with SOD) and H_2O_2 (no SOD) formation (Powers and Miller, 2016). Interestingly, H_2O_2 AQY spectra with added SOD suggested increased efficiency in the UV-B and often in the UV-A relative to those determined without SOD, supporting the idea that photoproduced transients contributed to oxidative superoxide decay in sunlit waters. To further examine the mechanistic relationship between O_2^- and H_2O_2 during irradiation, Arlinghaus et al. (2023) used the SOD method in irradiations of lake water (Georgia, USA) under varied conditions (i.e., changes in pH, buffer, and halides). In contrast to results from coastal and offshore waters, reductive superoxide sinks ($\text{O}_2^-:\text{H}_2\text{O}_2 < 2$) dominated with increasing pH and NaCl concentrations. Even over a relatively short 2 h irradiation, O_2^- photoproduction rates, determined as twice the CDOM-normalized H_2O_2 photoproduction rate in the presence of SOD, decreased for all samples due to a concomitant increase in O_2^- oxidative decay (Arlinghaus et al., 2023). Using SRFA solutions, Ma et al. (2019) suggested that O_2^- electron transfer to DOM may result in a reduced species that can also react with O_2^- to generate H_2O_2 , perhaps partly explaining the Arlinghaus et al. (2023) results. Ma et al. (2020) also examined IHSS materials (e.g., SRNOM, SRFA, SRHA, PLFA) and treated wastewater organic matter, finding that light-induced O_2^- loss did not result in H_2O_2 formation.

Even if the majority of photoproduced superoxide does not lead to H_2O_2 , photoproduction rates of H_2O_2 are significant in the global ocean. Zhu et al. (2022) used temperature-dependent AQY data for H_2O_2 photoproduction (Kieber et al., 2014) with remotely sensed ocean color and temperature to provide an updated estimate of annual H_2O_2 photoproduction in the open ocean, $21.1 \pm 7.5 \text{ Tmol H}_2\text{O}_2 \text{ yr}^{-1}$. This flux is well above those for well-studied carbon photoproducts, including CO ($2.5\text{--}4.2 \text{ Tmol yr}^{-1}$) and low molecular weight carbonyl compounds ($0.11\text{--}4.1 \text{ Tmol yr}^{-1}$). This work improves on the Powers and Miller (2014) global H_2O_2 photoproduction estimate by including depth-integrated rates and using H_2O_2 AQY spectra that were determined for shorter irradiation times when H_2O_2 accumulation was a linear function of photon exposure. Kieber et al. (2014) showed that temperature corrected marine H_2O_2 AQY spectra varied surprisingly little between diverse coastal and open-ocean waters when the condition of reciprocity was met. Additionally, H_2O_2 AQY values increased by ~ 1.8 with a 10°C temperature increase, consistent with its thermal production from O_2^- dismutation. Moreover, Zhu et al. (2022) observed that the marine-average H_2O_2 AQY spectrum computed from all AQY data reported in Kieber et al. (2014) only had an 11% error and was not statistically different from H_2O_2 AQY spectra determined for a diverse sample set including black-water rivers, inshore and offshore waters (Yocis et al., 2000). On the other hand, H_2O_2 AQY values reported for Lake Eire using an unconstrained single data-point AQY spectrum (see Section 11.6 on modeling) varied by a factor of five when evaluated for biweekly samples collected between June and September 2019 (Pandey et al., 2022). These results suggest that large variations in H_2O_2 AQYs are possible but have yet to be evaluated in seawater with high resolution.

Although nonphotochemical biological sources of O_2^- and H_2O_2 are well known (reviewed by [Morris et al., 2022](#)), an intriguing dark abiotic source for O_2^- , H_2O_2 , and the hydroxyl radical to the deep ocean is from water discharged from hydrothermal vents. Very high H_2O_2 concentrations (i.e., $1.1\text{--}1.6\text{ }\mu\text{mol L}^{-1}$ — $10\times$ higher than that found in sunlit surface waters) were measured in samples collected from high- and low-temperature vent plumes ([Shaw et al., 2021](#)). The authors concluded that the source of these ROS is Fe-catalyzed oxidation of sulfide as plume waters admixed with oxygenated bottom waters. The authors calculated an annual H_2O_2 flux of 0.7 Tmol yr^{-1} ([Shaw et al., 2021](#)), making vent systems an important ROS source in the deep sea.

11.5.1.2 Hydroxyl radical

The hydroxyl radical ($\cdot\text{OH}$) is the third step along the four-electron pathway between oxygen and water. Compared to O_2^- and H_2O_2 , $\cdot\text{OH}$ is a far more reactive and powerful oxidant, with rate constants at or near diffusion limits ($\sim 10^8\text{--}10^{10}\text{ L mol}^{-1}\text{ s}^{-1}$) with a variety of inorganic and organic compounds ([Kieber et al., 2003](#); [Gligorovski et al., 2015](#)). Primary abiotic $\cdot\text{OH}$ production mechanisms in natural waters include reactions of reduced metals with H_2O_2 and photochemical reactions involving DOM, nitrate, and nitrite. The kinetics of Fe(II) oxidation are different depending on whether iron is uncomplexed, complexed with DOM (e.g., SRFA) or standard ligands, and if samples are irradiated in freshwater versus seawater ([Miller et al., 2012](#); [Miller et al., 2016](#)). Intriguingly, when inorganic Fe(II) was not complexed at pH 8.2, the thermal reaction with H_2O_2 did not produce $\cdot\text{OH}$, contrary to its well-known production by reaction between Fe(II) and H_2O_2 at low pH ([Miller et al., 2016](#)). The Satilla River, an acidic black water river, with $\sim 10\text{ }\mu\text{mol L}^{-1}$ iron, was studied to investigate the role of photo-Fenton reactions in $\cdot\text{OH}$ photoproduction ([White et al., 2003](#)). In the presence of two strong iron ligands, fluoride and desferrioxamine mesylate, $\cdot\text{OH}$ photoproduction rates decreased by 10% and more than 75%, respectively. Thus even in the highly colored Satilla River, photo-Fenton processes dominated $\cdot\text{OH}$ photoproduction compared to CDOM.

In systems with low iron and nitrate/nitrite concentrations, or with a relatively high CDOM absorbance, CDOM dominates $\cdot\text{OH}$ photoproduction ([Altare and Vione, 2023](#)). It is well known that CDOM photoreactions produce $\cdot\text{OH}$, but reaction mechanisms are not well understood. A modeling study examining the relationships of CDOM (and its spectral slope) and nitrate/nitrite in $\cdot\text{OH}$ production showed that CDOM is the dominant $\cdot\text{OH}$ source in samples with high CDOM and lower spectral slopes (e.g., 0.012 nm^{-1}) ([Altare and Vione, 2023](#)). However, model conditions tested are representative of freshwaters (e.g., 5 mg L^{-1} DOC) but not marine systems. Similarly, $\cdot\text{OH}$ quantum yields were determined for a series of substituted phenols used as model components for the terrigenous CDOM pool and degradation products of lignin and tannins ([Sun et al., 2015](#)). Phenolics with carboxyl or phenolic groups in the para position (e.g., 4-hydroxybenzoic acid) had the highest quantum yields ($\sim 10^{-2}$) for $\cdot\text{OH}$ production. DOC normalized $\cdot\text{OH}$ photoproduction rates decreased from riverine waters in the Everglades to nearshore waters in the Florida Bay, USA ([Timko et al., 2014](#)), but $\cdot\text{OH}$ photoproduction rates normalized to CDOM absorbance were constant throughout this transect. Another study in the Everglades reported positive correlations between $\cdot\text{OH}$ AQYs and CDOM optical properties (e.g., ratio of absorption at 250 to that at 365 nm, spectral slope) ([McKay et al., 2017](#)). In prior work, $\cdot\text{OH}$ steady-state concentrations

were $12 \times 10^{-18} \text{ mol L}^{-1}$ (coastal) and $1.1 \times 10^{-18} \text{ mol L}^{-1}$ (open ocean) during irradiations, and photoproduction rates decreased from 110 to $10 \text{ nmol L}^{-1} \text{ h}^{-1}$ in a transect from coastal to offshore waters, with UV-B radiation and DOM dominating its production (Mopper and Zhou, 1990).

Typically, AQYs for many CDOM photoproducts (e.g., acetaldehyde, COS, CO, DIC, H_2O_2) are highest in the UV-B and decrease exponentially with increasing wavelength. On the other hand, $\cdot\text{OH}$ tends to have the highest AQY values in the UV-B and much lower values in the UV-A and visible that cannot be predicted by a simple exponential function (Bacilieri et al., 2022). Published $\cdot\text{OH}$ quantum yield values from the photolysis of nitrate range from 0.7% to 1.7% at 310 nm (Zepp et al., 1987; Jankowski et al., 1999; Mack and Bolton, 1999), with AQYs increasing with increasing temperature and pH (Chu and Anastasio, 2003; Jankowski et al., 1999). Similarly, AQY values for SRFA solutions were highest between 310 and 320 nm, and lower at both shorter and longer irradiation wavelengths, falling below detection at wavelengths greater than 350 nm (Vaughan and Blough, 1998). The AQYs determined for Chesapeake Bay and Delaware Bay samples were higher than those for SRFA. Work investigating radical photochemistry using terrestrial reference material such as Mississippi River natural organic matter and SRNOM (Bacilieri et al., 2022) or freshwater systems with CDOM sources from Arctic streams and rivers (Page et al., 2014) likely do not extrapolate to marine systems and as such more marine AQY data for $\cdot\text{OH}$ are needed to model its production in marine waters.

In freshwater systems, DOM is often the dominant sink for $\cdot\text{OH}$. Both SRFA and SRHA solutions exhibited second-order rate constants of $\sim 2\text{--}3 \times 10^4 \text{ s}^{-1} (\text{mg CL}^{-1})^{-1}$ when reacted with $\cdot\text{OH}$ generated by γ -radiolysis (Goldstone et al., 2002). The reaction between $\cdot\text{OH}$ and these terrestrial reference materials efficiently produced DIC (0.3 mol DIC per mol $\cdot\text{OH}$), low molecular weight organic acids, and resulted in losses of CDOM absorbance at 300 nm. In seawater, $\cdot\text{OH}$ reacts almost exclusively and irreversibly with bromide (97.7%), while CO_3^{2-} and HCO_3^- ions (1.8%) and DOM (0.2%) are minor competitors (Zafiriou, 1974; Zafiriou et al., 1987). The reaction between $\cdot\text{OH}$ and HCO_3^- or CO_3^{2-} can produce the carbonate radical ($\text{CO}_3^- \cdot$) (Zafiriou, 1974), but $\text{CO}_3^- \cdot$ has not been widely studied in natural systems (Burns et al., 2012) and, to our knowledge, has not been studied in seawater. However, $\text{CO}_3^- \cdot$ reactions may be important in surface seawater because (1) even if only 1.8% of $\cdot\text{OH}$ photoproduction results in the formation of $\text{CO}_3^- \cdot$, these rates may be significant (Kieber et al., 2003); (2) there are probably other routes for $\text{CO}_3^- \cdot$ production such as the reaction of the carbonate system with the peroxy nitrite, ONOO^- , radical (Medinas et al., 2007), photoreactions of metal-carbonate complexes, and reaction of the carbonate system with $^3\text{DOM}^*$ (Canonica et al., 2005); and (3) $\text{CO}_3^- \cdot$ is a selective oxidant reacting with reduced sulfur compounds (e.g., dibenzothiophene, Kieber et al., 2003) to produce sulfoxides (Huang and Mabury, 2000) and aromatic amine derivatives (Larson and Zepp, 1988). Unfortunately, most methods to determine $\text{CO}_3^- \cdot$ have $\mu\text{mol L}^{-1}$ detection limits (Burns et al., 2012), although the presence of carbonate radicals can usually be inferred when observing effects of $\text{HCO}_3^-/\text{CO}_3^{2-}$ on the oxidation of organic compounds by $\cdot\text{OH}$. Along those lines, Timko et al. (2014) estimated carbonate radical formation rates using alkalinity measurements and rate constants in the Shark River Estuary. Carbonate radical production rates were estimated from $\cdot\text{OH}$ production in samples with and without the carbonate system. It is unclear if this approach would work in evaluating $\text{CO}_3^- \cdot$ photochemistry in seawater.

11.5.1.3 Reactive halogen species (RHS)

The reaction between the bromide anion and $\cdot\text{OH}$ yields bromine atoms that can subsequently form reactive species such as BrCl^- , Br_2^- , and BrO^- , although the formation of Br_2^- dominates in seawater (Zafiriou et al., 1987). As noted by Zafiriou (1974), the fates of these halogenated daughter radicals involve reactions with DOM, though later work implied that Br_2^- decay involved the carbonate system (Zafiriou et al., 1987). When SRNOM and algal exudates containing 2.5–7.7 mg CL^{-1} DOC were irradiated, CDOM photobleaching rates increased by 20%–40% from 280 to 400 nm in a sample amended with halides at concentrations present in seawater relative to light controls with no added halides (Grebel et al., 2009). The halide-amended treatments confirmed that photobleaching enhancement was largely due to halides, although γ -radiolysis suggested that 12% of the increased CDOM degradation was also due to $\cdot\text{OH}$. In a study using artificial seawater and coastal seawater samples, halides increased the photodegradation of model compounds (e.g., domoic acid, thioethers) at high $\mu\text{mol L}^{-1}$ concentrations, compared to low ionic-strength controls (Parker and Mitch, 2016). Using γ -radiolysis and additional tests, the authors suggested that $^3\text{DOM}^*$ is also involved in RHS photoproduction. This idea is supported by prior work that used laser flash photolysis (LFP) to generate excited triplet state benzophenone ($^3\text{benzophenone}^*$) in the presence of halides (Jammouli et al., 2009). Halides quenched $^3\text{benzophenone}^*$ and formed several products, likely X_2^- , where $\text{X}=\text{Cl}$, Br , or I , with longer lifetimes than $^3\text{benzophenone}^*$. However, it is unknown whether similar results will be obtained using samples more representative of coastal or open-ocean waters with lower concentrations of DOC ($\sim 0.5\text{--}1\text{ mg C L}^{-1}$, Hansell et al., 2009), domoic acid ($\sim 1\text{--}20\text{ nmol L}^{-1}$, Mafra et al., 2009), and DMS ($\sim 2\text{ nmol L}^{-1}$, Hulswar et al., 2022). While it is well known that RHS are important oxidants in both engineered and natural aquatic systems (Yang and Pignatello, 2017; Zhang and Parker, 2018), the importance of RHS in photochemical DOM cycling in marine systems warrants further investigation.

There is some evidence that RHS reactions with DOM can form new halogenated organic compounds. When artificial seawater solutions of SRNOM and Nordic River natural organic matter were irradiated, the organic bromine and organic iodine content increased significantly providing evidence that photochemical production of RHS leads to subsequent reactions with DOM (Méndez-Díaz et al., 2014). Another study used HRMS to demonstrate the potential production of new bromine- and iodine-containing ions when SRFA was irradiated in solutions of bromide and iodide, respectively (Hao et al., 2017). The photoproduction of organic halogens in marine DOM has yet to be tested, but this process is likely complicated by dehalogenation reactions (Zepp and Ritmiller, 1995). Photochemical dehalogenation can occur through direct photolysis of excited-state organo-halogens or through indirect reactions involving organic halogens and a photoproduced reactive transient (Zepp and Ritmiller, 1995). Thus while DOM may be a dominant sink for RHS in marine systems, dehalogenation reactions, which can occur enzymatically and abiotically, need to be considered to fully understand the role of RHS in DOM cycling.

11.5.1.4 Excited triplet-state DOM ($^3\text{DOM}^*$)

$^3\text{DOM}^*$ (also reported as $^3\text{CDOM}^*$ or excited triplet-state natural organic matter $^3\text{NOM}^*$) reacts with a variety of organic compounds and is the main precursor for $^1\text{O}_2$ in natural waters

(McNeill and Canonica, 2016). In the Everglades, DOC-normalized $^1\text{O}_2$ photoproduction rates decreased by ~13% in the Harney River Estuary and ~56% in the Taylor River Estuary with increasing salinity (Timko et al., 2014). By contrast, DOC-normalized $^3\text{DOM}^*$ photoproduction rates, determined using the energy-transfer probe sorbic acid, did not change along either estuarine salinity transect. Although production rates were unchanged, $^3\text{DOM}^*$ decay constants decreased for all samples at high ionic strength thereby increasing $^3\text{DOM}^*$ steady-state concentrations. Timko et al. (2014) proposed that high ionic strength slowed $^3\text{DOM}^*$ electron-transfer pathways whereas $^3\text{DOM}^*$ energy-transfer pathways were unaffected. In support of this idea, $^3\text{DOM}^*$ rate constants for reaction with sorbic acid were similar and $^1\text{O}_2$ steady-state concentrations ($[^1\text{O}_2]_{ss}$) were similar for irradiated solutions of IHSS materials (SRNOM, Pahokee peat humic acid, and Leonardite humic acid) with DOC concentrations of ~4 mg CL⁻¹, regardless of ionic strength (Parker et al., 2013). However, McKay et al. (2017) noted that there was only either weak or no relationships between salinity and $^3\text{DOM}^*$ or $^1\text{O}_2$ AQYs in samples collected in the Everglades. They also observed a negative correlation between either $^3\text{DOM}^*$ or $^1\text{O}_2$ and the antioxidant capacity that was not seen for $\cdot\text{OH}$. When Sunday et al. (2020) irradiated Seto Inland Sea samples, with DOC ranging from 0.64 to 1.85 mg CL⁻¹, they observed $[^1\text{O}_2]_{ss}$ that differed by nearly an order of magnitude, from ~1 to 8×10^{-14} mol L⁻¹. $[^1\text{O}_2]_{ss}$ was highly correlated to a_{300} ($r^2 = 0.93$), but weakly correlated with DOC ($r^2 = 0.29$), highlighting that samples with similar DOC concentrations can yield very different $[^1\text{O}_2]_{ss}$. Metals can also impact $[^1\text{O}_2]_{ss}$ by affecting concentrations of $^3\text{DOM}^*$. In solutions containing 25–500 nmol L⁻¹ Cu(II), the $^3\text{DOM}^*$ and 2,4,6-trimethylphenol rate constant markedly decreased during irradiation as $^3\text{DOM}^*$ was quenched by photochemically produced Cu(I) (Pan et al., 2018). Taken as a whole, more work is needed to obtain a mechanistic understanding of both $^3\text{DOM}^*$ and $^1\text{O}_2$ photoreactivity and decay pathways in marine waters.

One way to potentially gain a better mechanistic understanding of excited-state species formed by photochemistry in marine systems is with LFP. As mentioned before, LFP has been used to examine the formation of RHS in seawater (Zafiriou et al., 1987) and in a model system (Jammouli et al., 2009). During LFP, UV excitation is produced with a nanosecond pulsed laser and visible to near-infrared absorption and/or emission bands are monitored (Cottrell et al., 2014; Wang et al., 2007). For instance, by minimizing multiphoton effects, hydrated electron quantum yields were determined using LFP with excitation at 308 nm and absorption at 633 nm for aqueous solutions of standard fulvic and humic acids (Wang et al., 2007). LFP with time-resolved $^1\text{O}_2$ phosphorescence monitoring was used to study $^1\text{O}_2$ directly without the need of a probe molecule (Appiani et al., 2017; Erickson et al., 2018). Again, studies in seawater are less common, but work characterizing Cu ligands also evaluated the production of reactive transients from marine samples using LFP (Cottrell et al., 2014). Coastal Pacific samples generated three reactive transients consistent with the solvated electron, a short-lived triplet excited state (lifetime of 1.1 μs), and a third longer-lived transient (lifetime of 9.9 ms). Intriguingly, BATS surface seawater also generated the solvated electron (lifetime of 3.8 μs) and the longer-lived transient (lifetime of 22.6 ms) similar to that observed in the coastal Pacific samples (Cottrell et al., 2014). The depth profile at BATS revealed that the lifetimes and absorbance of the other transients with lifetimes up to 3.5 μs were highest in samples from the surface and the chlorophyll maximum, and lowest in samples from the oxygen minimum zone. The solvated electron

was not generated at depths below 750 m whereas the long lived transient with average lifetime of 15.5 ms did not vary with depth (Cottrell et al., 2014).

11.5.2 Particles, photoflocculation, and photodissolution

Sunlight interacts not only with components of the dissolved phase, but also with particulate matter, and this interaction can result in photochemical transformations within or on the surface of living or nonliving POM or with the organic matter coating particles. Compared to DOC, scant research has been conducted on marine POM photochemistry largely because most of the organic matter in the open oceans is dissolved (POC is typically <2% of TOC); studies have focused on lacustrine environments and marine studies have been restricted to shallow nearshore, high-sediment load environments including salt marshes and estuaries; no work has been conducted to date in offshore open-ocean environments. Nearly all studies involve irradiating sediment suspensions, although a few studies focused on algal detrital matter, but none of these studies quantified the particle light field, which is an important component of any photochemical study. The photochemistry of POM was reviewed in detail in Mopper et al. (2015) and Hu et al. (2022a). The basic finding summarized in these reviews and confirmed in several other studies (Avery et al., 2017; Harfmann et al., 2021; Schiebel et al., 2015; Petit et al., 2015) is that organic matter and nutrients are “released” into the dissolved phase, including metals, toxins, DOC, DON, DIN, DOP, and DIP, but the mechanisms involved are lacking. The word released is in quotes because, although this is the term used in the literature, it is not clear whether particulate organic and inorganic matter are simply dissolved during the exposure of POM to a solar simulator or sunlight or new, water-soluble compounds are produced from POM photochemical transformations.

One mostly unrecognized but important finding is that photochemical AQYs may be quite different in the particulate phase compared to the dissolved phase. Song et al. (2015) exposed to sunlight unfiltered (with potassium cyanide added) and 0.2 μm -filtered water collected at multiple salinities and seasons along the main axis of the Delaware Estuary. They observed that AQYs for the photochemical production of CO from DOM were higher compared to POC AQYs. However, POC AQYs extended well into the visible while CO photochemical production from DOM was mainly confined to the UV. Using AQY data, Song et al. (2015) modeled rates in the estuary and determined that CO photoproduction from DOM dominated in surface waters with high UV exposure, but POM photogenerated CO dominated in deeper waters due to the rapid attenuation of UV and deeper penetration of visible solar radiation.

The particulate phase is also an important source of ROS, including the OH radical, superoxide, and singlet oxygen (Appiani and McNeill, 2015; Petit et al., 2015). However, given the increase in plastics, black carbon, and other natural and anthropogenic materials entering in the oceans and the high particle content of many rivers and estuaries and other shallow-water environments, particulate-phase photochemical processes should be considered, especially if there is no corresponding dissolved phase photochemical reaction that occurs at an appreciable rate. Two important challenges associated with POM photochemical studies are quantifying the light field (Song et al., 2015) and using appropriate probes to study POM-surface or interstitial reactions.

11.5.3 VOC photoproduction

Marine volatile organic compounds (VOC) are a minor component of DOM in the oceans, mainly produced through biological and/or photochemical processes. They are, nonetheless, important because the oceans are the main source of several VOC to the atmosphere wherein they are chemically reactive and a major source of secondary organic aerosol. Brüggemann et al. (2018) estimate the annual photochemically generated marine VOC annual emissions to range between 23 and 92 Tg C, and gas-phase photochemical oxidation products generated from the photolysis of marine-derived VOC potentially contribute 60% of the secondary organic aerosol mass produced over the remote oceans. A detailed discussion of marine VOC sources and sinks is given in Chapter 12 and will not be discussed here. Instead, we focus on photochemical processes that form VOC but only in the surface mixed layer, since sea-surface microlayer VOC photochemistry is discussed in detail in Section 11.5.5.

Multiple VOC are photochemically produced in the oceans across several compound classes including low molecular weight (one to three carbon atoms, C1–C3) carbonyl compounds, alkyl halides, alkyl nitrates, and hydrocarbons (e.g., acetaldehyde, glyoxal, acetone, ethene). As reviewed in Carpenter and Nightingale (2015), most work examining the photoproduction of VOC in the oceans has centered on the sea-surface microlayer, but a few studies focused on water-column VOC photoproduction. Of note, Zhu and Kieber (2018, 2019) determined wavelength- and temperature-dependent AQYs for the photochemical formation of acetaldehyde, glyoxal, and methylglyoxal in seawater collected from the subarctic Pacific and northwestern Atlantic Oceans. Using this dataset, they calculated a global surface mixed layer photochemical production of ~49 and 20 Tg Cyr⁻¹ for acetaldehyde and glyoxal, respectively, which is comparable to the global photochemical production estimate for CO of ~40–50 Tg Cyr⁻¹ (Fichot and Miller, 2010; Stubbins et al., 2006; Zafiriou et al., 2003). Zhu and Kieber (2019) estimated that photochemistry was responsible for 7%–23% of the total acetaldehyde production in the coastal waters and 26%–53% of its production in the oligotrophic waters of the northwest Atlantic Ocean.

Significant photoproduction rates in the nmol L⁻¹ h⁻¹ range have been reported for formaldehyde and acetone in estuarine and coastal waters, but open-ocean and global photochemical production estimates are still mostly lacking (Mopper et al., 2015). Reported photoproduction rates of hydrocarbons (e.g., methane, ethene) are in the pmol L⁻¹ h⁻¹ range (Li et al., 2020), consistent with findings from earlier studies (Mopper et al., 2015). Photochemistry has also been postulated to explain the “methane paradox,” the observation that surface seawater is supersaturated with respect to methane, although it should be noted that there are other surface sources of methane in aerobic seawater, such as degradation of phosphonates (Karl et al., 2008; Repeta et al., 2016) and in situ production during phytoplankton blooms (Damm et al., 2008). Li et al. (2020) measured CH₄ photoproduction rates in coastal to offshore waters and estimated an annual production rate in the global ocean of 118 Gg Cyr⁻¹, amounting to 20%–60% of the surface ocean methane efflux. Although photochemistry may play a role in the “methane paradox,” CH₄ photoproduction rates are more than 500 times lower than corresponding CO photoproduction rates. Thus, in terms of the photochemical cycling of DOC, the photoproduction of methane in the surface ocean likely plays a minor role. Furthermore, while methanol and ethanol are both important VOC in surface seawater, to date there is no evidence that they are photochemically produced in seawater.

11.5.4 Fate of compounds of concern and plastics

The role of DOM as a photosensitizer in the photochemical degradation and transformation of anthropogenic contaminants in aquatic environments is an active field and the subject of several reviews (Boreen et al., 2003; Pelletier et al., 2006; Remucal, 2014; Wilkinson et al., 2017; Yan and Song, 2014). Most work has focused on contaminant fate in freshwater or model systems (e.g., pure water with standard reference materials). In this section, we focus on work evaluating the role, or lack thereof, of photochemistry in the degradation and transformation of compounds of concern in seawater. We provide an update on harmful algal bloom (HAB) toxins (discussed in Mopper et al., 2015) and focus on the broad categories of oil spill contaminants, poly- and perfluoroalkyl substances (PFAS), and plastics.

11.5.4.1 Toxins

The photochemistry of the marine HAB toxins, domoic acid, which causes amnesic shellfish poisoning, and brevetoxins, which cause neurotoxic shellfish poisoning, was reviewed in Mopper et al. (2015). But of course, HAB species and the toxins they produce in both freshwater and seawater are diverse. A review of HAB data from 1990 to 2019 highlights that marine HAB problems in the US are rapidly increasing over time, and reoccurring blooms have become extensive along all US coastlines (Anderson et al., 2021). Most HABs are spreading into new regions beyond where they were initially detected, a process often linked to global warming but also due to increased monitoring and awareness of HABs. The photochemistry of a few freshwater (e.g., anatoxins, cylindrospermopsins, and microcystins) and two marine HAB toxins (i.e., domoic acids and nodularins) was reviewed, and while some toxins absorb solar UV radiation, indirect photoreactions are primarily responsible for their photodegradation (Kurtz et al., 2021). Indirect photochemistry is important in the photolysis of domoic acid via reaction with singlet oxygen, forming products that are not toxic as determined by the enzyme-linked immunosorbent assay (Jaramillo et al., 2020). The photochemical fate of the primarily freshwater HAB toxins microcystin and cylindrospermopsin was modeled under climate change scenarios (Vione and Rosario-Ortiz, 2021), but only freshwater systems were considered. While cyanobacterial toxins have typically been associated with freshwater systems, if they are produced in the land-sea interface, they can contaminate coastal systems. For example, freshwater microcystin from nutrient-rich rivers was linked to the deaths of marine mammals in the Monterey Bay National Marine Sanctuary, California, USA (Miller et al., 2010). Thus it may become increasingly important to study the photochemical fate and transformation of freshwater HAB toxins in estuarine and coastal systems. Seawater halides increased the photodegradation of domoic acid (Parker and Mitch, 2016), but environmentally relevant concentrations still need to be tested. Furthermore, photodegradation studies often only determine the loss of the toxin while photochemically produced products are rarely considered.

Previous work on the photochemistry of brevetoxin PbTx-2, a neurotoxin produced by the dinoflagellate *Karenia brevis*, determined photodegradation rate constants of 0.20 h^{-1} in coastal seawater (Kieber et al., 2010). In a subsequent study, the photochemical release of PbTx-2 was tested for coastal marine sediments from Florida that had been previously impacted by *K. brevis* blooms (Avery et al., 2017). While the depth of UV penetration may be limited to near surface waters, this work revealed that visible radiation (400–700 nm) is also

capable of releasing PbTx-2 from sediments. Concentrations of PbTx-2 released from resuspended sediments ranged from 1.3 to 36 pmol L⁻¹, approximately 0.5%–13% of the toxin present during a bloom (Avery et al., 2017). In addition to impacting marine sediments, brevetoxins can be transported into the atmosphere via sea salt aerosols and cause respiratory problems in humans. Sem et al. (2022) tested the atmospheric oxidation of brevetoxins in sea salt aerosols in the presence and absence of sunlight and ozone using an outdoor photochemical chamber. While brevetoxins in sea salt aerosols are stable under dark conditions, they decreased by ~80% between 8 and 11 am local time.

Kurtz (2021) examined the photodegradation of saxitoxin, which causes paralytic shellfish poisoning, gonyautoxin-2 and -3, and n-sulfocarbamoyl-gonyautoxin-1 and -2. None of these toxins degraded via direct photolysis, but saxitoxin and gonyautoxins photodegraded through a photosensitized pathway. Pan et al. (2020) examined the photochemical fate of diarrhetic shellfish poisoning toxins, okadaic acid and dinophysistoxin-1, in coastal seawater; under natural solar irradiation both toxins degraded slowly, with ~90% loss in 20 days. Ternon et al. (2022) examined the fate of toxic polyketides, the ovatoxin and the liguriatoxin family of toxins, produced by the HAB-forming benthic dinoflagellate *Ostreopsis cf. ovata*, which forms summer-time blooms in the Mediterranean Sea along the intertidal zone. These blooms are also a health risk to local communities due to their atmospheric input as part of seasalt aerosols. The toxins were readily degraded by microbes in the dark, and when samples were exposed to sunlight over a period of several days, the ovatoxins and liguriatoxins photodegraded, forming several new compounds as determined by ultrahigh performance liquid chromatography (UHPLC) with detection by HRMS (Ternon et al., 2022); the structure and toxicity of these products were not examined beyond untargeted metabolomics analysis to determine features lost or produced through microbial or photochemical pathways.

In general, the photochemical stability and toxicity of photoproducts produced for the photolysis of marine toxins are not known. Since most HABs occur in coastal waters, it is also possible that surface photochemistry of toxins on living or nonliving particulate matter will be important. Given the importance of marine toxins, it is surprising that toxin photochemistry has not been a research priority, as nearly all efforts have focused instead on toxin monitoring, predicting HAB events, and sensor development for HAB toxins.

11.5.4.2 Oil

For decades, oil spills have been studied because even if they are episodic, they cause major threats to environmental health. Reviews and perspectives have highlighted what we have learned about the photochemical weathering of oil (Aeppli, 2022; Farrington et al., 2021; Ward and Overton, 2020). As highlighted in these reviews, sunlight can rapidly change the physical and chemical properties of oil floating on the surface ocean. Therefore the photochemical oxidation of oil needs to be considered in oil spill fate and transport models, but specific mechanisms are still poorly understood (Farrington et al., 2021; Ward and Overton, 2020). Aeppli et al. (2022) summarized work published between 2019 and 2021 aimed at better understanding oil photochemical oxidation mechanisms and characterizing photochemical products, particularly by FT-ICR MS. Analyses conducted to characterize oil photochemical products vary widely, as summarized in a review of the techniques to study crude and weathered oil (Wise et al., 2022). These methods include targeted analyses of polycyclic aromatic hydrocarbons

(PAHs), hopanes, and steranes and nontargeted analyses using two-dimensional gas chromatography (GC), pyrolysis GC with mass spectroscopy (MS), GC with tandem MS, and HRMS. In general, it is nearly impossible to compare studies because of the variety of oil types (e.g., light vs. heavy crude), difference in additives (e.g., dispersants), and differences in experimental and irradiation conditions. Most studies do not determine photon doses or use actinometry, which again limits our understanding of oil photochemical transformations. In fact, only one study quantified DOC photoproduction AQYs from oil with careful laboratory irradiations meeting reciprocity considerations by irradiating samples at four different photon doses (Freeman and Ward, 2022). Here we summarize laboratory work not covered in prior reviews, though the reader is reminded that more quantitative photochemical experiments (e.g., AQY determinations) are required to better understand the fate of oil in the sea.

To better understand the photochemical transformation of insoluble oil compounds to soluble products, Freeman and Ward (2022) used UV and visible light emitting diode (LED) irradiations and measurements of DOC in water below oil films to determine the wavelength and photon-dose dependence of this process. The DOC photoproduction AQYs generated in this work were used along with a mass balance approach to determine that 3%–17% of the Deepwater Horizon surface oil was susceptible to photodissolution. DOC measurements and ESI-FT-ICR MS were used to evaluate this process over timescales from 6 to 120 h sunlight exposure, and in agreement with earlier work (Zito et al., 2020), water-soluble components were enriched in oxygen, nitrogen, and sulfur (Chen et al., 2022). Another study used UHPLC with ESI-Orbitrap MS detection, EEM-PARAFAC, and targeted PAHs analyses to understand changes in crude oil and diesel added to artificial seawater during 1- to 10-day irradiation experiments at 12°C to simulate high-latitude environments (Harsha et al., 2023). In addition to oxidation products observed by HRMS, unique EEM-PARAFAC signatures were observed and two oxygenated PAHs, phenanthrenequinone and 1,4-antraquinone, were identified. As the authors point out, photoproducts of oxygenated PAHs are typically missed by traditional total petroleum hydrocarbon analysis (Harsha et al., 2023), and therefore they should be incorporated into routine analysis used to track oil spill influences and weathering. While ESI-FT-ICR MS is suitable for evaluating oil photooxidation products like carboxylic acids, neutral nonpolar molecules, which are highly abundant in oil, will not be detected using this technique. Roman-Hubers et al. (2022) conducted mesocosm experiments in which oil slicks on top of natural seawater were exposed to sunlight for 8 days. They used atmospheric pressure photoionization coupled with ion mobility spectrometry-mass spectrometry to show that irradiation increased ketones and alcohols, and spectra were abundant in features containing oxygen and sulfur in the mass-to-charge ratio between 150 and 350. In a similar mesocosm experiment, Aeppli et al. (2022) observed results consistent with Roman-Hubers et al. (2022) after 11 days of sunlight exposure, including linear increases in oxygen and carbonyl content as well as increases in oil viscosity. The effectiveness of the dispersants Corexit EC9500A and EC9500B was also tested throughout these exposures. When the oxygen content increased to 3%, dispersant effectiveness decreased to ~40% compared to ~80% effectiveness prior to solar exposure (Aeppli et al., 2022).

The bioavailability of neutral and ionized oil photoproducts was evaluated using biomimetic extraction, a test that assumes that components extracted using solid-phase microextraction fibers coated with polydimethylsiloxane are representative of the water-soluble components that would react with target lipids (Roman-Hubers et al., 2022).

Calculated toxicity units via this method increased twofold for nonirradiated samples and fourfold for irradiated samples over 8 days, which was mostly due to ionized components. In another study, biomimetic extraction also showed increased toxicity for water below irradiated oil, which agreed with microbial (King et al., 2011) and copepod toxicity tests (Katz et al., 2022). While toxic water-soluble photoproducts are likely diluted and pose lower risk in situ, Chen et al. (2022) found the highest toxicity per unit carbon to bioluminescent bacteria during the early stages of irradiation, peaking at ~6 h. For weathered oil, DOM leached during an irradiation may be more biolabile and stimulate more microbial activity than DOM leached from nonirradiated oil. For example, when highly weathered sand patties (i.e., oil-laden sand) collected on the beach in the Gulf of Mexico in 2014 were exposed to simulated sunlight in seawater, the released DOM enhanced microbial respiration (Harriman et al., 2017). Thus the inhibitory effects, or lack thereof, of oil photoproducts on marine organisms will depend on exposure history and relative rates of abiotic and biological transformations.

11.5.4.3 Poly- and perfluoroalkyl substances (PFAS)

PFAS are a class of substances that have been used widely in commercial and industrial applications since the 1940s. PFAS are generally resistant to degradation in most natural settings, have high water solubilities, and are ubiquitous in the global ocean which may serve as a sink for these anthropogenic chemicals (Yamashita et al., 2008). Vertical profiles of perfluorooctanesulfonate and perfluorooctanoate (PFOA) concentrations were consistent with global circulation patterns, indicating that these chemically and biologically unreactive chemicals may serve as chemical tracers to study major oceanic currents (Yamashita et al., 2008). Perfluorooctanesulfonate and PFOA concentrations ranged from 9 to 73 pg L^{-1} and 52 to 440 pg L^{-1} , respectively, in Mid and North Atlantic surface waters and were much lower (~1–10 pg L^{-1}) in the surface waters of the South Pacific and Indian Oceans (Yamashita et al., 2008). Total concentrations of 21 PFAS measured on a circumnavigation cruise in the Atlantic, Indian, and Pacific Oceans ranged from 130 to 11,000 pg L^{-1} in the deep chlorophyll maximum (González-Gaya et al., 2019).

In addition to the extreme difficulty in breaking carbon-fluorine bonds, most PFAS do not absorb sunlight, even UV-B radiation, and therefore do not participate in direct photoreactions but secondary reactions are possible. One study observed the photochemical degradation of PFOA in the presence of Fe(III) during a 28-day rooftop exposure experiment (Liu et al., 2013). Even though samples were irradiated in borosilicate tubes with ~80% transmission of UV-A, ~98% of the PFOA degraded and the defluorination extent was ~13%. However, mg L^{-1} concentrations of PFOA and Fe(III) used in this study were well above concentrations found in seawater. In a similar study, indirect photodegradation of PFOA was tested in Baltic Sea seawater and artificial samples containing reference Nordic Aquatic Fulvic Acid (15 mg CL^{-1} and pH 4.4), Fe(III) (2.8 mg L^{-1} and pH 3.9), or nitrate (1 mg L^{-1} and pH 5.9) and amended with 100 ng L^{-1} PFOA (Vaalgamaa et al., 2011). Even though PFOA concentrations in this work are still three to four orders of magnitude higher than those found in coastal and open-ocean seawater and self-shading and high Fe were an issue, PFOA did not degrade during 66 and 165 h solar simulator irradiations, albeit losses were observed when samples were exposed to a Hg lamp after 48 h due to exposure to radiation $\ll 290\text{ nm}$ (Vaalgamaa et al., 2011). Javad et al. (2020) studied the reaction of PFOA with superoxide. The PFOA did not degrade after a 24 h incubation indicating that it was not reactive toward

this ROS. These studies suggest that PFAS and PFOA will not degrade in seawater when exposed to natural sunlight, but the photochemical stability needs to be tested under environmentally relevant conditions and at ambient pg L^{-1} concentrations.

While the molecular diversity of PFAS is admittedly much smaller than DOM and other anthropogenic compounds (e.g., plastics), various PFAS chemicals will indeed have different photochemical reactivity and environmental persistence. For example, the PFOA substitute GenX, or hexafluoropropylene oxide dimer acid, only degraded by 5% using common advanced oxidation processes such as UV/persulfate, whereas PFOA degraded by 27% (Bao et al., 2018). Though these experiments are not representative of reactions in natural water systems, they are important for understanding which chemicals are likely to be missed using standard remediation.

11.5.4.4 Plastics

Plastics are anthropogenic, ultrahigh molecular weight organic polymers first produced at an industrial scale in the 1950s (Geyer et al., 2017). Since that time, plastics production has accelerated and plastics have accumulated to become a globally significant pool of organic carbon (Stubbins et al., 2021). Plastic pollution in the ocean has been known for some time (Buchanan, 1971; Carpenter and Smith, 1972), but the magnitude of the problem has only now been documented in detail (e.g., Eriksen et al., 2023). The mass of microplastics floating at or near the sea surface is estimated to be 93–236 thousand metric tons (Eriksen et al., 2014; van Sebille et al., 2015) or 0.07–0.20 Tg plastic carbon (Stubbins et al., 2021). In surface waters of the open-ocean gyres, buoyant polyethylene (PE) and polypropylene (PP) dominate particle counts, with additional buoyant (e.g., expanded polystyrene; EPS) and easily suspended (e.g., fibers) plastics found in coastal surface waters (Law, 2017). Plastics carry other “passenger” organic molecules (e.g., additives and other lower molecular weight organics sorbed to the plastics). Once in the ocean, these passenger organic molecules can desorb off plastics into the dissolved phase; leachable organic compounds include additives such as plasticizers (e.g., phthalates), colorants, and flame retardants, plus chemicals picked up during the plastics’ environmental lifetime, such as organic pollutants and natural organic matter (Gewert et al., 2015). If leached, these organics enter the local DOC pool. The common plastics found in ocean surface waters (PP, PE, EPS) are insoluble in water (Wypych, 2012a, b, c). Therefore, it is likely that the first flush of DOC released from uncleaned, postconsumer and standard plastics incubated in the dark (Romera-Castillo et al., 2018) is due to the release of passenger molecules or monomers and not polymer dissolution. However, chemical degradation can generate DOM directly from plastic polymers.

The main mechanism for the chemical breakdown of plastics in natural waters is photodegradation by sunlight (Gewert et al., 2015; Hakkarainen and Albertsson, 2004). Accordingly, the major identified pathway for DOM production from plastics is via the photodissolution of plastic polymers in sunlight (Romera-Castillo et al., 2018; Ward et al., 2019; Zhu et al., 2020a). Photodegradation reduces polymer molecular weight through scission reactions (Gewert et al., 2015), forms novel nonoligomer structures through cross-linking reactions (Tolinski, 2009), oxidizes the polymer hydrocarbons, and produces oxidized products, such as CO , CO_2 , and a suite of low molecular weight, soluble organic compounds (Ranby and Lucki, 1980; Gewert et al., 2015; Stubbins et al., 2023; Ward et al., 2019) some of which are consumed by microbes (Eyheraguibel et al., 2017; Hakkarainen and Albertsson,

2004; Walsh et al., 2022). In the ocean, sunlight can also degrade floating plastics to release ethylene and the greenhouse gas methane (Royer et al., 2018).

Polymer chemistry influences the photoreactivity of plastics. Here we focus on the buoyant plastics, PE, PP, and EPS, but will also consider nonexpanded polystyrene, PS, which has a density greater than seawater (Stubbins et al., 2021). EPS is the most photoreactive of these plastics in natural sunlight due to the aromatic rings in the polymer structure, while PP and PE are alkanes that lack moieties in the pure polymer that absorb solar radiation (Andrady et al., 2022; Gewert et al., 2015; Stubbins et al., 2021). As such, PE and PP should not absorb natural sunlight and be photoreactive. However, plastic polymers can include chromophoric oxygen-containing functional groups (e.g., carbonyl groups) formed during thermal processing or prior weathering (Gewert et al., 2015). They can also carry photosensitizing passenger chemicals, such as PAHs (Gewert et al., 2015), and be coated with biofilms (Zettler et al., 2013). Benzoate and acetophenone can both be produced from PS during photodegradation (Bianco et al., 2020) and benzoate can be toxic to higher organisms (Olofinnade et al., 2021). These aromatic photoproducts can undergo photodegradation, including via radical (e.g., $\cdot\text{OH}$) mediated reactions (Fabbri et al., 2023).

Additives modify the physical and chemical properties of plastics, including their photoreactivity (e.g., Andrady et al., 2022), and additives are estimated to account for 7% of the total mass of plastics produced in 2015 (Geyer et al., 2017). UV stabilizers are added to intentionally alter plastics' photoreactivity, specifically to increase resilience to UV weathering during outdoor use and are most commonly free-radical quenchers or UV absorbers (see Andrady et al., 2022). Although the efficacy of UV stabilizers to increase the lifetime of products in use is well established, whether UV stabilizers also increase the longevity of plastics in sunlit surface waters remains untested (Andrady et al., 2022). Other additives are not designed to intentionally alter a plastics' photoreactivity. However, they appear to do so. Opacifiers, such as the inorganic compounds titanium dioxide and calcium carbonate, are added to make plastics opaque but with ramifications for a plastic's optical properties. These additives are reported to increase the photodegradation of PE films (e.g., consumer grocery bags) compared to pure PE films (Walsh et al., 2021), while brominated organic flame retardants can accelerate the photooxidation of PS (Khaled et al., 2018). Thus, when possible, researchers should determine the inorganic and organic additive content in plastics irradiated to assess their impacts on plastic degradation mechanisms, rates, and product spectra.

Photochemistry also impacts the release of additives and their subsequent fate in natural waters. For example, UV exposure of PE can increase the leaching of toxic bisphenol A and phthalic acid esters (Dhavamani et al., 2022), the latter are a class of plasticizers toxic to humans and aquatic organisms (Huang et al., 2021). Once released to surface waters, phthalic acid esters are photoreactive, although their rates of photodegradation in aqueous solution are considerably slower than biodegradation under the same conditions leading to suggestions that sunlight is only a modest sink for phthalic acid esters in surface waters (Staples et al., 1997). For bisphenol A, direct photolysis rates under natural sunlight are also modest although CDOM can increase its photolysis such that photolysis rates may rival biodegradation rates in some surface waters (Chin et al., 2004). Thus the interactions of light and additives are manifold, with additives modifying the photoreactivity of polymers, and sunlight both increasing the leaching of additives from plastics and photolyzing additives once dissolved in surface waters.

Photodegradation of many organic molecules, including DOC, follows first-order kinetics, with rates slowing with increasing exposure (Spencer et al., 2009). By contrast, plastics photodegradation and DOC release may accelerate (Hakkarainen and Albertsson, 2004; Zhu et al., 2020a), potentially leading to increasingly efficient removal the longer plastics reside in sunlit environments. The acceleration in rates may result from both the accumulation of photosensitizing oxygen-containing moieties, particularly carbonyl and hydroperoxide groups (Hakkarainen and Albertsson, 2004; Kamal, 1967), and an increase in surface area-to-volume ratio as plastics photochemically fragment (Zhu et al., 2020a). If the photochemical dissolution of plastics to DOC is modeled using acceleratory kinetics, results suggest that 2–5 mm pieces of EPS, PP, and PE can be completely dissolved at the sea surface within 0.3, 0.3, and 0.5 yr, substantially shorter than would be suggested by linear kinetics (1.8 yr for EPS, 2.6 yr for PP, and 11–50 yr for PE; Zhu et al., 2020a). Even these longer estimates suggest all microplastics at sea would dissolve within decades if inputs ceased. Further, the rapid loss of EPS is consistent with the low mass of EPS found in the gyres, and the rapid loss of PP relative to PE could explain why the ratio of PE:PP increases from coastal waters outward to the subtropical gyres (Arthur et al., 2009).

If the mass of all marine plastic particles (0.07–0.20 Tg C; Stubbins et al., 2021) dissolved to DOC, it would be a tiny fraction of total ocean DOC stocks (662,000 Tg C; see Chapter 17). However, since plastic-derived DOM is produced in sunlit surface waters, the addition of plastic DOM could impact upper ocean ecology and biogeochemical function. Photoproduced plastic-derived DOM contains transphilic products such as carboxylic acids (Kamal, 1967) that may fractionate into the marine microlayer and impact trace gas and aerosol exchange with the atmosphere, surface ocean ecology, and surface ocean biogeochemistry (Boldrini et al., 2021; Galgani and Loiselle, 2021). Plastic photolysis also produces VOC that may impact atmospheric chemical cycles. In most cases, photoproduced, plastic-derived DOM is biolabile and utilized by bacteria causing no obvious adverse effects (Romera-Castillo et al., 2018; Zhu et al., 2020a; Mazzotta et al., 2022; Walsh et al., 2022), although Romera-Castillo et al. (2018) initially observed more microbial activity from DOC leached from plastics in the dark. In a subsequent study, DOC leached from aged plastics found on the beach was up to two orders of magnitude higher than that leached from virgin plastics when exposed to simulated sunlight (Romera-Castillo et al., 2022). The photooxidation of plastics' surfaces can also make the plastic more biolabile, allowing microbes to access what was once polymer carbon (Goudriaan et al., 2023), in a process analogous to the photopriming of refractory DOC biolability (Kieber et al., 1989). Dissolved photoproducts can also inhibit microbes. Photoproducts from one sample of PE inhibited microbial growth (Zhu et al., 2020a), and leachates generated from high-density PE grocery bags and polyvinylchloride matting impaired the photosynthetic capacity and growth of the globally abundant phytoplankton, *Prochlorococcus* (Tetu et al., 2019). Thus some plastic leachates appear to be toxic to both bacteria and phytoplankton (Focardi et al., 2022; Wang et al., 2021a, b), so their impacts on marine microbial ecology and carbon biogeochemistry warrant further investigation.

Although the estimates mentioned before provide insight into the potential photochemical lifetimes of plastics at sea, these rates will be modified by environmental conditions, such as photon exposure, pH, temperature, and biofilm formation. Photon exposures will decrease exponentially with depth in the water column, especially UV, which will affect plastics that are mixed downward in the water column. Large buoyant plastics >1 mm in diameter are

likely to remain at the sea surface under calm conditions but become mixed to depth by high turbulence, while smaller buoyant microplastics and nanoplastics are increasingly likely to be entrained into deeper, darker waters as their size decreases (Enders et al., 2015). Biofouling can shield microplastics from sunlight (Nelson et al., 2021). Thus photodegradation rates in open-ocean waters may be slower than predicted based on laboratory studies without turbulence or biofouling.

Studies examining plastic photodegradation kinetics were generally conducted under near-environmental conditions in terms of temperature, wetness (i.e., they were floating on either fresh or saline water), and light exposure. However, there is a wealth of knowledge in the material science literature gained from experiments under different conditions. Some of this literature is noted later as it provides insight into how plastic degradation varies with environmental conditions (e.g., UV photon exposure or temperature) and whether accelerated weathering rates can be used to estimate field rates.

Photochemical oxidation rates of plastics increase with temperature, with the degree of temperature sensitivity varying by polymer. Activation energies calculated using Arrhenius plots of empirical data (carbonyl production measured by Fourier Transform Infrared Spectroscopy) from photodegradation experiments at fixed photon exposures were $\sim 74 \text{ kJ mol}^{-1}$ for linear low-density PE (Therias et al., 2021), $86 \pm 28 \text{ kJ mol}^{-1}$ for high-density PE (Fairbrother et al., 2019), and $29\text{--}54 \text{ kJ mol}^{-1}$ for PP films (Audouin et al., 1998). For PP, the activation energy determined between 40°C and 55°C was lower compared to that determined between 55°C and 70°C , indicating that PP photochemical oxidation kinetics do not obey the Arrhenius equation (Audouin et al., 1998). These irradiation studies determined activation energies at temperature $>30^\circ\text{C}$ and most were $>40^\circ\text{C}$. As the apparent activation energies of photooxidation can vary with temperature for a given polymer, it is unclear if the temperature sensitivities determined at these higher temperatures can be extrapolated to lower temperatures in the oceans. An added uncertainty is that temperature sensitivities of different photoreactions can vary within the same plastic polymer. For instance, photochemical oxidation of high-density PE, quantified as an increase in carbonyl groups in the polymer, was more temperature sensitive (activation energy: $86 \pm 28 \text{ kJ mol}^{-1}$) than changes in polymer physical properties, such as elongation at break and crystallinity (activation energy: $30\text{--}33 \text{ kJ mol}^{-1}$; Fairbrother et al., 2019). Variations in temperature sensitivity observed for different polymers, for different reactions within the same polymer, and across different temperature ranges indicate that the temperature sensitivity of reactions should be determined directly for polymers and reactions of interest, and under the range of environmental conditions of interest (e.g., in water across relevant temperature ranges) to better model rates at sea.

Since all plastics will be exposed to photon exposures that will vary with depth in the water column, latitude, season, cloud cover, and time of day, it is important to consider photon-exposure-dependent kinetics for plastic photodegradation. Although a literature search found no studies of reciprocity for plastic photodegradation in aqueous media, reciprocity is not observed for various photodegradation reactions of PP and PE in air with the Schwarzschild p-coefficient (a measure of reciprocity, where 1 = reciprocity) varying from ~ 0.5 for some degradation metrics (e.g., the elastic modulus for PE) but exceeding 1 for others (e.g., the chemical oxidation of PE quantified as carbonyl formation; Fairbrother et al., 2019). Further, if photon exposures were increased sufficiently above ambient levels in accelerated

weathering experiments, additive-free linear low-density PE photooxidation stopped (Therias et al., 2021). The fact that reciprocity is not met in these studies, and that different measures of photodegradation within a single experiment using the same plastics can show differing degrees of reciprocity argues that photon-exposure-dependent kinetics should be determined for the various polymers and photoreactions of interest in ocean waters. Accelerated weathering experiments using long photon exposures and/or high temperatures may not provide rates that can be applied in field settings and may even alter the predominance of different photodegradation mechanisms observed (e.g., Audouin et al., 1998).

Excellent reviews present what is known about plastics photochemistry in marine systems in further detail (Andrady et al., 2022; Masry et al., 2021). As we seek to understand the fate and impact of plastics at sea, it will be important to consider the wealth of information in the materials science literature and to obtain critical data regarding mechanisms, rates, and products of plastic photodegradation in marine waters. On first consideration, plastics can be viewed as simpler analogs of natural organic matter, dominated by a few polymers of known chemistries and production rates globally. However, the plastics encountered at sea have added chemical complexity in the form of additives, passenger pollutants, biofilms, and photochemically altered surface chemistries and topographies. Understanding the photochemistry of plastics at sea will require understanding and quantifying these complexities along with their influence on plastic photoreaction rates and mechanisms. In addition, the data about plastics at sea will need to be standardized and adapted to enable better quantification both of plastics but also their photoreactivity. For instance, many studies report plastics in terms of counts (i.e., pieces of plastics), some report masses of plastics, and even fewer report plastic organic carbon—the unit we use in studies of other forms of organic carbon to enable standardized budgeting. Calculating photodegradation rates of plastics at sea depends on knowing their surface area, mass, and polymer type. Thus, fieldwork to quantify plastics in surface waters should report sizes, masses, C content, and polymer type to allow improved assessment of plastic photoreactivity.

11.5.5 Sea-surface microlayer

The thin interface between the oceans and atmosphere, the sea-surface microlayer, is a photochemically active layer that is physically and chemically distinct from the underlying “bulk” seawater. Depending on one’s perspective, the microlayer thickness can range from angstroms to millimeters (MacIntyre, 1974), but in practice it is operationally defined by the method used to sample it (e.g., $\sim 50\text{ }\mu\text{m}$ using a glass plate, $\sim 200\text{ }\mu\text{m}$ using a stainless steel screen). Dissolved and particulate surface active living (e.g., viruses and bacteria) and nonliving organic and inorganic matter are deposited into the microlayer by settling particles or gases from the atmosphere or by rising bubble plumes generated from breaking waves in the ocean (Engel et al., 2017), the latter of which also serve to disrupt the microlayer. Unlike bulk seawater, additional significant thermal reactions in the microlayer can be initiated by atmospheric-derived oxidants such as ozone, NO, NO_2 , and nitrous acid (Thompson and Zafiriou, 1983), thus adding to the complexity of quantifying photochemical reactions. Another critical difference between the sea-surface microlayer and bulk seawater is that the microlayer is highly enriched in DOM and POM, both natural and anthropogenic, including

combined amino acids, carbohydrates, lipids, mycosporine like amino acids, transparent exopolymer particles, plastics, and compounds derived from oil, with enrichments occasionally exceeding several fold above concentrations in the underlying seawater (e.g., Wurl et al., 2011). It is therefore unsurprising that this is a photochemically reactive environment, even though residence times can be short (Blough, 1997) and the microlayer is optically thin with very little actinic UV and visible radiation absorbed within it.

Microlayer photochemical reactions have drawn considerable attention over the decades (Carlson, 1983; Henrichs and Williams, 1985; Zafiriou, 1986), highlighted by two reviews (Zafiriou, 1996; Blough, 1997). Early research focused on what reactions and transformations were possible and how these transformations might affect particle dynamics, surface-active biota, surface tension, and gas exchange. Studies then focused on disentangling specific reactions and processes leading to the formation of VOC, largely spearheaded by atmospheric scientists trying to understand and constrain the atmospheric cycling of VOC and secondary organic aerosol in the troposphere (Brüggemann et al., 2018; Carpenter and Nightingale, 2015; Novak and Bertram, 2020).

In most studies, surfactants and oxidants are added to laboratory water and irradiated using high concentrations of reactants, orders of magnitude higher than expected in seawater. Chiu et al. (2017) determined that organic films of several C7–C9 carboxylic acids overlying simple salt solutions produced glyoxal when exposed to a solar simulator followed by ozone treatment. Lin et al. (2021) added 1% by volume of 1-nonalol to air-saturated laboratory water. When the two layers were irradiated the main products detected in solution were nonanal and 1-heptene, with traces of C4–C6 carbon alkenes. Very little product formation was observed in a nitrogen atmosphere or when a singlet oxygen quencher was added to the reaction mixture, confirming that singlet oxygen was likely involved in 1-nonalol photo-oxidation. Similarly, several studies have been conducted using natural sea-surface microlayer water, biofilm-enriched groundwater, or a salt solution with added high DOM or photosensitizer concentration (e.g., 20–40 mg CL⁻¹ commercial humic acids; 0.1 mmol L⁻¹ 4-benzoyl benzoic acid), high concentrations of surfactants (mmol L⁻¹ range) including C7–C9 carbon carboxylic acids or alcohols (Alpert et al., 2017; Brüggemann et al., 2017; Chiu et al., 2017; Ciuraru et al., 2015a, b; Fu et al., 2015; Rossignol et al., 2016). Penežić et al. (2023) irradiated unfiltered and filtered diatom culture samples (collected during senescence) in parallel with lipid-extracted culture samples (\sim 0.8 mg lipids L⁻¹) and analyzed VOC generated from photolysis of these solutions in-line using proton transfer time of flight mass spectrometry. Multiple VOC molecules were generated in all studies, including a series of aliphatic alkanes and alkenes, dienes, and carbonyl compounds. In one study, surfactant activity was tested and shown to increase after irradiation compared to the dark control (Penežić et al., 2023). The photon exposure in the reaction chamber was not reported in any of these studies nor was the spectral output typically documented. Given the high concentrations of DOM, surfactants, and sensitizers used in these studies, results should be viewed as proof of concept only. The VOC product distribution may be quite different under ambient conditions in the oceans where the main surfactants are not C7–C9 organic acids or alcohols, but rather carbohydrates, peptides/proteins, and uncharacterized refractory DOM. Likewise, commercially available humic acids are not a good proxy for marine DOM.

The role of metals has also been considered in VOC formation. Iron is of particular interest because it is an important constituent of aged dust or volcanic ash deposited to the sea

surface. [Huang et al. \(2020\)](#) irradiated a pH 3.0 solution containing nonanoic acid and Fe(III). Fenton chemistry resulted in the decarboxylation of the nonanoic acid and production of the volatile compounds, octanol and octane, in the gas phase, with heptane and heptanal produced in minor quantities; water-soluble products were not examined. [Hamdun et al. \(2016\)](#) irradiated microlayer and bulk seawater samples collected from Japanese coastal waters containing $\sim 100 \text{ nmol L}^{-1}$ total iron mostly as Fe(III), with and without added $50 \mu\text{mol L}^{-1}$ hydrogen peroxide. Samples were irradiated for 30 min using an optically filtered high pressure mercury lamp. No differences were observed in hydrogen peroxide decay or Fe(II) formation in the sea-surface microlayer water compared to the bulk seawater, and $\cdot\text{OH}$ radical formation only occurred when hydrogen peroxide was added to the reaction mixture. From this, they concluded that in coastal seawater the Fenton reaction was a much more important removal mechanism for H_2O_2 compared to its direct photolysis, but it was not an important source of $\cdot\text{OH}$ in these samples.

[Saint-Macary et al. \(2022\)](#) used a sipper to collect $\sim 1 \text{ mm}$ thick layer microlayer samples from the southwestern Pacific Ocean. Unfiltered samples were exposed to sunlight for 6 h to determine DMS photolysis rates. Photolysis rate constants ($0.004\text{--}0.035 \text{ h}^{-1}$) were significantly lower than reported in the literature, and likely resulted from biological DMS production in the samples; it would have been advantageous to examine photolysis rates in parallel filtered samples. [Rickard et al. \(2022\)](#) collected sea-surface microlayer samples from the River Tyne Estuary and irradiated the samples for up to 24 h, which resulted in CDOM photobleaching and an increase in surfactant activity. The photochemically induced increase in surfactant activity was estimated to decrease the gas transfer velocity, which they suggest is a hitherto unknown process affecting gas exchange at the sea surface on a global scale. Microlayer studies almost without exception have not employed actinometers to quantify photon exposures, and therefore results from these studies are not directly comparable.

Conditions used in several studies (e.g., [Jiang et al., 2022](#); [Rossignol et al., 2016](#)) limit their usefulness in understanding authentic marine surface-microlayer photochemistry due to using high concentrations of reactants, low pH, or by excluding gas-phase oxidants. Improved experimental designs with chemical concentrations approaching ambient conditions are needed to study the microlayer. One important limitation of microlayer photochemical research is a repeatable and consistent definition of the microlayer, which is currently characterized by the method used to sample it. Microlayer samplers collect a different microlayer thickness depending on their design (e.g., screen, glass plate, sipper, rotating drum), and each sampler will have different efficiencies for collecting low and high molecular weight organic matter that will depend on the material used to sample the microlayer (e.g., glass vs. stainless steel). Typically, large stainless-steel rotation drums or screens are used to collect microlayer material because they can collect large volumes of microlayer, but the trade-off is these methods collect a much thicker microlayer thickness with different collection efficiencies for DOM compared to that obtained with a glass plate that only collects a few milliliters per dip (c.10 mL). As such, results using these different samplers are not comparable. From a photochemical perspective, samplers that collect a thinner microlayer thickness (e.g., glass plate) provide a better assessment of photochemical processes and rates in the microlayer. Standard protocols are needed ([Cunliffe et al., 2013](#); [Engel et al., 2017](#)) to directly compare results. From a photochemical perspective, studies are needed to define the optical properties of the microlayer and conduct experiments using authentic microlayer samples, with consideration of atmospherically derived gases on mechanisms and rates.

11.6 Modeling photochemical rates

11.6.1 Fundamental approaches

All photochemical models must quantify the individual elements that drive photochemical reactions. These normally vary with wavelength (λ) and include the irradiance ($E_{o,\lambda}$) and the absorption of available photons (a_{λ}), which together define the photon absorption rate ($Q_{a,\lambda}$). The efficiency (referred to as the quantum yield, ϕ_{λ}) with which the absorption of these photons results in a particular photochemical reaction then defines the rate of photochemical change in solution. In simplest terms, the total measured production or loss rate (R_{tot}) for any photochemical reaction in natural water is integrated as a function of wavelength and defined as follows:

$$R_{\text{tot}} = \sum_{\lambda} Q_{a,\lambda} \times \phi_{\lambda} \quad (11.1)$$

where $Q_{a,\lambda}$ is the product of the wavelength-dependent solar irradiance ($E_{o,\lambda}$) and the wavelength-dependent photon absorption (a_{λ}).

Models used to describe photochemistry under an artificial light source in a beaker are fundamentally the same as those used to estimate global oceanic photochemical budgets in this regard. Even though these components usually vary spectrally, and assumptions about extrapolation, scaling, and optics are made to accommodate environmental conditions, every model must respect these fundamental relationships. Estimates of regional to global in situ photochemical rates in the ocean require a complex mix of optical and photochemical considerations but, as is the case with all models, they are only as good as the assumptions and parameterizations that are included. Rigorous determination of each component is required for improved estimates of the role of photochemistry in marine biogeochemical cycles.

11.6.1.1 Photon absorption

Quantifying $Q_{a,\lambda}$ in laboratory containers must account for the spectral transparency and reflective/refractive properties related to specific materials and irradiation configurations. [Hu et al. \(2002\)](#) provide methods to account for most of these optical complexities. Discussion of optical issues and the degree of detail required to accurately quantify $Q_{a,\lambda}$ can be found in numerous publications (e.g., [Gu et al., 2017](#); [Hu et al., 2002](#); [Kirk, 1994](#); [Mobley, 2022](#); [Powers et al., 2015](#); [Ward et al., 2021](#); [Zhu and Kieber, 2018](#)). In all studies, regardless of the rigor with which optics are defined, it is essential to include appropriate actinometers to confirm the accuracy of $Q_{a,\lambda}$ in laboratory irradiations as described in [Section 11.2.1](#) and in multiple publications ([Jankowski et al., 1999](#); [Kieber et al., 2007](#); [Kuhn et al., 2004](#); [Laszakovits et al., 2017](#)).

Defining $Q_{a,\lambda}$ in the ocean is a more complex undertaking and requires a thorough understanding of ocean optics. Luckily, marine photochemists can draw from a long history and substantial body of environmental optical knowledge available (e.g., [Kirk, 1994](#); [Mobley, 2022](#)) to support models for photosynthetic and photochemical processes in sunlit marine systems. The inherent assumptions and models to quantify incident solar radiation, its reflection and refraction at the air-sea interface, and the underwater geometry of UV radiation that drives photochemical reactions have all received considerable attention (e.g., [Fichot and Miller, 2010](#); [Miller et al., 2002](#); [Powers and Miller, 2014](#); [Smyth, 2011](#); [Stubbins et al., 2006](#); [Zafiriou et al., 2003](#)). Models have used “average” CDOM absorbance spectra to estimate

the proportion of light absorbed by CDOM (e.g., [Stubbins et al., 2006](#); [Zafiriou et al., 2003](#)), but temporal, spatial, and compositional variations in CDOM can greatly influence photochemical rate calculations ([Powers and Miller, 2015a](#); [Reader and Miller, 2011](#)). Accurate estimates of the spectral scalar radiation in the water column, partitioning of UV photons between dissolved and particulate absorption, and the spectral vertical attenuation are all required for realistic ocean photochemical models.

11.6.1.2 Photochemical reaction efficiency

The critical chemical component for these *in situ* models is the photochemical reaction efficiency, ϕ , for the process of interest. This component is normally quantified using well-defined and controlled conditions in the laboratory but has also been estimated with suspended samples distributed down an attenuating UV light field *in situ* ([Vähäalo et al., 2000](#)). With accurate measurements of photochemical rates, R_{tot} , and exact knowledge of $Q_{a,\lambda}$, the determination of ϕ should be relatively straightforward. For the ocean, however, CDOM is generally responsible for the initial capture of UV solar energy that initiates almost all photochemical reactions. Since the chromophores that comprise CDOM are generally not known, wavelength-dependent AQYs are used in Eq. (11.1) (instead of ϕ_λ) to quantify the efficiency of photochemical transformations using the absorbance from all chromophores (i.e., CDOM) and not specific precursors used to calculate ϕ_λ . Since AQYs implicitly include many chromophores not involved in the photoreaction being evaluated, AQYs are significantly lower than ϕ_λ ; the latter being defined using only photons absorbed by the photochemical precursor in the reaction being evaluated.

The ϕ_λ for direct photolysis is independent of wavelength for small molecules with one chromophore ([Calvert and Pitts, 1966](#)), albeit this can vary for larger molecules with multiple chromophores. CDOM, however, is a complex mixture of dissolved organic compounds and inorganic solutes. Typically, researchers have determined wavelength-dependent AQYs using monochromatic (usually with a bandwidth $<20\text{ nm}$; e.g., [Toole et al., 2003](#); [Ward et al., 2021](#)) or broadband (using long-pass filters; e.g., [Johannessen and Miller, 2001](#)) irradiations, and have repeatedly shown that, with the exception of $\cdot\text{OH}$ radical production, AQY spectra for most photochemical reactions (e.g., DMS photolysis, CO or DIC photoproduction) that involve CDOM decrease exponentially with increasing wavelength (for review and references, see [Mopper et al., 2015](#)). However, given the extreme drop in $E_{o,\lambda}$ from visible to UV-B wavelengths that overlap with AQYs over the same range, small errors in AQY spectral shape can result in significant deviations for modeled photochemical rates. Consequently, whenever possible, multiple experimental and mathematical approaches should be compared to verify the magnitude of AQYs and AQY spectral shape before use in photochemical models.

Many AQY determinations have used the broadband irradiation method introduced by [Johannessen and Miller \(2001\)](#) (e.g., [Koehler et al., 2014, 2022](#); [Powers and Miller, 2015a](#)) rather than monochromatic irradiations (e.g., [Zhu and Kieber, 2018, 2020](#)). The broadband method allows simultaneous exposure of a single water sample, distributed into multiple quartz containers, to multiple spectral irradiances (using five to eight different long-pass cutoff filters) resulting in a different R_{tot} for each light treatment, thus allowing a statistical determination of the one, unique AQY spectrum that best describes all the R_{tot} data. The more R_{tot} data collected for a given sample with differing $Q_{a,\lambda}$, the more robust the statistical

determination of the AQY spectrum. Advantages of the broadband method over most monochromatic methods include increased analytical signal for better evaluation of initial rates, the ability to capture potential cross-spectral interactions within the CDOM pool, and simulation of the natural spectral changes that occur with depth in the photic zone. Potential disadvantages include the necessity to assume a mathematical shape for the AQY spectral fit and analytical challenges to precisely quantify a small change between spectral treatments within an overall large production signal. Detailed descriptions of the multicutoff filter “broadband” AQY method can be found in numerous publications (Neale and Kieber, 2000; Powers and Miller, 2015a; Rundel, 1983).

A distortion of this method has been used to estimate AQY spectra using only a single, full spectral irradiation and a single measurement of R_{tot} (Aarnos et al., 2018; Gu et al., 2017). This “1-point” method yields an AQY spectrum by using one chemical measurement, the spectral $Q_{a,\lambda}$, and a restricted statistical evaluation that limits the values for exponential fitting parameters within a predetermined range based on published AQY spectra for the same reaction (e.g., DIC photoproduction; Johannessen and Miller, 2001; White et al., 2010). This “1-point” method can be used to confirm consistency with previous findings, but it should not be confused with AQY methods that use multiple (\sim 5–8) spectral treatments to intentionally vary R_{tot} and constrain a single, robust statistical solution for the AQY spectrum. With only one chemical measurement to constrain photochemical production, the “1-point” method cannot provide a unique AQY spectral solution for an unknown photochemical reaction or poorly described reaction such as OCS photoproduction for which AQY spectra vary by more than two orders of magnitude in the literature (Section 11.3.2.2). The single R_{tot} measurement resulting from full spectral irradiation can, however, be used with $Q_{a,\lambda}$ integrated over an appropriate wavelength range to produce a nonspectral, “average” AQY that can be scaled with solar irradiance for in situ estimates. This approach has been used for a tDOC-loss model in the northern Gulf of Mexico (Fichot and Benner, 2014), and other studies have also used an average AQY to good effect (e.g., Song et al., 2015; Lennartz et al., 2019; Zhang and Xie, 2015).

The availability of a variety of high-output LEDs, including those that emit UV, has led to development of new systems for monochromatic irradiations that can be used to determine AQY spectra for DOC/CDOM-driven photochemical reactions. Ward et al. (2021) described the construction and use of an LED system that exposes samples to narrow-band UV radiation (e.g., 275, 309, 348, 369, and 406 nm). With this method, they reported the AQY spectra for O₂ consumption and oil dissolution in seawater (Freeman and Ward, 2022). A similar system with LED exposure bands centered more toward the visible (375, 387, 425, 461, 490, 531, 591, and 632 nm) has been used to determine AQY spectra for photochemically produced RIs from CDOM and black carbon (Wu et al., 2021; Wang et al., 2023). These LED systems provide both advantages and disadvantages relative to the multicutoff filter “broadband” method (see Ward et al., 2021). However, given that AQYs are cited in many model applications as the dominant source of error (Whelan et al., 2018; Launois et al., 2015), new LED irradiation systems should provide opportunities to confirm AQY spectral shape and magnitude with multiple methods and allow photochemical models to be applied to the ocean with greater confidence.

With accurate AQY spectra for photochemical processes and well-defined ocean optics, it is possible to implement fully spectral, depth-resolved photochemical models in the marine photic zone. The additional evaluation of temperature dependence for AQYs, particularly for

secondary photochemical reactions with a known thermal component (Estapa et al., 2012; Kieber et al., 2014; Zhu et al., 2020b), can significantly improve ocean models for CDOM-driven photoreactions. Unfortunately, understanding of the spatial and temporal variations is lacking for nearly all AQYs determined to date. Simple correlations between photochemical transformations and CDOM absorption currently used to extrapolate from easily measured coastal samples to oligotrophic waters may not be appropriate, as discussed in Section 11.2.2. Photochemical fading of CDOM, the lack of reciprocity, and/or molecular transformations of DOM during prolonged exposure of seawater to sunlight can alter AQY spectra (Section 11.2.1); these factors give rise to important uncertainties when using CDOM as the “chromophore” to define AQY spectra that drive photochemical reactions in the ocean.

11.6.2 Scaling to oceans

Ideally, CDOM-driven photochemical models will allow extrapolation beyond site- and time-specific studies that measure the rate of a photoreaction at a given depth, for a given sample, on a given day in the ocean. By measuring chemical and optical changes (CDOM, FDOM) in surface waters or in drifter buoy experiments with quartz flasks containing seawater suspended in the water column where solar irradiation is quantified, extrapolation to larger scales has been made (e.g., del Valle et al., 2007; Kieber et al., 1997, 2007, 2014; Toole et al., 2006; Yocis et al., 2000). Rate measurements, R_{tot} , can be correlated with modeled solar irradiation and $Q_{a,\lambda}$ to give regional and global estimates as has been done for the in situ loss of several micropollutants that result from secondary, CDOM-generated photochemical reactions (Zhou et al., 2018). Although this approach offers an empirical measure of photochemical rates at water column light levels, it can be untenable to extrapolate such data to larger temporal and spatial scales. Measurements made in the photic zone will reflect a “net” rate that incorporates both homogenous and particle-based production and loss, as well as biological processes. These direct field measurements, if light is quantified in a meaningful way, can be extremely valuable in constraining the potential magnitude of a given photochemical process, provide relative importance for reactions involving DOM versus POM, and help constrain photochemical significance in a “real world” setting.

11.6.2.1 Scaling and extrapolation

Global models of photoproduction have used “average” CDOM absorbance spectra to estimate the proportion of light absorbed by CDOM (Stubbins et al., 2006; Zafiriou et al., 2003). However, this approach is limited by CDOM variations as already mentioned. A significant advance for capturing oceanic CDOM variability for use in photochemical models over large spatial and temporal scales was introduced by Fichot and Miller (2010). This approach linked remotely sensed ocean color in visible wavelengths to downward attenuation in the UV (K_{dUV} , Fichot et al., 2008) and allowed depth-resolved estimates for photochemical rates. $Q_{a,\lambda}$ was calculated using a global insolation model and climatological ocean color data that informed CDOM values extrapolated from K_{dUV} . Using a single averaged AQY spectrum for CO production yielded a global yearly oceanic CO photoproduction of $\sim 41 \times 10^{12} \text{ g Cyr}^{-1}$, in reasonable agreement with previous estimates (Stubbins et al., 2006; Zafiriou et al., 2003).

As defined by the photochemical rate equation used to calculate AQYs (Section 11.6.1), a critical condition is that the production, or loss, of a compound is a linear function of photon exposure. If the condition of reciprocity is not met, then calculated rates will underestimate AQYs. As shown earlier in this chapter, laboratory determined AQYs often change over lengthy irradiations. However, this can reflect experimental design rather than in situ oceanic conditions, especially with respect to the timescale over which these changes might occur. Laboratory-based AQYs are typically determined using photon doses well above those received daily by a parcel of seawater exposed to sunlight in situ. In the ocean, a water parcel is exposed to variable solar irradiance that accumulates between the dawn and dark of night while mixing vertically through varying light fields. This will decrease its photon exposure compared to that for a sample “trapped” at the surface or irradiated in the lab. Additionally, vertical mixing may replenish lost chromophores both during the day and night, while no such condition is possible in the laboratory during long irradiations equivalent to multiday exposures to sunlight. Consequently, initial rates remain a valid representation in models of in situ photochemical rates. While long irradiation experiments should not be used for this purpose, they can nonetheless be informative in revealing important mechanistic information (Zhu et al., 2020b).

Another issue arising from using laboratory determined, CDOM-based AQY spectra for in situ photochemical models is that almost all AQYs are determined in $0.2\text{ }\mu\text{m}$ filtered samples. Since these only capture photochemical reactions stemming from photon absorbance by CDOM, it is of critical importance to know the CDOM/ K_{dUV} ratio for proper photochemical calculations in natural waters (e.g., Estapa et al., 2012; Song et al., 2015). Previous empirical CDOM/ K_{dUV} spectral ratios developed for clear oligotrophic waters do not perform well in coastal systems or in blooms with high particle attenuation. Cao and Miller (2015) developed empirical algorithms to retrieve 5 nm resolved CDOM spectra (275–450 nm) directly from ocean color data, independent of K_{dUV} ; their algorithms showed improved performance compared to Swan et al. (2013) who used the semianalytical Garver and Siegel GSM 01 algorithms (Garver and Siegel, 1997; Maritorena et al., 2002). Considering CDOM as a distinct inherent optical property separate from K_{dUV} , Cao and Miller (2015) obtained a unique estimate of CDOM/ K_{dUV} for each image pixel. This allowed CDOM-based AQY spectra to be appropriately partitioned for accurate depth-resolved photochemical models.

Cao et al. (2018) used this approach with a hyperspectral image from coastal Georgia, USA, to determine the photochemical CO production in nearshore and inshore waters with high gradients for particle load and CDOM. They estimated that rates may be miscalculated by $\pm 100\%$ when using CDOM based on K_{dUV} extrapolations, as would result from using the method of Fichot and Miller (2010) in these nearshore environments. With the ability to describe CDOM absorption in the UV relative to the total photon attenuation, the allocation of UV radiation among different phases should improve “photochemistry from space” models that address photoreactions involving POC and allow increased confidence to a wider variety of water types.

Previous models that address the known direct photochemical oxidation of DOM and subsequent formation of CO and DIC have been developed to better understand this likely significant component in the ocean organic carbon cycle (for review, see Mopper et al., 2015). Due to the extreme analytical difficulty of measuring DIC photoproduction in oligotrophic waters, proxies or extrapolations from coastal waters with more CDOM and higher

production rates have been used and global estimates from previous models are presented in [Section 11.3.1.1](#) and in previous reviews ([Mopper and Kieber, 2002](#); [Mopper et al., 2015](#)). Compilation of current results for DIC clearly shows that a great deal of work lies ahead to constrain this presumed major photochemical carbon sink for DOM.

As with all models, the accuracy of ocean photochemical models reflects the confidence level to which parameters are defined. Modelers have struggled to accurately represent the substantial temporal and spatial variability of AQYs, CDOM, and UV distribution in marine surface waters as they relate to a variety of photochemical reactions. In doing so, however, photochemical modeling studies have identified specific parameterizations that limit the development of more accurate photochemical approaches, and by extension, better regional and global biogeochemical ocean models, providing useful recommendations for future study.

11.6.2.2 Modeling examples

Photochemical proxies, even if later proven to be only loosely constrained, have moved models forward when direct measurements are not possible. As pointed out in [Section 11.3.1.1](#), using CO as a proxy for DIC photoproduction has turned out, for various reasons, to be less useful than initially proposed, having ratios ranging from 2 to more than 60 ([Powers and Miller, 2015a](#); [Reader and Miller, 2012](#); [White et al., 2010](#)). [Powers and Miller \(2015a, 2015b\)](#) proposed H_2O_2 as a better proxy for DIC photoproduction, with a more constrained relationship across the gradient from coastal to offshore waters ($\text{DIC}/\text{H}_2\text{O}_2 = 6.6 \pm 1.8$). Additional evidence that this proxy might be robust is that the nonlinear accumulation in irradiations observed for DIC was also seen equivalently for H_2O_2 such as to maintain the ratio even as production and accumulation changed during extended irradiations (unlike CO). This relationship was used by [Zhu et al. \(2022\)](#) with their updated satellite-based global model for H_2O_2 photoproduction to estimate the photoproduction of DIC. The estimated annual DIC photoproduction was 139 Tmol yr^{-1} , which is about two to four times higher than the DIC budget estimated using CO as a proxy. This DIC: H_2O_2 relationship is based on a limited dataset and more work is needed to determine the spatial and temporal variability of this ratio, particularly in blue water, in order to confirm or further constrain the potential use of H_2O_2 as a DIC proxy.

CO was again used as a proxy for methane photoproduction by [Li et al. \(2020\)](#), developing CH_4/CO production ratios for a variety of surface ocean waters including the Gulf of St. Lawrence, the Canadian Arctic, the coastal northeastern United States, the Sargasso Sea, and the subtropical North Pacific. While both CH_4 and CO exhibited linear relations with salinity and CDOM absorbance coefficient at 320 nm (a_{320}), CH_4 rates increased considerably in waters with a_{320} less than $\sim 2 \text{ m}^{-1}$ while CO did not. This in turn increased the CH_4/CO ratio when surface waters absorbed less UV, resulting in oligotrophic ocean water having a CH_4/a_{320} ratio ~ 7 times that of freshwater impacted estuarine and coastal waters. The AQYs for CH_4 photoproduction at 320 nm increased as photochemical fading proceeded, demonstrated by linear production despite significant fading. Using the relationships between CH_4/CO ratio and a_{320} together with the remote-sensing-informed model of [Fichot and Miller \(2010\)](#), the photoproduction of CH_4 in the global ocean was estimated to be 121 Ggyr^{-1} , with the open ocean (water depth $< 200 \text{ m}$) accounting for 97% of the total production (i.e., 118 Ggyr^{-1}). This work clearly shows the potential pitfalls of simply extrapolating nearshore photochemical

results to the globally dominant oligotrophic waters to estimate photochemical impacts on biogeochemical cycles.

Evidence for the importance of accurate estimates of CDOM in photochemical models comes from [Conte et al. \(2019\)](#). They imbedded the [Fichot and Miller \(2010\)](#) approach with its assumption of a single AQY for CO (by averaging [Zafiriou et al. \(2003\)](#) and [Ziolkowski and Miller \(2007\)](#)) to generate photochemical rates as part of a global 3-D biogeochemical model. This model, designed to explicitly represent CO cycling via biological, chemical, physical, and photochemical processes in the ocean, showed that the global CO photoproduction component varied by a factor of three ($\sim 14\text{--}49\text{ Tg Cyr}^{-1}$), strongly dependent on the CDOM parameterization used in the model. While this may be true for CO, other photoreactions that do not scale directly with CDOM or result from secondary photochemistry can create challenges beyond simply choosing accurate CDOM values.

The complexity of secondary photochemical reactions like DMS photolysis magnifies the importance of quantifying AQYs. Working to consolidate the disparate published AQY data to construct a comprehensive global DMS model, [Galí et al. \(2016\)](#) organized published DMS studies into several categories and developed a method to estimate the AQY at 330 nm (AQY_{330}). The AQY data from monochromatic or broadband studies designed specifically to determine wavelength-dependent AQYs were used to define its spectral shape (S_{DMS}), while studies using a “1-point” full spectrum exposure were constrained with S_{DMS} from monochromatic or broadband studies ([Section 11.6.1.2](#)) to derive AQY_{330} for use in the model. Confirming the importance of addressing AQY variability, both for laboratory determinations and in extrapolating from limited data, [Galí et al. \(2016\)](#) noted that CDOM composition or quality, rather than CDOM level, as well as the secondary role of nitrate and temperature, controlled AQY spectral values in the ocean. They also noted that current models used a fixed linear function of irradiance without using any of these variables as input ([Bopp et al., 2008](#); [Vogt et al., 2010](#)). In subsequent work, [Galí et al. \(2023\)](#) developed a DMS photolysis satellite-based model using two parameterizations: one using temperature and one with nitrate. From these improved constraints on DMS photolysis AQY spectra, they estimated a global photolysis rate of $13\text{--}15\text{ Tg Cyr}^{-1}$, with 73% of the total annual loss in the Southern Ocean. The previous models using photolysis proportional to visible radiation yielded a global estimate that was 150% larger.

In a review and synthesis of OCS as a tracer for carbon cycles, [Whelan et al. \(2018\)](#) make a strong argument for the critical importance of accurate AQY spectra in global estimates of OCS photoproduction. They found that modeled surface mixed-layer OCS production can vary by a factor of 40 depending on the methodology used. They examined published approaches by [Lennartz et al. \(2019\)](#) and [Launois et al. \(2015\)](#) and performed a sensitivity analysis with different published AQY spectra ([Cutter et al., 2004](#); [Weiss et al., 1995](#); [Zepp and Andreae, 1994](#)) using the model of [Fichot and Miller \(2010\)](#). They report that the heart of the problem in modeling OCS is the limited knowledge of the magnitude, spectral characteristics, and spatial and temporal variability of AQYs for OCS production.

Although photochemistry plays a significant role in the biogeochemistry of DOM, it remains challenging to constrain real-world rates of photochemical processes. Analytical methods for the diminishingly small concentrations of some photoproducts are often the primary limitation, creating the need for optical and chemical proxies. These creative approaches have led photochemical modelers to new estimates and improved understanding

of the impact of photochemistry in the ocean. A pressing issue for continued progress remains the limited ability to quantify the variability of AQY spectra for many reactions. Fully formed biogeochemical models with imbedded photochemistry, biological sources and sinks, and accurate UV optics and surface mixing will eventually provide meaningful comparison with observations.

11.7 Future directions

Over the last 50 years, the field of marine photochemistry has made significant advances, but much of what was stated in Zafiriou's "Marine Organic Photochemistry Previewed" (Zafiriou, 1977) remains true. Namely, marine photochemical systems are not well understood because (1) we do not know the structures of most organic reactants and products, (2) environmental rates are poorly constrained, and (3) basic mechanisms are not known (Zafiriou, 1977). Today, HRMS and NMR techniques are available, which have greatly improved our understanding of DOM transformations due to sunlight. However, as before (Mopper and Kieber, 2002; Mopper et al., 2015), distinguishing which compounds absorb sunlight and initiate marine photochemical DOM or POM transformations remains unresolved.

To better constrain photochemical reaction rates in any aquatic system, laboratory experiments should use environmentally relevant concentrations whenever possible. This rule is especially true for understanding the fate and transport of natural and anthropogenic contaminants in marine systems. A common theme throughout this review is that photochemical processes for DOM and ROS are examined at concentrations orders of magnitude above ambient concentrations, which can lead to erroneous conclusions when extrapolated to ambient seawater conditions. This was the case for acrylate, which photolyzes in seawater at $\mu\text{mol L}^{-1}$ levels but not at low nmol L^{-1} levels (Xue and Kieber, 2021). It is undoubtedly true that not all compounds will behave like acrylate, and many methods are not sensitive enough to examine photoreactions at pmol L^{-1} to nmol L^{-1} concentrations. However, as analytical techniques improve, it should be possible for researchers interested in the photochemistry of specific toxins, pollutants, or natural compounds to accurately quantify the trace concentrations of both photoproducts and photodegradable compounds under ambient seawater conditions. New precolumn derivatization techniques coupled to GC- or UHPLC-MS may allow analysis of low molecular weight photoproducts that have so far been missed by traditional "bulk DOM" analyses. For example, a benzoyl chloride derivatization method, coupled with UHPLC coupled to ESI and tandem MS, was developed and quantify 73 polar microbial metabolites in culture media and in seawater (Widner et al., 2021). Including advanced analytical approaches in future investigations of coupled photochemical-microbial DOM cycling should reveal new insights into these complex interactions.

Another common theme throughout this chapter is that obvious gaps remain in our understanding of the impact of photochemistry on multiple biogeochemical cycles. This condition is especially true in quantifying the production and/or loss of biolabile substrates. Work to date on the coupled photochemical-microbial cycling of DOM has relied heavily on measuring oxygen and/or DOC loss. Oxygen measurements do not necessarily reflect complete

oxidation of DOC to DIC, and measurements of direct DOC loss often require long irradiations to observe an effect. New approaches are needed to unravel the coupled photochemical-microbial transformations of DOM in more detail than afforded by incubation studies using changes in bulk chemical and biological parameters alone. A large body of work has focused on DOC photomineralization, and while justified, this focus may miss important aspects of the intricate interplay between carbon and other elemental cycles that are connected via photochemistry and biology. As discussed before, DOM-containing heteroatoms, such as N and S, appear to be preferentially photodegraded (Stubbins and Dittmar, 2015). Moreover, Ferrer-González et al. (2021) identified 36 phytoplankton metabolites readily consumed by marine microbes, 53% and 11% of which contained nitrogen and sulfur, respectively. Thus the photoproduction of biolabile nitrogen- and sulfur-containing compounds warrants future study. Postirradiation, molecular techniques such as metatranscriptomics (Vorobev et al., 2018; Nalven et al., 2022) and FT-ICR MS should be used together to reveal genes that are expressed and molecular formulae that are produced or lost during the cycling of BLP, possibly via coupling these data to machine learning algorithms (Pan et al., 2023). Likewise, isotopes have been used in studies related to marine photochemistry to gain mechanistic insights into biological and chemical processes (e.g., Moffett and Zafiriou, 1993; Sutherland et al., 2021, 2022; Zafiriou et al., 1990; Zhu and Kieber, 2019). These studies have shown isotopes are powerful tools to study photoreactions, and they should be used in future studies to study photochemical reaction mechanisms.

In addition to the need for new analytical tools to study photochemically reactive species, we still know very little about reaction mechanisms and the specific chromophores giving rise to direct photoproducts and reactive transients of interest. Future studies would benefit greatly from better structural information on reactive marine chromophores as well as the interactions between chromophores, nonchromophoric organic matter, and inorganic solutes in seawater. Chemical tests have been used to better understand CDOM photophysical properties, such as pH titrations, size fractionation, and borohydride reduction but these tests have mostly been done using isolates (e.g., Li and McKay, 2021; Ma et al., 2010; McKay et al., 2016; Schendorf et al., 2019).

CDOM photobleaching is not a trivial process to model due to the polychromatic nature of sunlight, its spectral changes in the photic zone, and the changes in spectral slopes due to wavelength-dependent CDOM photobleaching. New approaches to quantify CDOM photobleaching AQY matrices will allow photochemists to capture the effect of direct and indirect photobleaching on DOM photochemistry. Zhu et al. (2020b) introduced a new partial-least-squares optimized method for modeling natural waters, demonstrating that both temperature and prior irradiation history have a large effect on the magnitude and spectral shape of the photobleaching AQY matrix. These parameters will be important to consider in future models of photoreactions in cases where bleaching is significant relative to the supply of “fresh” CDOM. While HRMS has provided a wealth of information regarding DOM molecular composition, it contains limited structural information. High-field NMR has been used, sometimes in concert with FT-ICR MS (Hertkorn et al., 2006, 2013; Powers et al., 2019), which may help us better understand structural changes in DOM due to photochemistry (Gonsior et al., 2014). Keep in mind, SPE is most often used to prepare samples for both HRMS and NMR analysis, which imposes specific analytical windows on results; limitations that should always be considered (Section 11.2.3).

Optical models for UV irradiance in the ocean are much improved. New work to support NASA satellite capabilities having hyperspectral and UV sensors (e.g., Plankton, Aerosol, Cloud, ocean Ecosystem, PACE), and geostationary missions (e.g., Geosynchronous Littoral Imaging and Monitoring Radiometer, GLIMR) will see these algorithms mature with in situ calibration and validation campaigns to take advantage of novel high-resolution spatial and temporal data. As the mechanisms and variations that underpin photochemical AQY spectra and rates are revealed with new approaches and tools, future estimates that integrate UV optics and AQYs in the ocean will provide increasing confidence for quantifying the role of photochemistry in marine DOM cycles.

Acknowledgments

The authors gratefully acknowledge financial support provided through NSF Chemical Oceanography (OCE-1756907 and OCE-2023104 to DJK; OCE-2242014 to LCP and DJK; OCE-1635618 to WLM, LCP, and AS, and OCE-1924763 to WLM and LCP; OCE-2127669 to AS), NSF Environmental Engineering (CBET-1910621 to AS), and NSF Earth Sciences (CAS-MNP-2219334 to AS).

References

- Aarnos, H., Gélinas, Y., Kasurinen, V., Gu, Y., Puupponen, V.-M., Vähätalo, A.V., 2018. Photochemical mineralization of terrigenous DOC to dissolved inorganic carbon in ocean. *Global Biogeochem. Cycles* 32, 250–266. <https://doi.org/10.1002/2017GB005698>.
- Adesina, A.O., Sakugawa, H., 2021. Photochemically generated nitric oxide in seawater: the peroxy nitrite sink and its implications for daytime air quality. *Sci. Total Environ.* 781, 146683. <https://doi.org/10.1016/j.scitotenv.2021.146683>.
- Adesina, A.O., Anifowose, A.J., Takeda, K., Sakugawa, H., 2018. Photogeneration and interactive reactions of three reactive species in the Seto Island Sea, Japan. *Environ. Chem.* 15, 236–245. <https://doi.org/10.1071/EN18035>.
- Adesina, A.O., Takeda, K., Sakugawa, H., 2020. A fluorescence method for the determination of photochemically generated peroxy nitrite in seawater. *Anal. Chim. Acta* 1132, 83–92. <https://doi.org/10.1016/j.aca.2020.06.063>.
- Aeppli, C., 2022. Recent advance in understanding photooxidation of hydrocarbons after oil spills. *Curr. Opin. Chem. Eng.* 36, 100736. <https://doi.org/10.1016/j.coche.2021.100736>.
- Aeppli, C., Mitchell, D.A., Keyes, P., Beirne, E.C., McFarlin, K.M., Roman-Hubers, A.T., Rusyn, I., Prince, R.C., Zhao, L., Parkerton, T.F., Nedwed, T., 2022. Oil irradiation experiments document changes in oil properties, molecular composition, and dispersant effectiveness associated with oil photo-oxidation. *Environ. Sci. Technol.* 56, 7789–7799. <https://doi.org/10.1021/acs.est.1c06149>.
- Almuhtaram, H., Wang, C., Hofmann, R., 2021. The importance of measuring ultraviolet fluence accurately: a review of microcystin-LR removal by direct photolysis. *Environ. Sci. Technol.* 8, 199–205. <https://doi.org/10.1021/acs.estlett.0c00923>.
- Alongi, D.M., 2018. Blue Carbon Coastal Sequestration for Climate Change Mitigation. Springer, Cham, Switzerland, <https://doi.org/10.1007/978-3-319-91698-9>.
- Alpert, P.A., Ciuraru, R., Rossignol, S., Passananti, S., Tinel, L., Perrier, S., Dupart, Y., Steimer, S.S., Ammann, M., Donaldson, D.J., George, C., 2017. Fatty acid surfactant photochemistry results in new particle formation. *Sci. Rep.* 7, 12693. <https://doi.org/10.1038/s41598-017-12601-2>.
- Altare, N., Vione, D., 2023. Photochemical implications of changes in the spectral properties of chromophoric dissolved organic matter: a model assessment for surface waters. *Molecules* 28, 2664. <https://doi.org/10.3390/molecules28062664>.
- Amado, A.M., Cotner, J.B., Cory, R.M., Edlund, B.L., McNeill, K., 2015. Disentangling the interactions between photochemical and bacterial degradation of dissolved organic matter: amino acids play a central role. *Microb. Ecol.* 69, 554–566. <https://doi.org/10.1007/s00248-014-0512-4>.

- Anderson, D.M., Fensin, E., Gobler, C.J., Hoeglund, A.E., Hubbard, K.A., Kulis, D.M., Landsberg, J.H., Lefebvre, K.A., Provoost, P., Richlen, M.L., Smith, J.L., Solow, A.R., Trainer, V.L., 2021. Marine harmful algal blooms (HABs) in the United States: history, current status and future trends. *Harmful Algae* 102, 101975. <https://doi.org/10.1016/j.hal.2021.101975>.
- Andrady, A.L., Barnes, P.W., Bornman, J.F., Gouin, T., Madronich, S., White, C.C., Zepp, R.G., Jansen, M.A.K., 2022. Oxidation and fragmentation of plastics in a changing environment; from UV-radiation to biological degradation. *Sci. Total Environ.* 851, 158022. <https://doi.org/10.1016/j.scitotenv.2022.158022>.
- Andrew, A.A., del Vecchio, R., Subramaniam, A., Blough, N.V., 2013. Chromophoric dissolved organic matter (CDOM) in the Equatorial Atlantic Ocean: optical properties and their relation to CDOM structure and source. *Mar. Chem.* 148, 33–43. <https://doi.org/10.1016/j.marchem.2012.11.001>.
- Andrew, A.A., del Vecchio, R., Zhang, Y., Subramaniam, A., Blough, N.V., 2016. Are extracted materials truly representative of original samples? Impact of C18 extraction on CDOM optical and chemical properties. *Front. Chem.* 4, 4. <https://doi.org/10.3389/fchem.2016.00004>.
- Antony, R., Willoughby, A.S., Grannas, A.M., Catanzano, V., Sleighter, R.L., Thamban, M., Hatcher, P.G., 2018. Photo-biochemical transformation of dissolved organic matter on the surface of the coastal East Antarctic ice sheet. *Biogeochemistry* 141, 229–247. <https://doi.org/10.1007/s10533-018-0516-0>.
- Appiani, E., McNeill, K., 2015. Photochemical production of singlet oxygen from particulate organic matter. *Environ. Sci. Technol.* 49, 3514–3522. <https://doi.org/10.1021/es505712e>.
- Appiani, E., Ossola, R., Latch, D.E., Erickson, P.R., McNeill, K., 2017. Aqueous singlet oxygen reaction kinetics of furfuryl alcohol: effect of temperature, pH, and salt content. *Environ. Sci.: Processes Impacts* 19, 507–516. <https://doi.org/10.1039/c6em00646a>.
- Arlinghaus, K., Frossard, A.A., Miller, W.L., 2023. Examining superoxide dynamics in irradiated natural waters. *Limnol. Oceanogr.* 68, 878–890. <https://doi.org/10.1002/lo.12316>.
- Arthur, C., Bamford, H., Baker, J., 2009. Proceedings of the International Research Workshop on the Occurrence, Effects and Fate of Microplastic Marine Debris, Tacoma, WA. https://marinedebris.noaa.gov/sites/default/files/publications-files/TM_NOS-ORR_30.pdf.
- Audouin, L., Girois, S., Achimsky, L., Verdu, J., 1998. Effect of temperature on the photooxidation of polypropylene films. *Polym. Degrad. Stab.* 60, 137–143. [https://doi.org/10.1016/S0141-3910\(97\)00042-6](https://doi.org/10.1016/S0141-3910(97)00042-6).
- Avery Jr., B., Mickler, W., Probst, E., Mead, R.N., Skrabal, S.A., Kieber, R.J., Felix, J.D., 2017. Photochemical release of sediment bound brevetoxin (PbTx-2) from resuspended sediments. *Mar. Chem.* 189, 25–31. <https://doi.org/10.1016/j.marchem.2016.12.003>.
- Ayeni, T.T., Iwamoto, Y., Takeda, K., Sakugawa, H., Mostofa, K.M.G., 2022. Optical properties of dissolved organic matter in Japanese rivers and contributions to photoformation of reactive oxygen species. *Sci. Total Environ.* 826, 153671. <https://doi.org/10.1016/j.scitotenv.2022.153671>.
- Bacilieri, F., Vähätalo, A.V., Carena, L., Wang, M., Gao, P., Minella, M., Vione, D., 2022. Wavelength trends of photoproduction of reactive transient species by chromophoric dissolved organic matter (CDOM), under steady-state polychromatic irradiation. *Chemosphere* 306, 135502. <https://doi.org/10.1016/j.chemosphere.2022.135502>.
- Bao, Y., Deng, S., Jiang, X., Qu, Y., He, Y., Liu, L., Chai, Q., Mumtaz, M., Huang, J., Cagnetta, G., Yu, G., 2018. Degradation of PFOA substitute: GenX (HFPO-DA ammonium salt): oxidation with UV/persulfate or reduction with UV/sulfite? *Environ. Sci. Technol.* 52, 11728–11734. <https://doi.org/10.1021/acs.est.8b02172>.
- Barbeau, K., 2006. Photochemistry of organic iron (III) complexing ligands in oceanic systems. *Photochem. Photobiol.* 82, 1505–1516. <https://doi.org/10.1111/j.1751-1097.2006.tb09806.x>.
- Barrios, B., Mohrhardt, B., Doskey, P.V., Minakata, D., 2021. Mechanistic insight into the reactivities of aqueous-phase singlet oxygen with organic compounds. *Environ. Sci. Technol.* 55, 8054–8067. <https://doi.org/10.1021/acs.est.1c01712>.
- Berggren, M., Guillemette, F., Bieroza, M., Buffam, I., Deininger, A., Hawkes, J.A., Kothawala, D.N., LaBrie, R., Lapierre, J.F., Murphy, K.R., Al-Kharusi, E.S., Rulli, M.P.D., Hensgens, G., Younes, H., Wünsch, U.J., 2022. Unified understanding of intrinsic and extrinsic controls of dissolved organic carbon reactivity in aquatic ecosystems. *Ecology* 103, e3763. <https://doi.org/10.1002/ecy.3763>.
- Bianco, A., Sordello, F., Ehn, M., Vione, D., Passananti, M., 2020. Degradation of nanoplastics in the environment: reactivity and impact on atmospheric and surface waters. *Sci. Total Environ.* 742, 140413. <https://doi.org/10.1016/j.scitotenv.2020.140413>.

- Bittar, T.B., Vieira, A.A., Stubbins, A., Mopper, K., 2015. Competition between photochemical and biological degradation of dissolved organic matter from the cyanobacteria *Microcystis aeruginosa*. Limnol. Oceanogr. 60, 1172–1194. <https://doi.org/10.1002/lno.10090>.
- Blanchet, M., Fernandez, C., Joux, J., 2018. Photoreactivity of riverine and phytoplanktonic dissolved organic matter and its effects on the dynamics of a bacterial community from the coastal Mediterranean Sea. Prog. Oceanogr. 163, 82–93. <https://doi.org/10.1016/j.pocean.2017.03.003>.
- Blough, N.V., 1997. Photochemistry in the sea-surface microlayer. In: Liss, P.S., Duce, R.A. (Eds.), *The Sea Surface and Global Change*. Cambridge University Press, Oxford, UK, pp. 383–424.
- Blough, N.V., Zepp, R.G., 1995. Reactive oxygen species in natural waters. In: Foote, C.S., Greenberg, A., Valentine, J.S., Liebman, J.F. (Eds.), *Active Oxygen in Chemistry*, second ed. Springer, Dordrecht, pp. 280–333, <https://doi.org/10.1007/978-94-007-0874-7>.
- Boldrini, A., Galgani, L., Consumi, M., Loiselle, S.A., 2021. Microplastics contamination versus inorganic particles: effects on the dynamics of marine dissolved organic matter. Environments 8, 21. <https://doi.org/10.3390/environments8030021>.
- Bopp, L., Aumont, O., Belviso, S., Blain, S., 2008. Modelling the effect of iron fertilization on dimethylsulphide emissions in the Southern Ocean. Deep Sea Res. II 55, 901–912. <https://doi.org/10.1016/j.dsr2.2007.12.002>.
- Boreen, A.L., Arnold, W.A., McNeill, K., 2003. Photodegradation of pharmaceuticals in the aquatic environment: a review. Aquat. Sci. 65, 320–341. <https://doi.org/10.1007/s00027-003-0672-7>.
- Bouillon, R.-C., Miller, W.L., 2004. Determination of apparent quantum yield spectra of DMS photo-degradation in an *in situ* iron-induced Northeast Pacific Ocean bloom. Geophys. Res. Lett. 31, L06310. <https://doi.org/10.1029/2004GL019536>.
- Bouillon, R.-C., Miller, W.L., 2005. Photodegradation of dimethyl sulfide (DMS) in natural waters: laboratory assessment of the nitrate-photolysis-induced DMS oxidation. Environ. Sci. Technol. 39, 9471–9477. <https://doi.org/10.1021/es048022z>.
- Bowen, J.C., Kaplan, L.A., Cory, R.M., 2020a. Photodegradation disproportionately impacts biodegradation of semi-labile DOM in streams. Limnol. Oceanogr. 65, 13–26. <https://doi.org/10.1002/lno.11244>.
- Bowen, J.C., Ward, C.P., Kling, G.W., Cory, R.M., 2020b. Arctic amplification of global warming strengthened by sunlight oxidation of permafrost carbon to CO₂. Geophys. Res. Lett. 47, e2020GL087085. <https://doi.org/10.1029/2020GL087085>.
- Boyle, E.S., Guerriero, N., Thiallet, A., del Vecchio, R., Blough, N.V., 2009. Optical properties of humic substances and CDOM: relation to structure. Environ. Sci. Technol. 43, 2262–2268. <https://doi.org/10.1021/es803264g>.
- Braslavsky, S.E., 2007. Glossary of terms used in photochemistry (IUPAC Recommendations 2006), 3rd Ed. Pure Appl. Chem. 79, 293–465. <https://doi.org/10.1351/pac200779030293>.
- Brimblecombe, P., Shooter, D., 1986. Photo-oxidation of dimethylsulphide in aqueous solution. Mar. Chem. 19, 343–353. [https://doi.org/10.1016/0304-4203\(86\)90055-1](https://doi.org/10.1016/0304-4203(86)90055-1).
- Brüggemann, M., Hayeck, N., Bonnneau, C., Pesce, S., Alpert, P.A., Perrier, S., Zuth, C., Hoffmann, T., Chen, J., George, C., 2017. Interfacial photochemistry of biogenic surfactants: a major source of abiotic volatile organic compounds. Faraday Discuss. 200, 59–74. <https://doi.org/10.1039/c7fd00022g>.
- Brüggemann, M., Hayeck, N., George, C., 2018. Interfacial photochemistry at the ocean surface is a global source of organic vapors and aerosols. Nat. Commun. 9, 2101. <https://doi.org/10.1038/s41467-018-04528-7>.
- Buchanan, J.B., 1971. Pollution by synthetic fibres. Mar. Pollut. Bull. 2, 23. [https://doi.org/10.1016/0025-326X\(71\)90136-6](https://doi.org/10.1016/0025-326X(71)90136-6).
- Burns, S.E., Hassett, J.P., Rossi, M.V., 1997. Mechanistic implications of the intrahumic dechlorination of mirex. Environ. Sci. Technol. 31, 1365–1371. <https://doi.org/10.1021/es9605811>.
- Burns, J.M., Cooper, W.J., Ferry, J.L., King, D.W., DiMento, B.P., McNeill, K., Miller, C.J., Miller, W.L., Peake, B.M., Rusak, S.A., Rose, A.L., Waite, T.D., 2012. Methods for reactive oxygen species (ROS) detection in aqueous environments. Aquat. Sci. 74, 683–734. <https://doi.org/10.1007/s00027-012-0251-x>.
- Bushaw, K.L., Zepp, R.G., Tarr, M.A., Schultz-Jander, D., Bourbonniere, R.A., Hodson, R.E., Miller, W.L., Bronk, D.A., Moran, M.A., 1996. Photochemical release of biologically available nitrogen from aquatic dissolved organic matter. Nature 381, 404–407. <https://doi.org/10.1038/381404a0>.
- Butler, A., Harder, T., Ostrowski, A.D., Carrano, C.J., 2021. Photoactive siderophores: structure, function and biology. J. Inorg. Biochem. 221, 111457. <https://doi.org/10.1016/j.jinorgbio.2021.111457>.
- Calvert, J.G., Pitts, J.N., 1966. *Photochemistry*. Wiley & Sons, New York, NY.

- Calza, P., Vione, D., Novelli, A., Pelizzetti, E., Minero, C., 2012. The role of nitrite and nitrate ions as photosensitizers in the phototransformation of phenolic compounds in seawater. *Sci Total Environ.* 439, 67–75. <https://doi.org/10.1016/j.scitotenv.2012.09.009>.
- Canadell, J.G., Monteiro, P.M.S., Costa, M.H., Cotrim da Cunha, L., Cox, P.M., Eliseev, A.V., Henson, S., Ishii, M., Jaccard, S., Koven, C., Lohila, A., Patra, P.K., Piao, S., Rogelj, J., Syampungani, S., Zaehle, S., Zickfeld, K., 2021. Global carbon and other biogeochemical cycles and feedbacks. In: Masson-Delmotte, V., Zhai, P., Pirani, A., Connors, S.L., Péan, C., Berger, S., Zhou, B. (Eds.), *Climate Change 2021: The Physical Science Basis. Contribution of Working Group I to the Sixth Assessment Report of the Intergovernmental Panel on Climate Change*. Cambridge University Press, Cambridge, United Kingdom and New York, NY.
- Canonica, S., Kohn, T., Mac, M., Real, F.J., Wirz, J., von Gunten, U., 2005. Photosensitizer method to determine rate constants for the reaction of carbonate radical with organic compounds. *Environ. Sci. Technol.* 39, 9182–9188. <https://doi.org/10.1021/es051236b>.
- Cao, F., Medeiros, P.M., Miller, W.L., 2016. Optical characterization of dissolved organic matter in the Amazon River plume and the adjacent ocean: examining the relative role of mixing, photochemistry, and microbial alterations. *Mar. Chem.* 186, 178–188. <https://doi.org/10.1016/j.marchem.2016.09.007>.
- Cao, F., Miller, W.L., 2015. A new algorithm to retrieve chromophoric dissolved organic matter (CDOM) absorption spectra in the UV from ocean color. *J. Geophys. Res. Oceans* 120, 496–516. <https://doi.org/10.1002/2014JC010241>.
- Cao, F., Mishra, D.R., Schalles, J.F., Miller, W.L., 2018. Evaluating ultraviolet (UV) based photochemistry in optically complex coastal waters using the Hyperspectral Imager for the Coastal Ocean (HICO). *Estuar. Coast. Shelf Sci.* 215, 199–206. <https://doi.org/10.1016/j.ecss.2018.10.013>.
- Cao, F., Zhu, Y., Kieber, D.J., Miller, W.L., 2020. Distribution and photo-reactivity of chromophoric and fluorescent dissolved organic matter in the Northeastern North Pacific Ocean. *Deep Sea Res. I* 155, 103168. <https://doi.org/10.1016/j.dsr.2019.103168>.
- Carlson, D.J., 1983. Dissolved organic materials in surface microlayers: temporal and spatial variability and relation to sea state. *Limnol. Oceanogr.* 28, 415–431. <https://doi.org/10.4319/lo.1983.28.3.0415>.
- Carpenter, L.J., Nightingale, P.D., 2015. Chemistry and release of gases from the surface ocean. *Chem. Rev.* 115, 4015–4034. <https://doi.org/10.1021/cr5007123>.
- Carpenter, E.J., Smith, K.L., 1972. Plastics on the Sargasso Sea surface. *Science* 175, 1240–1241. <https://doi.org/10.1126/science.175.4027.1240>.
- Cartisano, C.M., del Vecchio, R., Bianca, M.R., Blough, N.V., 2018. Investigating the sources and structure of chromophoric dissolved organic matter (CDOM) in the North Pacific Ocean (NPO) utilizing optical spectroscopy combined with solid phase extraction and borohydride reduction. *Mar. Chem.* 204, 20–35. <https://doi.org/10.1016/j.marchem.2018.05.005>.
- Caukins, J., 1982. *The Role of Solar Ultraviolet Radiation in Marine Ecosystems*. Springer, New York, <https://doi.org/10.1007/978-1-4684-8133-4>.
- Charlson, R.J., Lovelock, J.E., Andreae, M.O., Warren, S.G., 1987. Oceanic phytoplankton, atmospheric sulphur, cloud albedo and climate. *Nature* 326, 655–661. <https://doi.org/10.1038/326655a0>.
- Chen, H., McKenna, A.M., Niles, S.F., Frye, J.W., Glattke, T.J., Rodgers, R.P., 2022. Time-dependent molecular progression and acute toxicity of oil-soluble, interfacially-active, and water-soluble species reveals their rapid formation in the photodegradation of Macondo Well Oil. *Sci. Total Environ.* 813, 151884. <https://doi.org/10.1016/j.scitotenv.2021.151884>.
- Cheng, K., Zhang, L., McKay, G., 2023. Evaluating the microheterogeneous distribution of photochemically generated singlet oxygen using furfuryl amine. *Environ. Sci. Technol.* 57, 7568–7577. <https://doi.org/10.1021/acs.est.3c01726>.
- Chin, Y.-P., Miller, P.L., Zeng, L., Cawley, K., Weavers, L.K., 2004. Photosensitized degradation of bisphenol A by dissolved organic matter. *Environ. Sci. Technol.* 38, 5888–5894. <https://doi.org/10.1021/es0496569>.
- Chiu, R., Tiné, L., Gonzalez, L., Ciuraru, R., Bernard, F., George, C., Volkamer, R., 2017. UV photochemistry of carboxylic acids at the air-sea boundary: a relevant source of glyoxal and other oxygenated VOC in the marine atmosphere. *Geophys. Res. Lett.* 44, 1079–1087. <https://doi.org/10.1002/2016GL071240>.
- Chu, L., Anastasio, C., 2003. Quantum yields of hydroxyl radical and nitrogen dioxide from the photolysis of nitrate on ice. *J. Phys. Chem. A* 107, 9594–9602. <https://doi.org/10.1021/jp0349132>.
- Ciuraru, R., Fine, L., van Pinxteren, M., D'Anna, B., Herrmann, H., George, C., 2015a. Photosensitized production of functionalized and unsaturated organic compounds at the air-sea interface. *Sci. Reports* 5, 12741. <https://doi.org/10.1038/srep12741>.

- Ciuraru, R., Fine, L., van Pinxteren, M., D'Anna, B., Herrmann, H., George, C., 2015b. Unravelling new processes at interfaces: photochemical isoprene production at the sea surface. *Environ. Sci. Technol.* 49, 13199–13205. <https://doi.org/10.1021/acs.est.5b02388>.
- Clark, J.B., Neale, P., Tzortziou, M., Cao, F., Hood, R.R., 2019. A mechanistic model of photochemical transformation and degradation of colored dissolved organic matter. *Mar. Chem.* 214, 103666. <https://doi.org/10.1016/j.marchem.2019.103666>.
- Conte, L., Szopa, S., Séferian, R., Bopp, L., 2019. The oceanic cycle of carbon monoxide and its emissions to the atmosphere. *Biogeoscience* 16, 881–902. <https://doi.org/10.5194/bg-16-881-2019>.
- Cooper, W.J., Zika, R.G., Petasne, R.G., Fischer, A.M., 1989. Sunlight-induced photochemistry of humic substances in natural waters: major reactive species. In: Sutfet, I.H., MacCarthy, P. (Eds.), *Aquatic Humic Substances, Influence on Fate and Treatment of Pollutants*. *Adv. Chem. Ser.* 219. Amer. Chem. Soc., Washington, DC, pp. 333–362, <https://doi.org/10.1021/ba-1988-0219.ch022>.
- Cory, R.M., Kling, G.W., Stanley, E., del Giorgio, P., 2018. Interactions between sunlight and microorganisms influence dissolved organic matter degradation along the aquatic continuum. *Limnol. Oceanogr. Lett.* 3, 102–116. <https://doi.org/10.18739/A2SV8Z>.
- Cotner Jr., J.B., Heath, R.T., 1990. Iron redox effects on photosensitive phosphorus release from dissolved humic materials. *Limnol. Oceanogr.* 35, 1175–1181. <https://doi.org/10.4319/lo.1990.35.5.1175>.
- Cottrell, B.A., Gonsior, M., Timko, S.A., Simpson, A.J., Cooper, W.J., van der Veer, W., 2014. Photochemistry of marine and fresh waters: a role for copper-dissolved organic matter ligands. *Mar. Chem.* 162, 77–88. <https://doi.org/10.1016/j.marchem.2014.03.005>.
- Cudd, A., Fridovich, I., 1982. Electrostatic interactions in the reaction mechanism of bovine erythrocyte superoxide dismutase. *J. Biol. Chem.* 257, 11443–11447. [https://doi.org/10.1016/S0021-9258\(18\)33779-7](https://doi.org/10.1016/S0021-9258(18)33779-7).
- Cunliffe, M., Engel, A., Frka, S., Gašparović, B., Guitart, C., Murrell, J.C., et al., 2013. Sea surface microlayers: a unified physicochemical and biological perspective of the air-ocean interface. *Prog. Oceanogr.* 109, 104–116. <https://doi.org/10.1016/j.pocean.2012.08.004>.
- Cutter, G.A., Cutter, L.S., Filippino, K.C., 2004. Sources and cycling of carbonyl sulfide in the Sargasso Sea. *Limnol. Oceanogr.* 49, 555–565. <https://doi.org/10.4319/lo.2004.49.2.0055>.
- Damm, E., Kiene, R.P., Schwarz, J., Falck, E., Dieckmann, G., 2008. Methane cycling in Arctic shelf water and its relationship with phytoplankton biomass and DMSP. *Mar. Chem.* 109, 45–59. <https://doi.org/10.1016/j.marchem.2007.12.003>.
- Davidson, C., Amrani, A., Angert, A., 2021. Tropospheric carbonyl sulfide mass balance based on direct measurements of sulfur isotopes. *Proc. Natl. Acad. Sci.* 118, e2020060118. <https://doi.org/10.1073/pnas.2020060118>.
- Deal, C.J., Kieber, D.J., Toole, D.A., Starnes, K., Jiang, S., Uzuka, N., 2005. Dimethylsulfide photolysis rates and apparent quantum yields in Bering Sea seawater. *Cont. Shelf Res.* 25, 1825–1835. <https://doi.org/10.1016/j.csr.2005.06.006>.
- del Valle, D.A., Kieber, D.J., Bisgrove, J., Kiene, R.P., 2007. Light-stimulated production of dissolved DMSO by a particle-associated process in the Ross Sea, Antarctica. *Limnol. Oceanogr.* 52, 2456–2466. <https://doi.org/10.4319/lo.2007.52.6.2456>.
- del Vecchio, R., Blough, N.V., 2002. Photobleaching of chromophoric dissolved organic matter in natural waters: kinetics and modeling. *Mar. Chem.* 78, 231–253. [https://doi.org/10.1016/S0304-4203\(02\)00036-1](https://doi.org/10.1016/S0304-4203(02)00036-1).
- del Vecchio, R., Blough, N.V., 2004a. Spatial and seasonal distribution of chromophoric dissolved organic matter and dissolved organic carbon in the Middle Atlantic Bight. *Mar. Chem.* 89, 169–187. <https://doi.org/10.1016/j.marchem.2004.02.027>.
- del Vecchio, R., Blough, N.V., 2004b. On the origin of the optical properties of humic substances. *Environ. Sci. Technol.* 38, 3885–3891. <https://doi.org/10.1021/es049912h>.
- Dhavamani, J., Beck, A.J., Gledhill, M., El-Shahawi, M.S., Kadi, M.W., Ismail, I.M.I., Achterberg, E.P., 2022. The effects of salinity, temperature, and UV irradiation on leaching and adsorption of phthalate esters from polyethylene in seawater. *Sci. Total Environ.* 838, 155461. <https://doi.org/10.1016/j.scitotenv.2022.155461>.
- Dister, B., Zafiriou, O.C., 1993. Photochemical free radical production rates in the eastern Caribbean. *J. Geophys. Res. C* 98, 2341–2352. <https://doi.org/10.1029/92JC02765>.
- Dittmar, T., Koch, B., Hertkorn, N., Kattner, G., 2008. A simple and efficient method for the solid-phase extraction of dissolved organic matter (SPE-DOM) from seawater. *Limnol. Oceanogr. Methods* 6, 230–235. <https://doi.org/10.4319/lom.2008.6.230>.
- Dittmar, T., Stubbins, A., Ito, T., Jones, D.C., 2017. Comment on “Dissolved organic sulfur in the ocean: biogeochemistry of a petagram inventory”. *Science* 356, 813. <https://doi.org/10.1126/science.aam6039>.

- Doney, S.C., Najjar, R.G., Stewart, S., 1995. Photochemistry, mixing and diurnal cycles in the upper ocean. *J. Mar. Res.* 53, 341–369. <https://doi.org/10.1357/0022240953213133>.
- Enders, K., Lenz, R., Stedmon, C.A., Nielsen, T.G., 2015. Abundance, size and polymer composition of marine microplastics \geq 10 μ m in the Atlantic Ocean and their modelled vertical distribution. *Mar. Pollut. Bull.* 100, 70–81. <https://doi.org/10.1016/j.marpolbul.2015.09.027>.
- Engel, A., Bange, H.W., Cunliffe, M., Burrows, S.M., Friedrichs, G., Galgani, L., Herrmann, H., Hertkorn, N., Johnson, M., Liss, P.S., Quinn, P.K., Schartau, M., Soloviev, A., Stolle, C., Upstill-Goddard, R.C., van Pinxteren, M., Zäncker, B., 2017. The Ocean's vital skin: toward an integrated understanding of the sea surface microlayer. *Front. Mar. Sci.* 4, 165. <https://doi.org/10.3389/fmars.2017.00165>.
- Erickson, P.R., Moor, K.J., Werner, J.J., Latch, D.E., Arnold, W.A., McNeill, K., 2018. Singlet oxygen phosphorescence as a probe for triplet-state dissolved organic matter reactivity. *Environ. Sci. Technol.* 52, 9170–9178. <https://doi.org/10.1021/acs.est.8b02379>.
- Eriksen, M., Lebreton, L.C.M., Carson, H.S., Thiel, M., Moore, C.J., Borerro, J.C., Galgani, F., Ryan, P.G., Reisser, J., 2014. Plastic pollution in the World's oceans: more than 5 trillion plastic pieces weighing over 250,000 tons afloat at sea. *PLoS One* 9, e111913. <https://doi.org/10.1371/journal.pone.0111913>.
- Eriksen, M., Cowger, W., Erdle, L.M., Coffin, S., Villarrubia-Gómez, P., Moore, C.J., Carpenter, E.J., Day, R.H., Thiel, M., Wilcox, C., 2023. A growing plastic smog, now estimated to be over 170 trillion plastic particles afloat in the world's oceans—urgent solutions required. *PLoS ONE* 18, e0281596. <https://doi.org/10.1371/journal.pone.0281596>.
- Estapa, M.L., Mayer, L.M., Boss, E., 2012. Rate and apparent quantum yield of sedimentary organic matter. *Limnol. Oceanogr.* 57, 1743–1756. <https://doi.org/10.4319/lo.2012.57.6.1743>.
- Eyheragüibel, B., Traikia, M., Fontanella, S., Sancelme, M., Bonhomme, S., Fromageot, D., Lemaire, J., Lauranson, G., Lacoste, J., Delort, A.M., 2017. Characterization of oxidized oligomers from polyethylene films by mass spectrometry and NMR spectroscopy before and after biodegradation by a *Rhodococcus rhodochrous* strain. *Chemosphere* 184, 366–374. <https://doi.org/10.1016/j.chemosphere.2017.05.137>.
- Fabbri, D., Carena, L., Bertone, D., Brigante, M., Passananti, M., Vione, D., 2023. Assessing the photodegradation potential of compounds derived from the photoinduced weathering of polystyrene in water. *Sci. Total Environ.* 876, 162729. <https://doi.org/10.1016/j.scitotenv.2023.162729>.
- Fairbrother, A., Hsueh, H.-C., Kim, J.H., Jacobs, D., Perry, L., Goodwin, D., White, C., Watson, S., Sung, L.-P., 2019. Temperature and light intensity effects on photodegradation of high-density polyethylene. *Polym. Degrad. Stab.* 165, 153–160. <https://doi.org/10.1016/j.polymdegradstab.2019.05.002>.
- Farrington, J.W., Overton, E.B., Passow, U., 2021. Biogeochemical processes affecting the fate of discharged deepwater horizon gas and oil. *Oceanogr.* 34, 76–97. <https://doi.org/10.2307/27020062>.
- Ferek, R.J., Andreae, M.O., 1984. Photochemical production of carbonyl sulfide in marine surface waters. *Nature* 307, 148–150. <https://doi.org/10.1038/307148a0>.
- Ferrer-González, F.X., Widner, B., Holderman, N.R., Glushka, J., Edison, A.S., Kujawinski, E.B., Moran, M.A., 2021. Resource partitioning of phytoplankton metabolites that support bacterial heterotrophy. *ISME J.* 15, 762–773. <https://doi.org/10.1038/s41396-020-00811-y>.
- Fichot, C.G., Benner, R., 2014. The fate of terrigenous dissolved organic carbon in a river-influenced ocean margin. *Global Biogeochem. Cycles* 28, 300–318. <https://doi.org/10.1002/2013GB004670>.
- Fichot, C.G., Miller, W.L., 2010. An approach to quantify depth-resolved marine photochemical fluxes using remote sensing: application to carbon monoxide (CO) photoproduction. *Remote Sens. Environ.* 114, 1363–1377. <https://doi.org/10.1016/j.rse.2010.01.019>.
- Fichot, C.G., Miller, W.L., Sathyendranath, S., 2008. SeaUV and SeaUVC: algorithms for the retrieval of UV/visible diffuse attenuation coefficients from ocean color. *Remote Sens. Environ.* 112, 1584–1602. <https://doi.org/10.1016/j.rse.2007.08.009>.
- Field, C.B., Behrenfeld, M.J., Randerson, J.T., Falkowski, P., 1998. Primary production of the biosphere: integrating terrestrial and oceanic components. *Science* 281, 237–240. <https://doi.org/10.1126/science.281.5374.237>.
- Fitch, A., Orland, C., Willer, D., Emilson, E.J.S., Tanentzap, A.J., 2018. Feasting on terrestrial organic matter: dining in a dark lake changes microbial decomposition. *Glob. Change Biol.* 24, 5110–5122. <https://doi.org/10.1111/gcb.14391>.
- Flöck, O.R., Andreae, M.O., 1996. Photochemical and non-photochemical formation and destruction of carbonyl sulfide and methyl mercaptan in ocean waters. *Mar. Chem.* 54, 11–26. [https://doi.org/10.1016/0304-4203\(96\)00027-8](https://doi.org/10.1016/0304-4203(96)00027-8).
- Flöck, O.R., Andreae, M.O., Dräger, M., 1997. Environmentally relevant precursors of carbonyl sulfide in aquatic systems. *Mar. Chem.* 59, 71–85. [https://doi.org/10.1016/S0304-4203\(97\)00012-1](https://doi.org/10.1016/S0304-4203(97)00012-1).

- Focardi, A., Moore, L.R., Raina, J.-B., Seymour, J.R., Paulsen, I.T., Tetu, S.G., 2022. Plastic leachates impair picophytoplankton and dramatically reshape the marine microbiome. *Microbiome* 10, 179. <https://doi.org/10.1186/s40168-022-01369-x>.
- Freeman, D.H., Ward, C.P., 2022. Sunlight-driven dissolution is a major fate of oil at sea. *Sci. Adv.* 8, eabl7605. <https://doi.org/10.1126/sciadv.abl7605>.
- Fu, H., Ciuraru, R., Dupart, Y., Passananti, M., Tiné, L., Rossignol, S., Perrier, S., Donaldson, D.J., Chen, J., George, C., 2015. Photosensitized production of atmospherically reactive organic compounds at the air/aqueous interface. *J. Am. Chem. Soc.* 137, 8348–8351. <https://doi.org/10.1021/jacs.5b04051>.
- Fujii, M., Otani, E., 2017. Photochemical generation and decay kinetics of superoxide and hydrogen peroxide in the presence of standard humic and fulvic acids. *Water Res.* 123, 642–654. <https://doi.org/10.1016/j.watres.2017.07.015>.
- Galgani, L., Loiselle, S.A., 2021. Plastic pollution impacts on marine carbon biogeochemistry. *Env. Pollut.* 268, 115598. <https://doi.org/10.1016/j.envpol.2020.115598>.
- Galí, M., Simó, R., Vila-Costa, M., Ruiz-González, C., Gasol, J.M., Matrai, P., 2013a. Diel patterns of oceanic dimethylsulfide (DMS) cycling: microbial and physical drivers. *Global Biogeochem. Cycles* 27, 620–636. <https://doi.org/10.1002/gbc.20047>.
- Galí, M., Ruiz-González, C., Lefort, T., Gasol, J.M., Cardelus, C., Romera-Castillo, C., Simó, R., 2013b. Spectral irradiance dependence of sunlight effects on plankton dimethylsulfide production. *Limnol. Oceanogr.* 58, 489–504. <https://doi.org/10.4319/lo.2013.58.2.0489>.
- Galí, M., Kieber, D.J., Romera-Castillo, C., Kinsey, J.D., Devred, E., Pérez, G.L., Westby, G.R., Marrasé, C., Babin, M., Levasseur, M., Duarte, C.M., Agustí, S., Simó, R., 2016. CDOM sources and photobleaching control quantum yields for oceanic DMS photolysis. *Environ. Sci. Technol.* 50, 13361–13370. <https://doi.org/10.1021/acs.est.6b04278>.
- Galí, M., Devred, E., Pérez, G.L., Kieber, D.J., Simó, R., 2023. Global ocean dimethylsulfide photolysis rates quantified with a spectrally and vertically resolved model. *Limnol. Oceanogr. Lett.* 8, 760–769. <https://doi.org/10.1002/lol2.10342>.
- Garg, S., Rose, A.L., Waite, T.D., 2011. Photochemical production of superoxide and hydrogen peroxide from natural organic matter. *Geochim. Cosmochim. Acta* 75, 4310–4320. <https://doi.org/10.1016/j.gca.2011.05.014>.
- Garver, S.A., Siegel, D.A., 1997. Inherent optical property inversion of ocean color spectra and its biogeochemical interpretation. 1. Time series from the Sargasso Sea. *J. Geophys. Res. C* 102, 18607–18625. <https://doi.org/10.1029/96JC03243>.
- Gewert, B., Plassmann, M.M., MacLeod, M., 2015. Pathways for degradation of plastic polymers floating in the marine environment. *Environ. Sci.: Processes Impacts* 17, 1513–1521. <https://doi.org/10.1039/C5EM00207A>.
- Geyer, R., Jambeck, J.R., Law, K.L., 2017. Production, use, and fate of all plastics ever made. *Sci. Adv.* 3, e1700782. <https://doi.org/10.1126/sciadv.1700782>.
- Gieskes, W.W.C., Laane, R.W.P.M., Ruardij, P., 2015. Photo-oxidation: major sink of oxygen in the ocean surface layer. *Mar. Chem.* 177, 472–475. <https://doi.org/10.1016/j.marchem.2015.06.003>.
- Gligorovski, S., Strelkowski, R., Barbati, S., Vione, D., 2015. Environmental implications of hydroxyl radicals (OH). *Chem. Rev.* 114, 13051–13092. <https://doi.org/10.1021/cr500310b>.
- Gobler, C.J., Hutchins, D.A., Fisher, N.S., Cosper, E.M., Sanudo-Wilhelmy, S.A., 1997. Release and bioavailability of C, N, P, Se and Fe following viral release of a marine chrysophyte. *Limnol. Oceanogr.* 42, 1492–1504. <https://doi.org/10.4319/lo.1997.42.7.1492>.
- Goldstone, J.V., Pullin, M.J., Bertilsson, S., Voelker, B.M., 2002. Reactions of hydroxyl radical with humic substances: bleaching, mineralization, and production of bioavailable carbon substrates. *Environ. Sci. Technol.* 36, 364–372. <https://doi.org/10.1021/es0109646>.
- Goldstone, J.V., Voelker, B.M., 2000. Chemistry of superoxide radical in seawater: CDOM associated sink of superoxide in coastal waters. *Environ. Sci. Technol.* 34, 1043–1048. <https://doi.org/10.1021/es9905445>.
- Gomez-Saez, G.V., Pohlabeln, A.M., Stubbins, A., Marsay, C.M., Dittmar, T., 2017. Photochemical alteration of dissolved organic sulfur from sulfidic porewater. *Environ. Sci. Technol.* 51, 14144–14154. <https://doi.org/10.1021/acs.est.7b03713>.
- Gonsior, M., Peake, B.M., Cooper, W.T., Podgorski, D., Andrilli, J.D., Cooper, W.J., 2009. Photochemically induced changes in dissolved organic matter identified by ultrahigh resolution Fourier transform ion cyclotron resonance mass spectrometry. *Environ. Sci. Technol.* 43, 698–703. <https://doi.org/10.1021/es8022804>.

- Gonsior, M., Schmitt-Kopplin, P., Bastviken, D., 2013. Depth-dependent molecular composition and photo-reactivity of dissolved organic matter in a boreal lake under winter and summer conditions. *Biogeoscience* 10, 6945–6956. <https://doi.org/10.5194/bg-10-6945-2013>.
- Gonsior, M., Hertkorn, N., Conte, M.H., Cooper, W.J., Bastviken, D., Druffel, E., Schmitt-Kopplin, P., 2014. Photochemical production of polyols arising from significant photo-transformation of dissolved organic matter in the oligotrophic surface ocean. *Mar. Chem.* 163, 10–18. <https://doi.org/10.1016/j.marchem.2014.04.002>.
- Gonsior, M., Powers, L., Lahm, M., McCallister, S.L., 2022. New perspectives on the marine carbon cycle—the marine dissolved organic matter reactivity continuum. *Environ. Sci. Technol.* 56, 5371–5380. <https://doi.org/10.1021/acs.est.1c08871>.
- González-Gaya, B., Casal, P., Jurado, E., Dachs, J., Jiménez, B., 2019. Vertical transport and sinks of perfluoroalkyl substances in the global open ocean. *Environ. Sci.: Processes Impacts* 21, 1957–1969. <https://doi.org/10.1039/C9EM00266A>.
- Goudriaan, M., Morales, V.H., van der Meer, M.T.J., Mets, A., Ndhlovu, R.T., van Heerwaarden, J., Simon, S., Heuer, V.B., Hinrichs, K.-U., Niemann, H., 2023. A stable isotope assay with ^{13}C -labeled polyethylene to investigate plastic mineralization mediated by *Rhodococcus ruber*. *Mar. Pollut. Bull.* 186, 114369. <https://doi.org/10.1016/j.marpolbul.2022.114369>.
- Grandbois, M., Latch, D.E., McNeill, K., 2008. Microheterogeneous concentrations of singlet oxygen in natural organic matter isolate solutions. *Environ. Sci. Technol.* 42, 9184–9190. <https://doi.org/10.1021/es8017094>.
- Grebel, J.E., Pignatello, J.J., Song, W., Cooper, W.J., Mitch, W.A., 2009. Impact of halides on the photobleaching of dissolved organic matter. *Mar. Chem.* 115, 134–144. <https://doi.org/10.1016/j.marchem.2009.07.009>.
- Grunert, B.K., Tzortziou, M., Neale, P., Menendez, A., Hernes, P., 2021. DOM degradation by light and microbes along the Yukon River-coastal ocean continuum. *Sci. Rep.* 11, 10236. <https://doi.org/10.1038/s41598-021-89327-9>.
- Grzybowski, W., Tranvik, L., 2008. Phototransformations of dissolved organic nitrogen. In: Capone, D.G., Bronk, D.A., Mulholland, M.R., Carpenter, E.J. (Eds.), *Nitrogen in the Marine Environment*, second ed. Academic Press, Boston, pp. 511–527, <https://doi.org/10.1016/B978-0-12-372522-6.00010-4>.
- Gu, Y., Lensu, A., Perämäki, S., Ojala, A., Väätäalo, A.V., 2017. Iron and pH regulating the photochemical mineralization of dissolved organic carbon. *ACS Omega* 2, 1905–1914. <https://doi.org/10.1021/acsomega.7b00453>.
- Guo, M., Li, X., Song, C., Liu, G., Zhou, Y., 2020. Photo-induced phosphate release during sediment resuspension in shallow lakes: a potential positive feedback mechanism of eutrophication. *Environ. Pollut.* 258, 113679. <https://doi.org/10.1016/j.envpol.2019.113679>.
- Hakkarainen, M., Albertsson, A.C., 2004. Environmental degradation of polyethylene. In: Albertsson, A.C. (Ed.), *Long Term Properties of Polyolefins, Advances in Polymer Science*. Vol. 169. Springer, Berlin, Heidelberg, pp. 177–200, <https://doi.org/10.1007/b13523>.
- Hamdun, A.M., Higaonna, Y., Uehara, H., Arakaki, T., 2016. Role of the Fenton reaction in coastal seawater samples collected in Okinawa, Japan. *Chem. Lett.* 46, 42–44. <https://doi.org/10.1246/cl.160894>.
- Hansell, D.A., Carlson, C.A., Repeta, D.J., Schlitzer, R., 2009. Dissolved organic matter in the ocean. *Oceanography* 22, 202–211. <https://doi.org/10.5670/oceanog.2009.109>.
- Hao, Z., Yin, Y., Cao, D., Liu, J., 2017. Probing and comparing the photobromination and photoiodination of dissolved organic matter by using ultra-high-resolution mass spectrometry. *Environ. Sci. Technol.* 51, 5464–5472. <https://doi.org/10.1021/acs.est.6b03887>.
- Harfmann, J.L., Avery Jr., G.B., Rainey, H.D., Mead, R.N., Skrabal, S.A., Kieber, R.J., Felix, J.D., Helms, J.R., Podgorski, D.C., 2021. Composition and lability of photochemically released dissolved organic matter from resuspended estuarine sediments. *Org. Geochem.* 151, 104164. <https://doi.org/10.1016/j.orggeochem.2020.104164>.
- Harriman, B.H., Zito, P., Podgorski, D.C., Tarr, M.A., Suflita, J.M., 2017. Impact of photooxidation and biodegradation on the fate of oil spilled during the Deepwater Horizon incident: advanced stages of weathering. *Environ. Sci. Technol.* 51, 7412–7421. <https://doi.org/10.1021/acs.est.7b01278>.
- Harsha, M.L., Redman, Z.C., Wesolowski, J., Podgorski, D.C., Tomco, P.L., 2023. Photochemical formation of water-soluble oxyPAHs, naphthenic acids, and other hydrocarbon oxidation products from Cook Inlet, Alaska crude oil and diesel in simulated seawater spills. *Environ. Sci. Adv.* 2, 447–461. <https://doi.org/10.1039/d2va00325b>.
- Hassett, J.P., 2006. Dissolved natural organic matter as a microreactor. *Science* 311, 1723–1724. <https://doi.org/10.1126/science.1123389>.
- Hatton, A.D., 2002. Influence of photochemistry on the marine biogeochemical cycle of dimethylsulphide in the northern North Sea. *Deep Sea Res. II* 49, 3039–3052. [https://doi.org/10.1016/S0967-0645\(02\)00070-X](https://doi.org/10.1016/S0967-0645(02)00070-X).

- Heller, M.I., Croot, P.L., 2010a. Kinetics of superoxide reactions with dissolved organic matter in tropical Atlantic surface waters near Cape Verde (TENATSO). *J. Geophys. Res. C* 115, C12. <https://doi.org/10.1029/2009JC006021>.
- Heller, M.I., Croot, P.L., 2010b. Superoxide decay kinetics in the Southern Ocean. *Environ. Sci. Technol.* 44, 191–196. <https://doi.org/10.1021/es901766r>.
- Heller, M.I., Croot, P.L., 2011. Superoxide decay as a probe for speciation changes during dust dissolution in Tropical Atlantic surface waters near Cape Verde. *Mar. Chem.* 126, 37–55. <https://doi.org/10.1016/j.marchem.2011.03.006>.
- Heller, M.I., Wuttig, K., Croot, P.L., 2016. Identifying the sources and sinks of CDOM/FDOM across the Mauritanian shelf and their potential role in the decomposition of superoxide (O_2^-). *Front. Mar. Sci.* 3, 132. <https://doi.org/10.3389/fmars.2016.00132>.
- Helms, J.R., Mao, J., Stubbins, A., Schmidt-Rohr, K., Spencer, R.G.M., Hernes, P.J., Mopper, K., 2014. Loss of optical and molecular indicators of terrigenous dissolved organic matter during long-term photobleaching. *Aquat. Sci.* 76, 353–373. <https://doi.org/10.1007/s00027-014-0340-0>.
- Henrichs, S.M., Williams, P.M., 1985. Dissolved and particulate amino acids and carbohydrates in the sea surface microlayer. *Limnol. Oceanogr.* 17, 141–163. [https://doi.org/10.1016/0304-4203\(85\)90070-2](https://doi.org/10.1016/0304-4203(85)90070-2).
- Hernes, P.J., Benner, R., 2003. Photochemical and microbial degradation of dissolved lignin phenols: implications for the fate of terrigenous dissolved organic matter in marine environments. *J. Geophys. Res. C* 108, 3291. <https://doi.org/10.1029/2002JC001421>.
- Hernes, P.J., Spencer, R.G.M., Dyda, R.Y., Pellerin, B.A., Bachand, P.A.M., Bergamaschi, B.A., 2008. The role of hydrologic regimes on dissolved organic carbon composition in an agricultural watershed. *Geochim. Cosmochim. Acta* 72, 5266–5277. <https://doi.org/10.1016/j.gca.2008.07.031>.
- Hertkorn, N., Benner, R., Frommberger, M., Schmitt-Kopplin, P., Witt, M., Kaiser, K., Kettrup, A., Hedges, J.I., 2006. Characterization of a major refractory component of marine dissolved organic matter. *Geochim. Cosmochim. Acta* 70, 2990–3010. <https://doi.org/10.1016/j.gca.2006.03.021>.
- Hertkorn, N., Harir, M., Koch, B.P., Michalke, B., Schmitt-Kopplin, P., 2013. High-field NMR spectroscopy and FTICR mass spectrometry: powerful discovery tools for the molecular level characterization of marine dissolved organic matter. *Biogeoscience* 10, 1583–1624. <https://doi.org/10.5194/bg-10-1583-2013>.
- Holt, A.D., Kellerman, A.M., Li, W., Stubbins, A., Wagner, S., McKenna, A., Fellman, J., Hood, E., Spencer, R.G., 2021. Assessing the role of photochemistry in driving the composition of dissolved organic matter in glacier runoff. *J. Geophys. Res. Biogeosci.* 126, e2021JG006516. <https://doi.org/10.1029/2021JG006516>.
- Hu, C., Muller-Karger, F.E., Zepp, R.G., 2002. Absorbance, absorption coefficient, and apparent quantum yield: a comment on common ambiguity in the use of these optical concepts. *Limnol. Oceanogr.* 47, 1261–1267. <https://doi.org/10.4319/lo.2002.47.4.1261>.
- Hu, B., Wang, P., Wang, C., Bao, T., 2022a. Photogeochemistry of particulate organic matter in aquatic systems: a review. *Sci. Total Environ.* 806, 150467. <https://doi.org/10.1016/j.scitotenv.2021.150467>.
- Hu, E., Hu, L., Zheng, Y., Wu, Y., Wang, X., Sun, C., Su, Y., 2022b. Bacterial abundance and community structure in response to nutrients and photodegraded terrestrial humic acids in a eutrophic lake. *Environ. Sci. Pollut. Res.* 29, 8218–8231. <https://doi.org/10.1007/s11356-021-16288-x>.
- Hu, B., Wang, P., Zhang, N., Wang, C., Ao, Y., 2016. Photoproduction of dissolved organic carbon and inorganic nutrients from resuspended lake sediments. *Environ. Sci. Pollut. Res.* 23, 22126–22135. <https://doi.org/10.1007/s11356-016-7327-4>.
- Huang, J., Mabury, S.A., 2000. The role of carbonate radical in limiting the persistence of sulfur-containing chemicals in sunlit natural waters. *Chemosphere* 41, 1775–1782. [https://doi.org/10.1016/S0045-6535\(00\)00042-4](https://doi.org/10.1016/S0045-6535(00)00042-4).
- Huang, D., Wang, J., Xia, H., Zhang, Y., Bao, F., Li, M., Chen, C., Zhao, J., 2020. Enhanced photochemical volatile organic compounds release from fatty acids by surface-enriched Fe(III). *Environ. Sci. Technol.* 54, 13448–13457. <https://doi.org/10.1021/acs.est.0c03793>.
- Huang, L., Zhu, X., Zhou, S., Cheng, Z., Shi, K., Zhang, C., Shao, H., 2021. Phthalic acid esters: natural sources and biological activities. *Toxins* 13, 495. <https://doi.org/10.3390/toxins13070495>.
- Huie, R.E., Padmaja, S., 1993. The reaction of NO with superoxide. *Free Radic. Res. Commun.* 18, 195–199. <https://doi.org/10.3109/10715769309145868>.
- Hulswar, S., Simó, R., Galí, M., Bell, T.G., Lana, A., Inamdar, S., Halloran, P.R., Manville, G., Mahajan, A.S., 2022. Third revision of the global surface seawater dimethyl sulfide climatology (DMS-Rev3). *Earth Syst. Sci. Data* 14, 2963–2987. <https://doi.org/10.5194/essd-14-2963-2022>.
- Jammoul, A., Dumas, S., D'anna, B., George, C., 2009. Photoinduced oxidation of sea salt halides by aromatic ketones: a source of halogenated radicals. *Atmos. Chem. Phys.* 9, 4229–4237. <https://doi.org/10.5194/acp-9-4229-2009>.

- Jankowski, J.J., Kieber, D.J., Mopper, K., 1999. Nitrate and nitrite ultraviolet actinometers. *Photochem. Photobiol.* 70, 319–328. <https://doi.org/10.1111/j.1751-1097.1999.tb08143.x>.
- Jaramillo, M., Joens, J.A., O'Shea, K.E., 2020. Fundamental studies of the singlet oxygen reactions with the potent marine toxin domoic acid. *Environ. Sci. Technol.* 54, 6073–6081. <https://doi.org/10.1021/acs.est.9b07380>.
- Javad, H., Metz, J., Eraslan, T.C., Mathieu, J., Wang, B., Wu, G., Tsai, A.-L., Wong, M.S., Alvarez, P.J.J., 2020. Discerning the relevance of superoxide in PFOA degradation. *Environ. Sci. Technol. Lett.* 7, 653–658. <https://doi.org/10.1021/acs.estlett.0c00505>.
- Jerusalén-Lléo, E., Nieto-Cid, M., Fuentes-Santos, I., Dittmar, T., Álvarez-Salgado, X.A., 2023. Solid phase extraction of ocean dissolved organic matter with PPL cartridges: efficiency and selectivity. *Front. Mar. Sci.* 10, 159762. <https://doi.org/10.3389/fmars.2023.1159762>.
- Jian, S., Zhang, H.-H., Zhang, J., Yang, G.-P., 2017. Spatiotemporal distribution characteristics and environmental control factors of biogenic dimethylated sulfur compounds in the East China Sea during spring and autumn. *Limnol. Oceanogr.* 63, S280–S298. <https://doi.org/10.1002/limo.10737>.
- Jiang, H., He, Y., Wang, Y., Li, S., Jiang, B., Carena, L., Li, X., Yang, L., Luan, T., Vione, D., Gligorovski, S., 2022. Formation of organic sulfur compounds through SO_2 -initiated photochemistry of PAHs and dimethylsulfoxide at the air-water interface. *Atmos. Chem. Phys.* 22, 4237–4252. <https://doi.org/10.5194/acp-22-4237-2022>.
- Johannessen, S.J., Miller, W.L., 2001. Quantum yield for the photochemical production of dissolved inorganic carbon in seawater. *Mar. Chem.* 76, 271–283. [https://doi.org/10.1016/S0304-4203\(01\)00067-6](https://doi.org/10.1016/S0304-4203(01)00067-6).
- Jones, M.W., Coppola, A.I., Santín, C., Dittmar, T., Jaffé, R., Doerr, S.H., Quine, T.A., 2020. Fires prime terrestrial organic carbon for riverine export to the global oceans. *Nat. Commun.* 11, 2791. <https://doi.org/10.1038/s41467-020-16576-z>.
- Kamal, M.R., 1967. *Weatherability of Plastic Materials*. Interscience Publishers, Easton, PA.
- Karl, D.M., Beversdorf, L., Björkman, K.M., Church, M.J., Martinez, A., Delong, E.F., 2008. Aerobic production of methane in the sea. *Nat. Geosci.* 1, 473–478. <https://doi.org/10.1038/ngeo234>.
- Katz, S.D., Chen, H., Fields, D.M., Beirne, E.C., Keyes, P., Drozd, G.T., Aepli, C., 2022. Changes in chemical composition and copepod toxicity during petroleum photo-oxidation. *Environ. Sci. Technol.* 56, 5552–5562. <https://doi.org/10.1021/acs.est.2c00251>.
- Kellerman, A.M., Vonk, J., McColaugh, S., Podgorski, D.C., van Winden, E., Hawkings, J.R., Johnston, S.E., Humayun, M., Spencer, R.G., 2021. Molecular signatures of glacial dissolved organic matter from Svalbard and Greenland. *Global Biogeochem. Cycles* 35, e2020GB006709. <https://doi.org/10.1029/2020GB006709>.
- Kemsley, J., 2015. Celebrating the international year of light. *Chem. Eng. News* 93, 13–19.
- Kettle, A.J., 2005. Diurnal cycling of carbon monoxide (CO) in the upper ocean near Bermuda. *Ocean Model.* 8, 337–367. <https://doi.org/10.1016/j.ocemod.2004.01.003>.
- Khaled, A., Rivaton, A., Richard, C., Jaber, F., Sleiman, M., 2018. Phototransformation of plastic containing brominated flame retardants: enhanced fragmentation and release of photoproducts to water and air. *Environ. Sci. Technol.* 52, 11123–11131. <https://doi.org/10.1021/acs.est.8b03172>.
- Khalil, M.A.K., Rasmussen, R.A., 1984. Global sources, lifetimes and mass balances of carbonyl sulfide (OCS) and carbon disulfide (CS_2) in the earth's atmosphere. *Atmos. Environ.* 18, 1805–1813. [https://doi.org/10.1016/0004-6981\(84\)90356-1](https://doi.org/10.1016/0004-6981(84)90356-1).
- Kieber, D.J., McDaniel, J.A., Mopper, K., 1989. Photochemical source of biological substrates in seawater: implications for carbon cycling. *Nature* 341, 637–639. <https://doi.org/10.1038/341637a0>.
- Kieber, D.J., Jiao, J.F., Kiene, R.P., Bates, T.S., 1996. Impact of dimethylsulfide photochemistry on methyl sulfur cycling in the equatorial Pacific Ocean. *J. Geophys. Res. C* 101, 3715–3722. <https://doi.org/10.1029/95JC03624>.
- Kieber, D.J., Yocis, B.H., Mopper, K., 1997. Free-floating drifter for photochemical studies in the water column. *Limnol. Oceanogr.* 42, 1829–1833. <https://doi.org/10.4319/lo.1997.42.8.1829>.
- Kieber, D.J., Peake, B.M., Scully, N.M., 2003. Reactive oxygen species in aquatic ecosystems. In: Helbling, E.W., Zagarese, H. (Eds.), *UV Effects on Aquatic Organisms and Ecosystems*, Comprehensive Series in Photochemistry and Photobiology. The Royal Society of Chemistry, Cambridge, UK, pp. 253–288, <https://doi.org/10.1039/9781847552266-00251>.
- Kieber, D.J., Toole, D.A., Jankowski, J.J., Kiene, R.P., Westby, G.R., del Valle, D.A., Slezak, D., 2007. Chemical “light meters” for photochemical and photobiological studies. *Aquat. Sci.* 69, 360–376. <https://doi.org/10.1007/s00027-007-0895-0>.
- Kieber, R.J., Pitt, J., Skrabal, S.A., Wright, J.L.C., 2010. Photodegradation of the brevetoxin PbTx-2 in coastal seawater. *Limnol. Oceanogr.* 55, 2299–2304. <https://doi.org/10.4319/lo.2010.55.6.2299>.

- Kieber, D.J., Miller, G.W., Neale, P.J., Mopper, K., 2014. Wavelength and temperature-dependent apparent quantum yields for photochemical formation of hydrogen peroxide in seawater. *Environ. Sci.: Processes Impacts* 16, 777–791. <https://doi.org/10.1039/c4em00036f>.
- King, S.M., Leaf, P.A., Tarr, M.A., 2011. Photochemistry of deepwater horizon oil. In: Benvenuto, M.A., Roberts-Kirchhoff, E.S., Murray, M.N., Garshott, D.M. (Eds.), *It's All in the Water: Studies of Materials and Conditions in Fresh and Salt Water Bodies*. American Chemical Society, Washington, DC, pp. 81–95, <https://doi.org/10.1021/bk-2011-1086.ch006>.
- King, D.W., Berger, E., Helm, Z., Irish, E., Mopper, K., 2016. Measurement of antioxidant activity toward superoxide in natural waters. *Front. Mar. Sci.* 3, 217. <https://doi.org/10.3389/fmars.2016.00217>.
- Kirk, J.T.O., 1994. *Light and Photosynthesis in Aquatic Ecosystems*, second ed. Cambridge University Press, Cambridge, UK, <https://doi.org/10.1017/CBO9780511623370>.
- Koehler, B., Landelius, T., Weyhenmeyer, G.A., Machida, N., Tranvik, L.J., 2014. Sunlight-induced carbon dioxide emissions from inland waters. *Global Biogeochem. Cycles* 28, 696–711. <https://doi.org/10.1002/2014GB004850>.
- Koehler, B., Powers, L.C., Cory, R.M., Einarsdóttir, K., Gu, Y., Tranvik, L.J., Vähätilo, A.V., Ward, C.P., Miller, W.L., 2022. Inter-laboratory differences in the apparent quantum yield for the photochemical production of dissolved inorganic carbon in inland waters and implications for photochemical rate modeling. *Limnol. Oceanogr. Methods* 20, 320–337. <https://doi.org/10.1002/lom3.10489>.
- Ksionzek, K.B., Lechtenfeld, O.J., McCallister, S.L., Schmitt-Kopplin, P., Geuer, J.K., Geibert, W., Koch, B.P., 2016. Dissolved organic sulfur in the ocean: biogeochemistry of a petagram inventory. *Science* 354, 456–459. <https://doi.org/10.1126/science.aaf7796>.
- Kuhn, H.J., Braslavsky, S.E., Schmidt, R., 2004. Chemical actinometry (IUPAC Technical Report). *Pure Appl. Chem.* 76, 2105–2146. <https://doi.org/10.1351/pac200476122105>.
- Kujawinski, E.B., del Vecchio, R., Blough, N.V., Klein, G.C., Marshall, A.G., 2004. Probing molecular-level transformations of dissolved organic matter: insights on photochemical degradation and protozoan modification of DOM from electrospray ionization Fourier transform ion cyclotron resonance mass spectrometry. *Mar. Chem.* 92, 23–37. <https://doi.org/10.1016/j.marchem.2004.06.038>.
- Kurtz, T.D., 2021. *The Photodegradation of Saxitoxins in Surface Waters*. MSc Thesis, University of Colorado, Boulder, CO.
- Kurtz, T.D., Zeng, T., Rosario-Ortiz, F.L., 2021. Photodegradation of cyanotoxins in surface waters. *Water Res.* 192, 116804. <https://doi.org/10.1016/j.watres.2021.116804>.
- Larson, R.A., Zepp, R.G., 1988. Reactivity of the carbonate radical with aniline derivatives. *Environ. Toxicol. Chem.* 7, 265–274. <https://doi.org/10.1002/etc.5620070403>.
- Laszakovits, J.R., Berg, S.M., Anderson, B.G., O'Brien, J.E., Wammer, K.H., Sharpless, C.M., 2017. p-Nitroanisole/pyridine and p-nitroacetophenone/pyridine actinometers revisited: quantum yield in comparison to ferrioxalate. *Environ. Sci. Lett.* 4, 11–14. <https://doi.org/10.1021/acs.estlett.6b00422>.
- Latch, D.E., McNeill, K., 2006. Microheterogeneity of singlet oxygen distributions in irradiated humic acid solutions. *Science* 311, 1743–1747. <https://doi.org/10.1126/science.1121636>.
- Launois, T., Belviso, S., Bopp, L., Fichot, C.G., Peylin, P., 2015. A new model for the global biogeochemical cycle of carbonyl sulfide. Part 1. Assessment of direct marine emissions with an oceanic general circulation and biogeochemistry model. *Atmos. Chem. Phys.* 15, 2295–2312. <https://doi.org/10.5194/acp-15-2295-2015>.
- Law, K.L., 2017. Plastics in the marine environment. *Annu. Rev. Mar. Sci.* 9, 205–229. <https://doi.org/10.1146/annurev-marine-010816-060409>.
- Le Roux, D.M., Powers, L.C., Blough, N.V., 2021. Photoproduction rates of one-electron reductants by chromophoric dissolved organic matter via fluorescence spectroscopy: comparison with superoxide and hydrogen peroxide rates. *Environ. Sci. Technol.* 55, 12095–12105. <https://doi.org/10.1021/acs.est.1c04043>.
- Le Roux, D.M., Powers, L.C., Blough, N.V., 2023. Direct evidence of a light-dependent sink of superoxide within chromophoric dissolved organic matter. *Environ. Sci. Technol.* 57, 20627–20635. <https://doi.org/10.1021/acs.est.3c08254>.
- Leifer, A., 1988. *The Kinetics of Environmental Aquatic Photochemistry: Theory and Practice*. American Chemical Society, Washington, DC.
- Lennartz, S.T., von Hobe, M., Booge, D., Bittig, H.C., Fischer, T., Gonçalves-Araujo, R., Ksionzek, K.B., Koch, B.P., Bracher, A., Röttgers, R., Quack, B., Marandino, C.A., 2019. The influence of dissolved organic matter on the marine production of carbonyl sulfide (OCS) and carbon disulfide (CS₂) in the Peruvian upwelling. *Ocean Sci.* 15, 1071–1090. <https://doi.org/10.5194/os-15-1071-2019>.

- Li, H., McKay, G., 2021. Relationships between the physicochemical properties of dissolved organic matter and its reaction with sodium borohydride. *Environ. Sci. Technol.* 55, 10843–10851. <https://doi.org/10.1021/acs.est.1c01973>.
- Li, Y., Fichot, C.G., Geng, L., Scarratt, M.G., Xie, H., 2020. The contribution of methane photoproduction to the oceanic methane paradox. *Geophys. Res. Lett.* 47, e2020GL088362. <https://doi.org/10.1029/2020GL088362>.
- Li, J.-L., Zhai, X., Du, L., 2021. Photosensitized formation of sulfate and volatile sulfur gases from dissolved organic sulfur: roles of pH, dissolved oxygen, and salinity. *Sci. Total Environ.* 786, 147449. <https://doi.org/10.1016/j.scitotenv.2021.147449>.
- Li, J.-L., Zhai, X., Du, L., 2022. Effect of nitrate on the photochemical production of carbonyl sulfide from surface seawater. *Geophys. Res. Lett.* 49, e2021GL097051. <https://doi.org/10.1029/2021GL097051>.
- Li, X., Zhou, Y., Liu, G., Lei, H., Zhu, D., 2017. Mechanisms of the photochemical release of phosphate from resuspended sediments under solar irradiation. *Sci. Total Environ.* 595, 779–786. <https://doi.org/10.1016/j.scitotenv.2017.04.039>.
- Liang, S.-M., Zhai, X., Li, C.-X., Xin, M., Sun, P., Liu, X.-L., Liu, L., Wang, B.-D., 2023. Distribution and physical-biological controls of dimethylsulfide in the western tropical Indian Ocean during winter monsoon. *Front. Mar. Sci.* 10, 1100678. <https://doi.org/10.3389/fmars.2023.1100678>.
- Lin, J., Dai, Q., Zhao, H., Cao, H., Wang, T., Wang, G., Chen, C., 2021. Photoinduced release of volatile organic compounds from fatty alcohols at the air-water interface: the role of singlet oxygen photosensitized by a carbonyl group. *Environ. Sci. Technol.* 55, 8683–8690. <https://doi.org/10.1021/acs.est.1c00313>.
- Liu, D., Xiu, Z., Liu, F., Wu, G., Adamson, D., Newell, C., Vikesland, P., Tsai, A.L., Alvarez, P.J., 2013. Perfluorooctanoic acid degradation in the presence of Fe(III) under natural sunlight. *J. Hazard. Mater.* 262, 456–463. <https://doi.org/10.1016/j.jhazmat.2013.09.001>.
- Logozzo, L., Tzortziou, M., Neale, P., Clark, J.B., 2021. Photochemical and microbial degradation of chromophoric dissolved organic matter exported from tidal marshes. *J. Geophys. Res. Biogeosci.* 126, e2020JG005744. <https://doi.org/10.1029/2020JG005744>.
- Lønborg, C., Nieto-Cid, M., Hernando-Morales, V., Hernández-Ruiz, M., Teira, E., Álvarez-Salgado, X.A., 2016. Photochemical alteration of dissolved organic matter and the subsequent effects on bacterial carbon cycling and diversity. *FEMS Microbiol. Ecol.* 92, fiw048. <https://doi.org/10.1093/femsec/fiw048>.
- Longnecker, K., Oswald, L., Kido Soule, M.C., Cutter, G.A., Kujawinski, E.B., 2020. Organic sulfur: a spatially variable and understudied component of marine organic matter. *Limnol. Oceanogr. Lett.* 5, 305–312. <https://doi.org/10.1002/lo2.10149>.
- Lu, X., Beaupré, S., 2021. Evaluation of the moderate $\Delta \text{I}^{13}\text{C}$ isotope enrichment method for measuring photochemical mineralization of marine dissolved organic carbon. *Limnol. Oceanogr. Met.* 19, 651–658. <https://doi.org/10.1002/lim3.10450>.
- Lueder, U., Jørgensen, B.B., Kappler, A., Schmidt, C., 2020. Photochemistry of iron in aquatic environments. *Environ. Sci.: Processes Impacts* 22, 12–24. <https://doi.org/10.1039/C9EM00415G>.
- Ma, J., del Vecchio, R., Golanski, K.S., Boyle, E.S., Blough, N.V., 2010. Optical properties of humic substances and CDOM: effects of borohydride reduction. *Environ. Sci. Technol.* 44 (14), 5395–5402. <https://doi.org/10.1021/es100880q>.
- Ma, J., Zhou, H., Yan, S., Song, W., 2019. Kinetics studies and mechanistic considerations on the reactions of superoxide radical ions with dissolved organic matter. *Water Res.* 149, 56–64. <https://doi.org/10.1016/j.watres.2018.10.081>.
- Ma, J., Nie, J., Zhou, H., Wang, H., Lian, L., Yan, S., Song, W., 2020. Kinetic consideration of photochemical formation and decay of superoxide radical in dissolved organic matter solutions. *Environ. Sci. Technol.* 54, 3199–3208. <https://doi.org/10.1021/acs.est.9b06018>.
- Ma, Q.-Y., Zhang, H.-H., Xu, F., Yang, G.-P., 2022. Transformation processes of biogenic dimethylated sulfur compounds in the northwestern Pacific continental sea. *Limnol. Oceanogr.* 67, 903–917. <https://doi.org/10.1002/lo.12044>.
- Maavara, T., Logozzo, L., Stubbins, A., Aho, K., Brinkerhoff, C., Hosen, J., Raymond, P., 2021. Does photomineralization of dissolved organics matter in temperate rivers? *J. Geophys. Res. Biogeosci.* 126, e2021JG006402. <https://doi.org/10.1029/2021JG006402>.
- MacIntyre, F., 1974. Chemical fractionation and sea-surface microlayer processes. In: Goldberg, E.D. (Ed.), *The Sea, Volume 5, Marine Chemistry*. Wiley Interscience, New York, pp. 245–299.
- Mack, J., Bolton, J.R., 1999. Photochemistry of nitrite and nitrate in aqueous solution: a review. *J. Photochem. Photobiol. A: Chem.* 128, 1–13. [https://doi.org/10.1016/S1010-6030\(99\)00155-0](https://doi.org/10.1016/S1010-6030(99)00155-0).

- Madsen-Østerbye, M., Kragh, T., Pedersen, O., Sand-Jensen, K., 2018. Coupled UV-exposure and microbial decomposition improves measures of organic matter degradation and light models in humic lake. *Ecol. Eng.* 118, 191–200. <https://doi.org/10.1016/j.ecoleng.2018.04.018>.
- Mafra, L.L., Léger, C., Bates, S.S., Quilliam, M.A., 2009. Analysis of trace levels of domoic acid in seawater and plankton by liquid chromatography without derivatization, using UV or mass spectrometry detection. *J. Chromatogr. A* 1216, 6003–6011. <https://doi.org/10.1016/j.chroma.2009.06.050>.
- Maie, N., Pisani, O., Jaffé, R., 2008. Mangrove tannins in aquatic ecosystems: their fate and possible influence on dissolved organic carbon and nitrogen cycling. *Limnol. Oceanogr.* 53, 160–171. <https://doi.org/10.2307/40006158>.
- Majumdar, R.D., Blumkin, L., Lane, D., Soong, R., Simpson, M., Simpson, A.J., 2017. Analysis of DOM phototransformation using a looped NMR system integrated with a sunlight simulator. *Water. Res.* 120, 64–76. <https://doi.org/10.1016/j.watres.2017.04.067>.
- Maritorena, S., Siegel, D.A., Peterson, A.R., 2002. Optimization of a semianalytical ocean color model for global-scale applications. *Appl. Opt.* 41, 2705–2714. <https://doi.org/10.1364/AO.41.002705>.
- Masry, M., Rossignol, S., Gardette, J.-L., Therias, S., Bussière, P.-O., Chung, P.W.-W., 2021. Characteristics, fate, and impact of marine plastic debris exposed to sunlight: a review. *Mar. Pollut. Bull.* 171, 112701. <https://doi.org/10.1016/j.marpolbul.2021.112701>.
- Mazoyer, F., Laurion, I., Rautio, M., 2022. The dominant role of sunlight in degrading winter dissolved organic matter from a thermokarst lake in a subarctic peatland. *Biogeosciences* 19, 3959–3977. <https://doi.org/10.5194/bg-19-3959-2022>.
- Mazzotta, M.G., Reddy, C.M., Ward, C.P., 2022. Rapid degradation of cellulose diacetate by marine microbes. *Env. Sci. Technol. Lett.* 9, 37–41. <https://doi.org/10.1021/acs.estlett.1c00843>.
- McCallister, S.L., Bauer, J.E., Kelly, J., Ducklow, H.W., 2005. Effects of sunlight on decomposition of estuarine dissolved organic C, N and P and bacterial metabolism. *Aquat. Microb. Ecol.* 40, 25–35. <https://doi.org/10.3354/ame040025>.
- McKay, G., 2020. Emerging investigator series: critical review of photophysical models for the optical and photochemical properties of dissolved organic matter. *Environ. Sci.: Processes Impacts* 22, 1139–1165. <https://doi.org/10.1039/D0EM00056F>.
- McKay, G., Couch, K.D., Mezyk, S.P., Rosario-Ortiz, F.L., 2016. Investigation of the coupled effects of molecular weight and charge-transfer interactions on the optical and photochemical properties of dissolved organic matter. *Environ. Sci. Technol.* 50, 8093–8102. <https://doi.org/10.1021/acs.est.6b02109>.
- McKay, G., Huang, W., Romera-Castillo, C., Crouch, J.E., Rosario-Ortiz, F.L., Jaffé, R., 2017. Predicting reactive intermediate quantum yields from dissolved organic matter photolysis using optical properties and antioxidant capacity. *Environ. Sci. Technol.* 51, 5404–5413. <https://doi.org/10.1021/acs.est.6b06372>.
- McNabb, B.J., Tortell, P.D., 2023. Oceanographic controls on Southern Ocean dimethylsulfide distributions revealed by machine learning algorithms. *Limnol. Oceanogr.* 68, 616–630. <https://doi.org/10.1002/lno.12298>.
- McNeill, K., Canonica, S., 2016. Triplet state dissolved organic matter in aquatic photochemistry: reaction mechanisms, substrate scope, and photophysical properties. *Environ. Sci.: Processes Impacts* 18, 1381–1399. <https://doi.org/10.1039/C6EM00408C>.
- Medeiros, P.M., Seidel, M., Powers, L.C., Dittmar, T., Hansell, D.A., Miller, W.L., 2015a. Dissolved organic matter composition and photochemical transformations in the northern North Pacific Ocean. *Geophys. Res. Lett.* 42, 863–870. <https://doi.org/10.1002/2014GL062663>.
- Medeiros, P.M., Seidel, M., Ward, N.D., Carpenter, E.J., Gomes, H.R., Niggemann, J., Krusche, A.V., Richey, J.E., Yager, P.L., Dittmar, T., 2015b. Fate of the Amazon River dissolved organic matter in the tropical Atlantic Ocean. *Global Biogeochem. Cycles* 29, 677–690. <https://doi.org/10.1002/2015GB005115>.
- Medinas, D.B., Cerchiaro, G., Trindade, D.F., Augusto, O., 2007. The carbonate radical and related oxidants derived from bicarbonate buffer. *IUBMB Life* 59, 255–262. <https://doi.org/10.1080/15216540701230511>.
- Méndez-Díaz, J.D., Shimabuku, K.K., Ma, J., Enumah, Z.O., Pignatello, J.J., Mitch, W.A., Dodd, M.C., 2014. Sunlight-driven photochemical halogenation of dissolved organic matter in seawater: a natural abiotic source of organobromine and organoiodine. *Environ. Sci. Technol.* 48, 7418–7427. <https://doi.org/10.1021/es5016668>.
- Miller, W.L., Zepp, R.G., 1995. Photochemical production of dissolved inorganic carbon from terrestrial organic matter: significance to the oceanic organic carbon cycle. *Geophys. Res. Lett.* 22, 417–420. <https://doi.org/10.1029/94GL03344>.
- Miller, W.L., Moran, M., Sheldon, W.M., Zepp, R.G., Opsahl, S., 2002. Determination of apparent quantum yield spectra for the formation of biologically labile photoproducts. *Limnol. Oceanogr.* 47, 343–352. <https://doi.org/10.4319/lo.2002.47.2.0343>.

- Miller, M.A., Kudela, R.M., Mekebri, A., Crane, D., Oates, S.C., Tinker, M.T., Staedler, M., Miller, W.A., Toy-Choutka, S., Dominik, C., Hardin, D., Langlois, G., Murray, M., Ward, K., Jessup, D.A., 2010. Evidence for a novel marine harmful algal bloom: cyanotoxin (microcystin) transfer from land to sea otters. *PLoS One* 5, 1–11. <https://doi.org/10.1371/journal.pone.0012576>.
- Miller, C.J., Vincent Lee, S.M., Rose, A.L., Waite, T.D., 2012. Impact of natural organic matter on H₂O₂-mediated oxidation of Fe(II) in coastal seawaters. *Environ. Sci. Technol.* 46, 11078–11085. <https://doi.org/10.1021/es3022792>.
- Miller, C.J., Rose, A.L., Waite, T.D., 2016. Importance of iron complexation for fenton-mediated hydroxyl radical production at circumneutral pH. *Front. Mar. Sci.* 3, 134. <https://doi.org/10.3389/fmars.2016.00134>.
- Mobley, C.D., 2022. The Oceanic Optics Book. International Ocean Colour Coordinating Group (IOCCG), Dartmouth, NS, Canada, <https://doi.org/10.25607/OBP-1710>.
- Modiri Gharehveran, M., Shah, A.D., 2018. Indirect photochemical formation of carbonyl sulfide and carbon disulfide in natural waters: role of organic sulfur precursors, water quality constituents, and temperature. *Environ. Sci. Technol.* 52, 9108–9117. <https://doi.org/10.1021/acs.est.8b01618>.
- Modiri Gharehveran, M., Shah, A.D., 2021. Influence of dissolved organic matter on carbonyl sulfide and carbon disulfide formation from dimethyl sulfide during sunlight photolysis. *Water Environ. Res.* 93, 2982–2997. <https://doi.org/10.1002/wer.1650>.
- Modiri Gharehveran, M., Hain, E., Blaney, L., Shah, A.D., 2020. Influence of dissolved organic matter on carbonyl sulfide and carbon disulfide formation from cysteine during sunlight photolysis. *Environ. Sci: Processes Impacts* 22, 1852–1864. <https://doi.org/10.1039/D0EM00219D>.
- Moffett, J.W., Zafiriou, O.C., 1993. The photochemical decomposition of hydrogen peroxide in surface waters of the eastern Caribbean and Orinoco River. *J. Geophys. Res. C* 98, 2307–2313. <https://doi.org/10.1029/92JC02768>.
- Montalti, M., Credi, A., Prodi, L., Gandolfi, M.T., 2006. Handbook of Photochemistry, third ed. CRC Press, Boca Raton, FL, <https://doi.org/10.1201/9781420015195>.
- Mopper, K., Kieber, D.J., 2002. Photochemistry and the cycling of carbon, sulfur, nitrogen, and phosphorus. In: Hansell, D.A., Carlson, C.A. (Eds.), Biogeochemistry of Marine Dissolved Organic Matter. Academic Press, Boston, pp. 455–508, <https://doi.org/10.1016/B978-012323841-2/50011-7>.
- Mopper, K., Zhou, X., 1990. Hydroxyl radical photoproduction in the sea and its potential impact on marine processes. *Science* 250, 661–664. <https://doi.org/10.1126/science.250.4981.661>.
- Mopper, K., Zhou, X., Kieber, R.J., Kieber, D.J., Sikorski, R.J., Jones, R.D., 1991. Photochemical degradation of dissolved organic carbon and its impact on the oceanic carbon cycle. *Nature* 353, 60–62. <https://doi.org/10.1038/353060a0>.
- Mopper, K., Kieber, D.J., Stubbins, A., 2015. Marine photochemistry of organic matter: processes and impacts. In: Hansell, D.A., Carlson, C.A. (Eds.), Biogeochemistry of Marine Dissolved Organic Matter, second ed. Academic Press, Boston, pp. 389–450, <https://doi.org/10.1016/B978-0-12-405940-5.00008-X>.
- Moran, M.A., Kujawinski, E.B., Stubbins, A., Fatland, R., Aluwihare, L.I., Buchan, A., Crump, B.C., Dorrestein, P.C., Dyhrman, S.T., Hess, N.J., Howe, B., Longnecker, K., Medeiros, P.M., Niggemann, J., Obernosterer, I., Repeta, D.J., Waldbauer, J.R., 2016. Deciphering ocean carbon in a changing world. *Proc. Natl. Acad. Sci.* 113, 3143–3151. <https://doi.org/10.1073/pnas.151464511>.
- Morel, F.M., Price, N.M., 2003. The biogeochemical cycles of trace metals in the oceans. *Science* 300, 944–947. <https://doi.org/10.1126/science.1083545>.
- Morris, J.J., Rose, A.L., Lu, Z., 2022. Reactive oxygen species in the world ocean and their impacts on marine ecosystems. *Redox Biol.* 22, 102285. <https://doi.org/10.1016/j.redox.2022.102285>.
- Mostovaya, A., Koehler, B., Guillemette, F., Brunberg, A.-K., Tranvik, L.J., 2016. Effects of compositional changes on reactivity continuum and decomposition kinetics of lake dissolved organic matter. *J. Geophys. Res. Biogeosci.* 121, 1733–1746. <https://doi.org/10.1002/2016JG003359>.
- Müller, E., von Gunten, U., Bouchet, S., Droz, B., Winkel, L.H.E., 2019. Hypobromous acid as an unaccounted sink for marine dimethylsulfide? *Environ. Sci. Technol.* 53, 13146–13157. <https://doi.org/10.1021/acs.est.9b04310>.
- Müller, E., von Gunten, U., Bouchet, S., Droz, B., Winkel, L.H.E., 2021. Reaction of DMS and HOBr as a sink for marine DMS and an inhibitor of bromoform formation. *Environ. Sci. Technol.* 55, 5547–5558. <https://doi.org/10.1021/acs.est.0c08189>.
- Najjar, R.G., Erickson III, D.J., Madronich, S., 1995. Modeling the air-sea fluxes of gases formed from the decomposition of dissolved organic matter: carbonyl sulfide and carbon monoxide. In: Zepp, R.G., Sonntag, C. (Eds.), Role of Nonliving Organic Matter in the Earth's Carbon Cycle. Wiley & Sons, Chichester, UK, pp. 107–132. <http://n2t.net/ark:/85065/d7h133dw>.

- Nalven, S.G., Ward, C.P., Payet, J.P., Cory, R.M., Kling, G.W., Sharpton, T.J., Sullivan, C.M., Crump, B.C., 2022. Experimental metatranscriptomics reveals the costs and benefits of dissolved organic matter photo-alteration for freshwater microbes. *Environ. Microbiol.* 22, 3505–3521. <https://doi.org/10.1111/1462-2920.15121>.
- Neale, P.J., Kieber, D.J., 2000. Assessing biological and chemical effects of UV in the marine environment: spectral weighting functions. In: Hester, R.E., Harrison, R.M. (Eds.), *Causes and Environmental Implications of Increased UV-B Radiation*. The Royal Society of Chemistry, Cambridge, UK, pp. 61–83, <https://doi.org/10.1039/9781847550354-00061>.
- Neilan, A.D., Carroll, A.R., Hawker, D.W., O'Brien, K.R., Burford, M.A., 2019. Effects of photochemical and microbial changes in terrestrial dissolved organic matter on its chemical characteristics and phytotoxicity towards cyanobacteria. *Sci. Total Environ.* 695, 133901. <https://doi.org/10.1016/j.scitotenv.2019.133901>.
- Nelson, N.B., Siegel, D.A., 2013. The global distribution and dynamics of chromophoric dissolved organic matter. *Ann. Rev. Mar. Sci.* 5, 447–476. <https://doi.org/10.1146/annurev-marine-120710-100751>.
- Nelson, N.B., Siegel, D.A., Michaels, A.F., 1998. Seasonal dynamics of colored dissolved material in the Sargasso Sea. *Deep Sea Res. I* 45, 931–957. [https://doi.org/10.1016/S0967-0637\(97\)00106-4](https://doi.org/10.1016/S0967-0637(97)00106-4).
- Nelson, N.B., Siegel, D.A., Carlson, C.A., Swan, C., Smethie, W.M., Khatiwala, S., 2007. Hydrography of chromophoric dissolved organic matter in the North Atlantic. *Deep Sea Res. I* 54, 710–731. <https://doi.org/10.1016/j.dsr.2007.02.006>.
- Nelson, T.F., Reddy, C.M., Ward, C.P., 2021. Product formulation controls the impact of biofouling on consumer plastic photochemical fate in the ocean. *Environ. Sci. Technol.* 55, 8898–8907. <https://doi.org/10.1021/acs.est.1c02079>.
- Novak, G.A., Bertram, T.H., 2020. Reactive VOC production from photochemical and heterogeneous reactions occurring at the air-ocean interface. *Acc. Chem. Res.* 53, 1014–1023. <https://doi.org/10.1021/acs.accounts.0c00095>.
- Olofinnade, A.T., Onaolapo, A.Y., Onaolapo, O.J., Olowe, O.A., 2021. The potential toxicity of food-added sodium benzoate in mice is concentration-dependent. *Toxicol. Res.* 10, 561–569. <https://doi.org/10.1093/toxres/tfab024>.
- Osburn, C.L., Morris, D.P., Thorn, K.A., Moeller, R.E., 2001. Chemical and optical changes in freshwater dissolved organic matter exposed to solar radiation. *Biogeochemistry* 54, 251–278. <https://doi.org/10.1023/A:1010657428418>.
- Ossola, R., Tolu, J., Clerc, B., Erickson, P.R., Winkel, L.H.E., McNeill, K., 2019. Photochemical production of sulfate and methanesulfonic acid from dissolved organic sulfur. *Environ. Sci. Technol.* 53, 13191–13200. <https://doi.org/10.1021/acs.est.9b04721>.
- Ossola, R., Jönsson, O.M., Moor, K., McNeill, K., 2021. Singlet oxygen quantum yields in environmental waters. *Chem. Rev.* 121, 4100–4146. <https://doi.org/10.1021/acs.chemrev.0c00781>.
- Ossola, R., Gruseck, R., Houska, J., Manfrin, A., Vallierès, M., McNeill, K., 2022. Photochemical production of carbon monoxide from dissolved organic matter: role of lignin methoxyarene functional groups. *Environ. Sci. Technol.* 56, 13449–13460. <https://doi.org/10.1021/acs.est.2c03762>.
- Paerl, R.W., Claudio, I.M., Shields, M.R., Bianchi, T.S., Osburn, C.L., 2020. Dityrosine formation via reactive oxygen consumption yields increasingly recalcitrant humic-like fluorescent organic matter in the ocean. *Limnol. Oceanogr. Lett.* 5, 337–345. <https://doi.org/10.1002/lol2.10154>.
- Page, S.E., Logan, J.R., Cory, R.M., McNeill, K., 2014. Evidence for dissolved organic matter as the primary source and sink of photochemically produced hydroxyl radical in arctic surface waters. *Environ. Sci.: Processes Impacts* 16, 807–822. <https://doi.org/10.1039/C3EM00596H>.
- Pan, Y., Garg, S., Waite, T.D., Yang, X., 2018. Copper inhibition of triplet-induced reactions involving natural organic matter. *Environ. Sci. Technol.* 52, 2742–2750. <https://doi.org/10.1021/acs.est.7b05655>.
- Pan, L., Chen, J., He, X., Zhan, T., Shen, H., 2020. Aqueous photodegradation of okadaic acid and dinophysistoxin-1: persistence, kinetics, photoproducts, pathways, and toxicity evaluation. *Sci. Total Environ.* 743, 140593. <https://doi.org/10.1016/j.scitotenv.2020.140593>.
- Pan, Q., Hu, W., He, D., He, C., Zhang, L., Shi, Q., 2023. Machine-learning assisted molecular formula assignment to high-resolution mass spectrometry data of dissolved organic matter. *Talanta* 259, 124484. <https://doi.org/10.1016/j.talanta.2023.124484>.
- Pandey, D.R., Polik, C., Cory, R.M., 2022. Controls on the photochemical production of hydrogen peroxide in Lake Erie. *Environ. Sci.: Processes Impacts* 24, 2108–2118. <https://doi.org/10.1039/D2EM00327A>.
- Parker, K.M., Mitch, W.A., 2016. Halogen radicals contribute to photooxidation in coastal and estuarine waters. *Proc. Natl. Acad. Sci.* 113, 5868–5873. www.pnas.org/cgi/doi/10.1073/pnas.1602595113.
- Parker, K.M., Pignatello, J.J., Mitch, W.A., 2013. Influence of ionic strength on triplet-state natural organic matter loss by energy transfer and electron transfer pathways. *Environ. Sci. Technol.* 47, 10987–10994. <https://doi.org/10.1021/es401900j>.

- Pelletier, É., Sargian, P., Payet, J., Demers, S., 2006. Ecotoxicological effects of combined UVB and organic contaminants in coastal waters: a review. *Photochem. Photobiol.* 82, 981–993. <https://doi.org/10.1562/2005-09-18-ra-688>.
- Penezić, A., Wang, X., Perrier, S., George, C., Frka, S., 2023. Interfacial photochemistry of marine diatom lipids: abiotic production of volatile organic compounds and new particle formation. *Chemosphere* 313, 137510. <https://doi.org/10.1016/j.chemosphere.2022.137510>.
- Petasne, R.G., Zika, R.G., 1987. Fate of superoxide in coastal sea water. *Nature* 325, 516–518. <https://doi.org/10.1038/325516a0>.
- Petit, M., Suroy, M., SempéRé, R., Vautier, F., Volkman, J.K., Goutx, M., Rontani, J.-F., 2015. Transfer of singlet oxygen from senescent irradiated phytoplankton cells to attached heterotrophic bacteria: effect of silica and carbonaceous matrices. *Mar. Chem.* 151, 87–95. <https://doi.org/10.1016/j.marchem.2015.02.007>.
- Phillips, A.A., White, M.E., Seidel, M., Wu, F., Pavia, F.F., Kemeny, P.C., Ma, A.C., Aluwihare, L.I., Dittmar, T., Sessions, A.L., 2022. Novel sulfur isotope analyses constrain sulfurized porewater fluxes as minor component of marine dissolved organic matter. *Proc. Natl. Acad. Sci.* 119, e2209152119. <https://doi.org/10.1073/pnas>.
- Pohlbeln, A.M., Dittmar, T., 2015. Novel insights into the molecular structure of non-volatile marine dissolved organic sulfur. *Mar. Chem.* 168, 86–94. <https://doi.org/10.1016/j.marchem.2014.10.018>.
- Porcal, P., Kopáček, J., 2018. Photochemical degradation of dissolved organic matter reduces the availability of phosphorus for aquatic primary producers. *Chemosphere* 193, 1018–1026. <https://doi.org/10.1016/j.chemosphere.2017.11.140>.
- Porcal, P., Frejlachová, K., Kopáček, J., Nedoma, J., Šavrlová, T., 2017. Photochemical cleaving of allochthonous organic-metal complexes contributes to phosphorus immobilization in surface waters. *Chemosphere* 167, 374–381. <https://doi.org/10.1016/j.chemosphere.2016.10.022>.
- Pos, W.H., Riemer, D.D., Zika, R.G., 1998. Carbonyl sulfide (OCS) and carbon monoxide (CO) in natural waters: evidence of a coupled production pathway. *Mar. Chem.* 62, 89–101. [https://doi.org/10.1016/S0304-4203\(98\)00025-5](https://doi.org/10.1016/S0304-4203(98)00025-5).
- Poulin, B.A., Ryan, J.N., Nagy, K.L., Stubbins, A., Dittmar, T., Orem, W., Krabbenhoft, D.P., Aiken, G.R., 2017. Spatial dependence of reduced sulfur in everglades dissolved organic matter controlled by sulfate enrichment. *Environ. Sci. Technol.* 51, 3630–3639. <https://doi.org/10.1021/acs.est.6b04142>.
- Powers, L.C., Miller, W.L., 2014. Blending remote sensing data products to estimate photochemical production of hydrogen peroxide and superoxide in the surface ocean. *Environ. Sci.: Processes Impacts* 16, 792–806. <https://doi.org/10.1039/C3EM00617D>.
- Powers, L.C., Miller, W.L., 2015a. Photochemical production of CO and CO₂ in the Northern Gulf of Mexico: estimates and challenges for quantifying the impact of photochemistry on carbon cycles. *Mar. Chem.* 171, 21–35. <https://doi.org/10.1016/j.marchem.2015.02.004>.
- Powers, L.C., Miller, W.L., 2015b. Hydrogen peroxide and superoxide photoproduction in diverse marine waters: a simple proxy for estimating direct CO₂ photochemical fluxes. *Geophys. Res. Lett.* 42, 7696–7704. <https://doi.org/10.1002/2015GL065669>.
- Powers, L.C., Miller, W.L., 2016. Apparent quantum efficiency spectra for superoxide photoproduction and its formation of hydrogen peroxide in natural waters. *Front. Mar. Sci.* 3, 235. <https://doi.org/10.3389/fmars.2016.00235>.
- Powers, L.C., Babcock-Adams, L.C., Enright, J.K., Miller, W.L., 2015. Probing the photochemical reactivity of deep ocean refractory carbon (DORC): lessons from hydrogen peroxide and superoxide kinetics. *Mar. Chem.* 177, 306–317. <https://doi.org/10.1016/j.marchem.2015.06.005>.
- Powers, L.C., Brandes, J.A., Stubbins, A., Miller, W.L., 2017. MoDIE: Moderate dissolved inorganic carbon (DI¹³C) isotope enrichment for improved evaluation of DIC photochemical production in natural waters. *Mar. Chem.* 194, 1–9. <https://doi.org/10.1016/j.marchem.2017.03.007>.
- Powers, L.C., Hertkorn, N., McDonald, N., Schmitt-Kopplin, P., del Vecchio, R., Blough, N.V., Gonsior, M., 2019. *Sargassum* sp. act as a large regional source of marine dissolved organic carbon and polyphenols. *Global Biogeochem. Cycles* 33, 1423–1439. <https://doi.org/10.1029/2019GB006225>.
- Powers, L.C., del Vecchio, R., Blough, N.V., McDonald, N., Schmitt-Kopplin, P., Gonsior, M., 2020. Optical properties and photochemical transformation of the dissolved organic matter released by *Sargassum*. *Front. Mar. Sci.* 7, 588287. <https://doi.org/10.3389/fmars.2020.588287>.
- Powers, L.C., Lapham, L., Malkin, S.Y., Heyes, A., Schmitt-Kopplin, P., Gonsior, M., 2021. Molecular and optical characterization reveals the preservation and sulfurization of chemically diverse porewater dissolved organic matter in oligohaline and brackish Chesapeake Bay sediments. *Org. Geochem.* 161, 104324. <https://doi.org/10.1016/j.orggeochem.2021.104324>.
- Rabani, J., Mamane, H., Pousty, D., Bolton, J.R., 2021. Practical chemical actinometry—a review. *Photochem. Photobiol.* 97, 873–902. <https://doi.org/10.1111/php.13429>.

- Rabek, J.F., 1982a. *Experimental Methods in Photochemistry and Photophysics. Part 1*. John Wiley & Sons, New York, NY.
- Rabek, J.F., 1982b. *Experimental Methods in Photochemistry and Photophysics. Part 2*. John Wiley & Sons, New York, NY.
- Ranby, B., Lucki, J., 1980. New aspects of photodegradation and photooxidation of polystyrene. *Pure Appl. Chem.* 52, 295–303. <https://doi.org/10.1351/pac198052020295>.
- Reader, H.E., Miller, W.L., 2011. Effect of estimations of ultraviolet absorption spectra of chromophoric dissolved organic matter on the uncertainty of photochemical production calculations. *J. Geophys. Res. C* 116, C08002. <https://doi.org/10.1029/2010JC006823>.
- Reader, H.E., Miller, W.L., 2012. Variability of carbon monoxide and carbon dioxide apparent quantum yield spectra in three coastal estuaries of the South Atlantic Bight. *Biogeoscience* 9, 4279–4294. <https://doi.org/10.5194/bg-9-4279-2012>.
- Reader, H.E., Miller, W.L., 2014. The efficiency and spectral photon dose dependence of photochemically induced changes to the bioavailability of dissolved organic carbon. *Limnol. Oceanogr.* 59, 182–194. <https://doi.org/10.4319/lo.2014.59.1.01082>.
- Remucal, C.K., 2014. The role of indirect photochemical degradation in the environmental fate of pesticides: a review. *Environ. Sci.: Processes Impacts* 16, 628–653. <https://doi.org/10.1039/c3em00549f>.
- Repeta, D.J., Ferrón, S., Sosa, O.A., Johnson, C.G., Repeta, L.D., Acker, M., DeLong, E.F., Karl, D.M., 2016. Marine methane paradox explained by bacterial degradation of dissolved organic matter. *Nat. Geosci.* 9, 884–887. <https://doi.org/10.1038/ngeo2837>.
- Rickard, P.C., Uher, G., Upstill-Goddard, R.C., 2022. Photoreactivity of surfactants in the sea-surface microlayer and subsurface water of the Tyne estuary, UK. *Geophys. Res. Lett.* 49, e2021GL095469. <https://doi.org/10.1029/2021GL095469>.
- Robinson, C., Williams, P.J., 2005. Respiration and its measurement in surface marine waters. In: del Giorgio, P., Williams, P.J. (Eds.), *Respiration in Aquatic Ecosystems*. Oxford University Press, New York, pp. 147–180, <https://doi.org/10.1093/acprof:oso/9780198527084.003.0009>.
- Rocher-Ros, G., Harms, T.K., Sponseller, R.A., Väistönen, M., Mört, C.M., Giesler, R., 2021. Metabolism overrides photo-oxidation in CO₂ dynamics of Arctic permafrost streams. *Limnol. Oceanogr.* 66, 169–181. <https://doi.org/10.1002/lnco.11564>.
- Roman-Hubers, A.T., Aepli, C., Dodds, J.N., Baker, E.S., McFarlin, K.M., Letinski, D.J., Zhao, L., Mitchell, D.A., Parkerton, T.F., Prince, R.C., Nedwed, T., Rusyn, I., 2022. Temporal chemical composition changes in water below a crude oil slick irradiated with natural sunlight. *Mar. Pollut. Bull.* 185, 114360. <https://doi.org/10.1016/j.marpolbul.2022.114360>.
- Romera-Castillo, C., Pinto, M., Langer, T.M., Álvarez-Salgado, X.A., Herndl, G.J., 2018. Dissolved organic carbon leaching from plastics stimulates microbial activity in the ocean. *Nat. Commun.* 9, 1430. <https://doi.org/10.1038/s41467-018-03798-5>.
- Romera-Castillo, C., Birnstock, S., Álvarez-Salgado, X.A., Sebastián, M., 2022. Aged plastic leaching of dissolved organic matter is two orders of magnitude higher than virgin plastic leading to a strong uplift in marine microbial activity. *Front. Mar. Sci.* 9, 861557. <https://doi.org/10.3389/fmars.2022.861557>.
- Rose, A.L., 2012. The influence of extracellular superoxide on iron redox chemistry and bioavailability to aquatic microorganisms. *Front. Microbiol.* 3, 124. <https://doi.org/10.3389/fmicb.2012.00124>.
- Rose, A.L., 2016. The influence of reactive oxygen species on local redox conditions in oxygenated natural waters. *Front. Earth Sci.* 4, 96. <https://doi.org/10.3389/feart.2016.00096>.
- Rose, A.L., Waite, T.D., 2006. Role of superoxide in the photochemical reduction of iron in seawater. *Geochim. Cosmochim. Acta* 70, 3869–3882. <https://doi.org/10.1016/j.gca.2006.06.008>.
- Rossignol, S., Tiné, L., Bianco, A., Passananti, M., Brigante, M., Donaldson, D.J., George, C., 2016. Atmospheric photochemistry at a fatty acid-coated air-water interface. *Science* 353, 699–702. <https://doi.org/10.1126/science.aaf361>.
- Royer, S.-J., Ferrón, S., Wilson, S.T., Karl, D.M., 2018. Production of methane and ethylene from plastic in the environment. *PLoS One* 13, e0200574. <https://doi.org/10.1371/journal.pone.0200574>.
- Rundel, R.D., 1983. Action spectra and estimation of biologically effective UV radiation. *Physiol. Plant.* 58, 360–366. <https://doi.org/10.1111/j.1399-3054.1983.tb04195.x>.
- Saint-Macary, A.D., Marriner, A., Deppeler, S., Safi, K.A., Law, C.S., 2022. Dimethylsulfide cycling in the sea surface microlayer in the southwestern Pacific. Part 2. Processes and rates. *Ocean Sci.* 18, 1559–1571. <https://doi.org/10.5194/os-18-1559-2022>.

- Schendorf, T.M., del Vecchio, R., Bianca, M., Blough, N.V., 2019. Combine effects of pH and borohydride reduction on the optical properties of humic substances (HS): a comparison of optical models. *Environ. Sci. Technol.* 53, 6310–6319. <https://doi.org/10.1021/acs.est.9b01516>.
- Schiebel, H.N., Wang, X., Chen, R.F., Peri, F., 2015. Photochemical release of dissolved organic matter from resuspended salt marsh sediments. *Estuar. Coasts* 38, 1692–1705. <https://doi.org/10.1007/s12237-014-9893-3>.
- Schmitt-Kopplin, P., Hertkorn, N., Schulten, H.R., Kettrup, A., 1998. Structural changes in a dissolved soil humic acid during photochemical degradation processes under O₂ and N₂ atmosphere. *Environ. Sci. Technol.* 32, 2531–2541. <https://doi.org/10.1021/es970636z>.
- Seidel, M., Yager, P.L., Ward, N.D., Carpenter, E.J., Gomes, H.R., Krusche, A.V., Richey, J.E., Dittmar, T., Medeiros, P.M., 2015. Molecular-level changes of dissolved organic matter along the Amazon river-to-ocean continuum. *Mar. Chem.* 177, 218–231. <https://doi.org/10.1016/j.marchem.2015.06.019>.
- Sem, K., Jang, M., Pierce, R., Blum, P., Yu, Z., 2022. Characterization of atmospheric processes of brevetoxins in sea spray aerosols from red tide events. *Environ. Sci. Technol.* 56, 1811–1819. <https://doi.org/10.1021/acs.est.1c05740>.
- Shank, G.C., Lee, R., Vähätalo, A., Zepp, R.G., Bartels, E., 2010a. Production of chromophoric dissolved organic matter from mangrove leaf litter and floating *Sargassum* colonies. *Mar. Chem.* 119, 172–181. <https://doi.org/10.1016/j.marchem.2010.02.002>.
- Shank, G.C., Zepp, R.G., Vähätalo, A., Lee, R., Bartels, E., 2010b. Photobleaching kinetics of chromophoric dissolved organic matter derived from mangrove leaf litter and floating *Sargassum* colonies. *Mar. Chem.* 119, 162–171. <https://doi.org/10.1016/j.marchem.2010.01.003>.
- Sharpless, C.M., Blough, N.V., 2014. The importance of charge-transfer interactions in determining chromophoric dissolved organic matter (CDOM) optical and photochemical properties. *Environ. Sci.: Processes Impacts* 16, 654–671. <https://doi.org/10.1039/C3EM00573A>.
- Shaw, T.J., Luther III, G.W., Rosas, R., Oldham, V.E., Coffey, N.R., Ferry, J.L., Dias, D.M.C., Yücel, M., Thibault de Chanvalon, A., 2021. Fe-catalyzed sulfide oxidation in hydrothermal plumes is a source of reactive oxygen species to the ocean. *Proc. Natl. Acad. Sci.* 118, e2026654118. <https://doi.org/10.1073/pnas.2026654118>.
- Simó, R., Archer, S.D., Pedrós-Alio, C., Gilpin, L., Stelfox-Widdicombe, C.E., 2002. Coupled dynamics of dimethylsulfoniopropionate and dimethylsulfide cycling and the microbial food web in surface waters of the North Atlantic. *Limnol. Oceanogr.* 47, 53–61. <https://doi.org/10.4319/lo.2002.47.1.0053>.
- Sleighter, R.L., Hatcher, P.G., 2008. Molecular characterization of dissolved organic matter (DOM) along a river to ocean transect of the lower Chesapeake Bay by ultrahigh resolution electrospray ionization Fourier transform ion cyclotron resonance mass spectrometry. *Mar. Chem.* 110, 140–152. <https://doi.org/10.1016/j.marchem.2008.04.008>.
- Smyth, T.J., 2011. Penetration of UV irradiance into the global ocean. *J. Geophys. Res. C* 116, C11020. <https://doi.org/10.1029/2011JC007183>.
- Song, G., Richardson, J.D., Werner, J.P., Xie, H., Kieber, D.J., 2015. Carbon monoxide photoproduction from particles and solutes in the Delaware Estuary under contrasting hydrological conditions. *Environ. Sci. Technol.* 49, 14048–14056. <https://doi.org/10.1021/acs.est.5b02630>.
- Southwell, M.W., Kieber, R.J., Mead, R.N., Brooks Avery, G., Skrabal, S.A., 2009. Effects of sunlight on the production of dissolved organic and inorganic nutrients from resuspended sediments. *Biogeochemistry* 98, 115–126. <https://doi.org/10.1007/s10533-009-9380-2>.
- Spencer, R.G.M., Aiken, G.R., Wickland, K.P., Striegl, R.G., Hernes, P.J., 2008. Seasonal and spatial variability in dissolved organic matter quantity and composition from the Yukon River basin, Alaska. *Global Biogeochem. Cycles* 22, GB4002. <https://doi.org/10.1029/2008GB003231>.
- Spencer, R.G.M., Stubbins, A., Hernes, P.J., Baker, A., Mopper, K., Aufdenkampe, A.K., Dyda, R.Y., Mwamba, V.L., Mangangu, A.M., Wabakanghanzi, J.N., Six, J., 2009. Photochemical degradation of dissolved organic matter and dissolved lignin phenols from the Congo River. *J. Geophys. Res. Biogeosci.* 114, G03010. <https://doi.org/10.1029/2009JG000968>.
- Spencer, R.G., Mann, P.J., Dittmar, T., Eglinton, T.I., McIntyre, C., Holmes, R.M., Zimov, N., Stubbins, A., 2015. Detecting the signature of permafrost thaw in Arctic rivers. *Geophys. Res. Lett.* 42, 2830–2835. <https://doi.org/10.1002/2015GL063498>.
- Stanley, R., Bell, T., Gao, Y., Gaston, C., Ho, D., Kieber, D.J., Mackey, K., Meskhidze, N., Miller, B., Potter, H., Vlahos, P., Yager, P., Alexander, B., Beaupré, S., Craig, S., Cutter, G., Emerson, S., Frossard, A., Gasso, S., Haus, B., Keene, W., Landing, W., Moore, R., Ortiz-Suslow, D., Palter, J., Paulot, F., Saltzman, E., Thornton, D., Wozniak, A., Zamora, L., Benway, H., 2021. US SOLAS Science Report. <https://doi.org/10.1575/1912/27821>.

- Staples, C.A., Peterson, D.R., Parkerton, T.F., Adams, W.J., 1997. The environmental fate of phthalate esters: a literature review. *Chemosphere* 35, 667–749. [https://doi.org/10.1016/S0045-6535\(97\)00195-1](https://doi.org/10.1016/S0045-6535(97)00195-1).
- Stenson, A.C., Marshall, A.G., Cooper, W.T., 2003. Exact masses and chemical formulas of individual Suwannee River fulvic acids from ultrahigh resolution electrospray ionization Fourier transform ion cyclotron resonance mass spectrometry. *Anal. Chem.* 75, 1275–1284. <https://doi.org/10.1021/ac026106p>.
- Stubbins, A., Dittmar, T., 2015. Illuminating the deep: molecular signatures of photochemical alteration of dissolved organic matter from North Atlantic Deep Water. *Mar. Chem.* 171, 318–324. <https://doi.org/10.1016/j.marchem.2015.06.020>.
- Stubbins, A., Uher, G., Law, C.S., Mopper, K., Robinson, C., Upstill-Goddard, R.C., 2006. Open-ocean carbon monoxide photoproduction. *Deep Sea Res. II* 53, 1695–1705. <https://doi.org/10.1016/j.dsr2.2006.05.011>.
- Stubbins, A., Hubbard, V., Uher, G., Law, C.S., Upstill-Goddard, R.C., Aiken, G.R., et al., 2008. Relating carbon monoxide photoproduction to dissolved organic matter functionality. *Environ. Sci. Technol.* 42, 3271–3276. <https://doi.org/10.1021/es703014q>.
- Stubbins, A., Spencer, R.G.M., Chen, H., Hatcher, P.G., Mopper, K., Hernes, P.J., Mwamba, V.L., Mangangu, A.M., Wabakanghanzi, J.N., Six, J., 2010. Illuminated darkness: molecular signatures of Congo River dissolved organic matter and its photochemical alteration as revealed by ultrahigh precision mass spectrometry. *Limnol. Oceanogr.* 55, 1467–1477. <https://doi.org/10.4319/lo.2010.55.4.1467>.
- Stubbins, A., Niggemann, J., Dittmar, T., 2012. Photo-lability of deep ocean dissolved black carbon. *Biogeosciences* 9, 1661–1670. <https://doi.org/10.5194/bg-9-1661-2012>.
- Stubbins, A., Mann, P.J., Powers, L., Bittar, T.B., Dittmar, T., McIntyre, C.P., Eglinton, T.I., Zimov, N., Spencer, R.G., 2017. Low photolability of yedoma permafrost dissolved organic carbon. *J. Geophys. Res. Biogeosci.* 122, 200–211. <https://doi.org/10.1002/2016JG003688>.
- Stubbins, A., Law, K.L., Muñoz, S.E., Bianchi, T.S., Zhu, L., 2021. Plastics in the Earth system. *Science* 373, 51–55. <https://doi.org/10.1126/science.abb035>.
- Stubbins, A., Zhu, L., Zhao, S., Spencer, R.G.M., Podgorski, D.C., 2023. Molecular signatures of dissolved organic matter generated from the photodissolution of microplastics in sunlit seawater. *Environ. Sci. Technol.* 57, 20097–20106. <https://doi.org/10.1021/acs.est.1c03592>.
- Sulzberger, B., Arey, J.S., 2016. Impacts of polar changes on the UV-induced mineralization of terrigenous dissolved organic matter. *Environ. Sci. Technol.* 50, 6621–6631. <https://doi.org/10.1021/acs.est.5b05994>.
- Sulzberger, B., Austin, A.T., Cory, R.M., Zepp, R.G., Paul, N.D., 2019. Solar UV radiation in a changing world: Roles of cryosphere-land-water-atmosphere interfaces in global biogeochemical cycles. *Photochem. Photobiol. Sci.* 18, 747–774. <https://doi.org/10.1039/C8PP90063A>.
- Sun, L., Qian, J., Blough, N.V., Mopper, K., 2015. Insights into the photoproduction sites of hydroxyl radicals by dissolved organic matter in natural waters. *Environ. Sci. Technol. Lett.* 2, 352–356. <https://doi.org/10.1021/acs.estlett.5b00294>.
- Sunda, W.G., 2012. Feedback interactions between trace metal nutrients and phytoplankton in the ocean. *Front. Microbiol.* 3, 204. <https://doi.org/10.3389/fmicb.2012.00204>.
- Sunday, M.O., Takeda, K., Sakugawa, H., 2020. Singlet oxygen photogeneration in coastal seawater: prospect of large-scale modeling in seawater surface and its environmental significance. *Environ. Sci. Technol.* 54, 6125–6133. <https://doi.org/10.1021/acs.est.0c00463>.
- Sutherland, K.M., Wankel, S.D., Hansel, C.M., 2020. Dark biological superoxide production as a significant flux and sink of marine dissolved oxygen. *Proc. Natl. Acad. Sci.* 117, 3433–3439. <https://doi.org/10.1073/pnas.1912313117>.
- Sutherland, K.M., Grabb, K.C., Karolewski, J.S., Taenzer, L., Hansel, C.M., Wankel, S.D., 2021. The redox fate of hydrogen peroxide in the marine water column. *Limnol. Oceanogr.* 66, 3828–3841. <https://doi.org/10.1002/limo.11922>.
- Sutherland, K.M., Johnston, D.T., Hemingway, J.D., Wankel, S.D., Ward, C.P., 2022. Revised microbial and photochemical triple-oxygen isotope effects improve marine gross oxygen production estimates. *PNAS Nexus* 1, pgac233. <https://doi.org/10.1093/pnasnexus/pgac233>.
- Swan, C.M., Nelson, N.B., Siegel, D.A., Fields, E.A., 2013. A model for remote estimation of ultraviolet absorption by chromophoric dissolved organic matter based on the global distribution of spectral slope. *Remote Sens. Environ.* 136, 277–285. <https://doi.org/10.1016/j.rse.2013.05.009>.
- Swarr, G.J., Kading, T., Lamborg, C.H., Hammerschmidt, C.R., Bowman, K.L., 2016. Dissolved low-molecular weight thiol concentrations from the U.S. GEOTRACES North Atlantic Ocean zonal transect. *Deep-Sea Res. I* 116, 77–87. <https://doi.org/10.1016/j.dsr.2016.06.003>.

- Takeda, K., Moriki, M., Oshiro, W., Sakugawa, H., 2013. Determination of phenolic concentrations in dissolved organic matter pre-concentrate using solid phase extraction from natural water. *Mar. Chem.* 157, 208–215. <https://doi.org/10.1016/j.marchem.2013.10.008>.
- Tang, D., Hung, C.-C., Warnken, K.W., Santschi, P.H., 2000. The distribution of biogenic thiols in surface waters of Galveston Bay. *Limnol. Oceanogr.* 45, 1289–1297. <https://doi.org/10.4319/lo.2000.45.6.1289>.
- Ternon, E., Thomas, O.P., Lemée, R., Gerwick, W.H., 2022. Rapid biotic and abiotic transformation of toxins produced by *Ostreopsis cf. ovata*. *Mar. Drugs* 20, 748. <https://doi.org/10.3390/MD2020748>.
- Tetu, S.G., Sarker, I., Schrammeyer, V., Pickford, R., Elbourne, L.D.H., Moore, L.R., Paulsen, I.T., 2019. Plastic leachates impair growth and oxygen production in *Prochlorococcus*, the ocean's most abundant photosynthetic bacteria. *Commun. Biol.* 2, 184. <https://doi.org/10.1038/s42003-019-0410-x>.
- Therias, S., Rapp, G., Masson, C., Gardette, J.-L., 2021. Limits of UV-light acceleration on the photooxidation of low-density polyethylene. *Polym. Degrad. Stab.* 183, 109443. <https://doi.org/10.1016/j.polymdegradstab.2020.109443>.
- Thompson, A.M., Zafiriou, O.C., 1983. Air-sea fluxes of transient atmospheric species. *J. Geophys. Res. C* 88, 6696–6708. <https://doi.org/10.1029/JC088iC11p06696>.
- Timko, S.A., Romera-Castillo, C., Jaffé, R., Cooper, W.J., 2014. Photo-reactivity of natural dissolved organic matter from fresh to marine waters in the Florida Everglades, USA. *Environ. Sci.: Processes Impacts* 16, 866–878. <https://doi.org/10.1039/c3em00591g>.
- Timko, S.A., Maydanov, A., Pittelli, S.L., Conte, M.H., Cooper, W.J., Koch, B.P., Schmitt-Kopplin, P., Gonsior, M., 2015. Depth-dependent photodegradation of marine dissolved organic matter. *Front. Mar. Sci.* 2, 66. <https://doi.org/10.3389/fmars.2015.00066>.
- Tolinski, M., 2009. Additives for Polyolefins. Chapter 15, Cross-linking. Elsevier, Oxford, UK, pp. 215–220, <https://doi.org/10.1016/B978-0-8155-2051-1.00015-7>.
- Toole, D.A., Kieber, D.J., Kiene, R.P., Siegel, D.A., Nelson, N.B., 2003. Photolysis and the dimethylsulfide (DMS) summer paradox in the Sargasso Sea. *Limnol. Oceanogr.* 48, 1088–1100. <https://doi.org/10.4319/lo.2003.48.3.1088>.
- Toole, D.A., Kieber, D.J., Kiene, R.P., White, E.M., Bisgrove, J., del Valle, D.A., et al., 2004. High dimethylsulfide photolysis rates in nitrate-rich Antarctic waters. *Geophys. Res. Lett.* 31, L11307. <https://doi.org/10.1029/2004GL019863>.
- Toole, D.A., Slezak, D., Kieber, D.J., Kiene, R.P., Siegel, D.A., 2006. Effects of solar radiation on dimethylsulfide cycling in the western Atlantic Ocean. *Deep Sea Res. I* 53, 136–153. <https://doi.org/10.1016/j.dsr.2005.09.003>.
- Uher, G., Pillans, J.J., Hatton, A.D., Upstill-Goddard, R.C., 2017. Photochemical oxidation of dimethylsulphide to dimethylsulphoxide in estuarine and coastal waters. *Chemosphere* 186, 805–816. <https://doi.org/10.1016/j.chemosphere.2017.08.050>.
- Vaalgamaa, S., Vähätilo, A.V., Perkola, N., Huhtala, S., 2011. Photochemical reactivity of perfluorooctanoic acid (PFOA) in conditions representing surface water. *Sci. Total Environ.* 409, 3043–3048. <https://doi.org/10.1016/j.scitotenv.2011.04.036>.
- Vähätilo, A.V., Zepp, R.G., 2005. Photochemical mineralization of dissolved organic nitrogen to ammonium in the Baltic Sea. *Environ. Sci. Technol.* 39, 6985–6992. <https://doi.org/10.1021/es050142z>.
- Vähätilo, A.V., Salkinoja-Salonen, M., Taalas, P., Salonen, K., 2000. Spectrum of the quantum yield for photochemical mineralization of dissolved organic carbon in a humic lake. *Limnol. Oceanogr.* 45, 664–676. <https://doi.org/10.4319/lo.2000.45.3.00664>.
- van Sebille, E., Wilcox, C., Lebreton, L., Maximenko, N., Hardesty, B.D., van Franeker, J.A., Eriksen, M., Siegel, D., Galgani, F., Law, K.L., 2015. A global inventory of small floating plastic debris. *Environ. Res. Lett.* 10, 124006. <https://doi.org/10.1088/1748-9326/10/12/124006>.
- Vaughan, P.P., Blough, N.V., 1998. Photochemical formation of hydroxyl radical by constituents of natural waters. *Environ. Sci. Technol.* 32, 2947–2953. <https://doi.org/10.1021/es9710417>.
- Vione, D., 2022. A model assessment of the occurrence and reactivity of the nitrating/nitrosating agent nitrogen dioxide (NO₂) in Sunlit natural waters. *Molecules* 27, 4855. <https://doi.org/10.3390/molecules27154855>.
- Vione, D., Rosario-Ortiz, F.L., 2021. Foreseen effects of climate-impacted scenarios on the photochemical fate of selected cyanotoxins in surface freshwaters. *Environ. Sci. Technol.* 55, 10928–10934. <https://doi.org/10.1021/acs.est.1c03440>.
- Vione, D., Minella, M., Maurino, V., Minero, C., 2014. Indirect photochemistry in sunlit surface waters: photoinduced production of reactive transient species. *Chem. Eur. J.* 20, 10590–10606. <https://doi.org/10.1002/chem.201400413>.
- Voelker, B.M., Sulzberger, B., 1996. Effects of fulvic acid on Fe(II) oxidation by hydrogen peroxide. *Environ. Sci. Technol.* 30, 1106–1114. <https://doi.org/10.1021/es9502132>.

- Vogt, M., Vallina, S.M., Buitenhuis, E.T., Bopp, L., Le Quéré, C., 2010. Simulating dimethylsulphide seasonality with the Dynamic Green Ocean Model PlankTOM5. *J. Geophys. Res. C* 115, C06021. <https://doi.org/10.1029/2009JC005529>.
- von Hobe, M., Najjar, R.G., Kettle, A.J., Andreae, M.O., 2003. Photochemical and physical modeling of carbonyl sulfide in the ocean. *J. Geophys. Res. C* 108, 3229. <https://doi.org/10.1029/2000JC000712>.
- Vorobev, A., Sharma, S., Yu, M., Lee, J., Washington, B.J., Whitman, W.B., Ballantyne IV, F., Medeiros, P.M., Moran, M.A., 2018. Identifying labile DOM components in a coastal ocean through depleted bacterial transcripts and chemical signals. *Environ. Microbiol.* 20, 3012–3030. <https://doi.org/10.1111/1462-2920.14344>.
- Wagner, S., Brandes, J., Spencer, R.G., Ma, K., Rosengard, S.Z., Moura, J.M.S., Stubbins, A., 2019. Isotopic composition of oceanic dissolved black carbon reveals non-riverine source. *Nat. Commun.* 10, 5064. <https://doi.org/10.1038/s41467-019-13111-7>.
- Walsh, A.N., Reddy, C.M., Niles, S.F., McKenna, A.M., Hansel, C.M., Ward, C.P., 2021. Plastic formulation is an emerging control of its photochemical fate in the ocean. *Environ. Sci. Technol.* 55, 12383–12392. <https://doi.org/10.1021/acs.est.1c02272>.
- Walsh, A.N., Mazzotta, M.G., Nelson, T.F., Reddy, C.M., Ward, C.P., 2022. Synergy between sunlight, titanium dioxide, and microbes enhances cellulose diacetate degradation in the ocean. *Environ. Sci. Technol.* 56, 13810–13819. <https://doi.org/10.1021/acs.est.2c04348>.
- Wang, W., Zafiriou, O.C., Chan, I.Y., Zepp, R.G., Blough, N.V., 2007. Production of hydrated electrons from photoionization of dissolved organic matter in natural waters. *Environ. Sci. Technol.* 41, 1601–1607. <https://doi.org/10.1021/es061069v>.
- Wang, W., Johnson, C.G., Takeda, K., Zafiriou, O.C., 2009. Measuring the photochemical production of carbon dioxide from marine dissolved organic matter by pool isotope exchange. *Environ. Sci. Technol.* 43, 8604–8609. <https://doi.org/10.1021/es901543e>.
- Wang, S.-C., Liu, F.-F., Huang, T.-Y., Fan, J.-L., Gao, Z.-Y., Liu, G.-Z., 2021a. Effects of nanoplastics on the dinoflagellate *Amphidinium carterae* Hulbert from the perspectives of algal growth, oxidative stress and hemolysin production. *Nanomaterials* 11, 2471. <https://doi.org/10.3390/nano1110247>.
- Wang, X., Dalton, E.Z., Payne, Z.C., Perrier, S., Riva, M., Raff, J.D., George, C., 2021b. Superoxide and nitrous acid production from nitrate photolysis is enhanced by dissolved aliphatic organic matter. *Environ. Sci. Technol. Lett.* 8, 53–58. <https://doi.org/10.1021/acs.estlett.0c00806>.
- Wang, Y., Wu, B., Zheng, X., Chen, B., Chu, C., 2023. Assessing the quantum yield spectrum of photochemically produced reactive intermediates from black carbon of various sources and properties. *Water Res.* 229, 119450. <https://doi.org/10.1016/j.watres.2022.119450>.
- Ward, C.P., Cory, R.M., 2020. Assessing the prevalence, products, and pathways of dissolved organic matter partial photo-oxidation in arctic surface waters. *Environ. Sci.: Processes Impacts* 22, 1214–1223. <https://doi.org/10.1039/C9EM00504H>.
- Ward, C.P., Overton, E.B., 2020. How the 2010 Deepwater Horizon spill reshaped our understanding of crude oil photochemical weathering at sea: a past, present, and future perspective. *Environ. Sci.: Processes Impacts* 22, 1125–1138. <https://doi.org/10.1039/d0em00027b>.
- Ward, C.P., Nalven, S.G., Crump, B.C., Kling, G.W., Cory, R.M., 2017. Photochemical alteration of organic carbon draining permafrost soils shifts microbial metabolic pathways and stimulates respiration. *Nat. Commun.* 8, 772. <https://doi.org/10.1038/s41467-017-00759-2>.
- Ward, C.P., Armstrong, C.J., Walsh, A.N., Jackson, J.H., Reddy, C.M., 2019. Sunlight converts polystyrene to carbon dioxide and dissolved organic carbon. *Environ. Sci. Lett.* 6, 669–674. <https://doi.org/10.1021/acs.estlett.9b00532>.
- Ward, C.P., Bowen, J.C., Freeman, D.H., Sharpless, C.M., 2021. Rapid and reproducible characterization of the wavelength dependence of aquatic photochemical reactions using light-emitting diodes. *Environ. Sci. Technol. Lett.* 8, 437–442. <https://doi.org/10.1021/acs.estlett.1c00172>.
- Wei, L., Ahner, B.A., 2005. Sources and sinks of dissolved phytochelatin in natural seawater. *Limnol. Oceanogr.* 50, 13–22. <https://doi.org/10.4319/lo.2005.50.1.00013>.
- Weiss, P.S., Andrews, S.S., Johnson, J.E., Zafiriou, O.C., 1995. Photoproduction of carbonyl sulfide in South Pacific Ocean waters as a function of irradiation wavelength. *Geophys. Res. Lett.* 22, 215–218. <https://doi.org/10.1029/94GL03000>.
- Whelan, M.E., Lennartz, S.T., Gimeno, T.E., Wehr, R., Wohlfahrt, G., Wang, Y., Kooijmans, L.M.J., Hilton, T.W., Belviso, S., Peylin, P., Commane, R., Sun, W., Chen, H., Kuai, L., Mammarella, I., Maseyk, K., Berkelhammer, M., Li, K.-F., Yakir, D., Zumkehr, A., Katayama, Y., Ogée, J., Spielmann, F.M., Kitz, F.,

- Rastogi, B., Kesselmeier, J., Marshall, J., Erkkilä, K.-M., Wingate, L., Meredith, L.K., He, W., Bunk, R., Launois, T., Vesala, T., Schmidt, J.A., Fichot, C.G., Seibt, U., Saleska, S., Saltzman, E.S., Montzka, S.A., Berry, J.A., Campbell, J.E., 2018. Reviews and syntheses: carbonyl sulfide as a multi-scale tracer for carbon and water cycles. *Biogeosciences* 15, 3625–3657. <https://doi.org/10.5194/bg-15-3625-2018>.
- White, E.M., Vaughan, P.P., Zepp, R.G., 2003. Role of the photo-Fenton reaction in the production of hydroxyl radicals and photobleaching of colored dissolved organic matter in a coastal river of the southeastern United States. *Aquatic Sci.* 65, 402–414. <https://doi.org/10.1007/s00027-003-0675-4>.
- White, E.M., Kieber, D.J., Mopper, M., 2008. Determination of photochemically produced carbon dioxide in seawater. *Limnol. Oceanogr. Methods* 6, 441–453. <https://doi.org/10.4319/lom.2008.6.441>.
- White, E.M., Kieber, D.J., Sherrard, J., Miller, W.L., Mopper, K., 2010. Carbon dioxide and carbon monoxide photoproduction quantum yields in the Delaware Estuary. *Mar. Chem.* 118, 11–21. <https://doi.org/10.1016/j.marchem.2009.10.001>.
- Widner, B., Kido Soule, M.C., Ferrer-González, F.X., Moran, M.A., Kujawinski, E.B., 2021. Quantification of amine- and alcohol-containing metabolites in saline samples using pre-extraction benzoyl chloride derivatization and ultrahigh performance liquid chromatography tandem mass spectrometry (UHPLC MS/MS). *Anal. Chem.* 93, 4809–4817. <https://doi.org/10.1021/acs.analchem.0c03769>.
- Wiegner, T.N., Seitzinger, S.P., 2001. Photochemical and microbial degradation of external dissolved organic matter inputs to rivers. *Aquat. Microb. Ecol.* 24, 27–40. <https://doi.org/10.3354/ame024027>.
- Wilkinson, J., Hooda, P.S., Barker, J., Barton, S., Swinden, J., 2017. Occurrence, fate and transformation of emerging contaminants in water: an overarching review of the field. *Environ. Pollut.* 231, 954–970. <https://doi.org/10.1016/j.envpol.2017.08.032>.
- Wise, S.A., Rodgers, R.P., Reddy, C.M., Nelson, R.K., Kujawinski, E.B., Wade, T.L., Campiglia, A.D., Liu, Z., 2022. Advances in chemical analysis of oil spills since the *Deepwater Horizon* disaster. *Crit. Rev. Anal. Chem.*, 1–60. <https://doi.org/10.1080/10408347.2022.2039093>.
- Wu, B., Liu, T., Wang, Y., Zhao, G., Chen, B., Chu, C., 2021. High sample throughput LED reactor for facile characterization of the quantum yield spectrum of photochemically produced reactive intermediates. *Environ. Sci. Technol.* 55, 16204–16214. <https://doi.org/10.1021/acs.est.1c04608>.
- Wünsch, U.J., Geuer, J.K., Lechtenfeld, O.J., Koch, B.P., Murphy, K.R., Stedmon, C.A., 2018. Quantifying the impact of solid-phase extraction on chromophoric dissolved organic matter composition. *Mar. Chem.* 207, 33–41. <https://doi.org/10.1016/j.marchem.2018.08.010>.
- Wurl, O., Wurl, E., Miller, L., Johnson, K., Vagle, S., 2011. Formation and global distribution of seasurface microlayers. *Biogeoscience* 8, 121–135. <https://doi.org/10.5194/bg-8-121-2011>.
- Wuttig, K., Heller, M.I., Croot, P.L., 2013a. Pathways of superoxide (O_2^-) decay in the Eastern Tropical North Atlantic. *Environ. Sci. Technol.* 47, 10249–10256. <https://doi.org/10.1021/es401658t>.
- Wuttig, K., Heller, M.I., Croot, P.L., 2013b. Reactivity of inorganic Mn and Mn desferrioxamine B with O_2 , O_2^- , and H_2O_2 in seawater. *Environ. Sci. Technol.* 47, 10257–10265. <https://doi.org/10.1021/es4016603>.
- Wypych, G., 2012a. PE polyethylene. In: Wypych, G., Wypych, G. (Eds.), *Handbook of Polymers*. Elsevier, Amsterdam, pp. 336–341, <https://doi.org/10.1016/B978-1-895198-47-8.50104-1>.
- Wypych, G., 2012b. PP polypropylene. In: Wypych, G., Wypych, G. (Eds.), *Handbook of Polymers*. Elsevier, Amsterdam, pp. 479–486, <https://doi.org/10.1016/B978-1-895198-47-8.50144-2>.
- Wypych, G., 2012c. PS polystyrene. In: Wypych, G. (Ed.), *Handbook of Polymers*. Elsevier, Amsterdam, p. 541, <https://doi.org/10.1016/B978-1-895198-47-8.50162-4>.
- Xie, H., Moore, R.M., Miller, W.L., 1998. Photochemical production of carbon disulfide in seawater. *J. Geophys. Res.* C 103, 5635–5644. <https://doi.org/10.1029/97JC02885>.
- Xu, F., Jin, N., Ma, Z., Zhang, H.-H., Yang, G.-P., 2019. Distribution, occurrence, and fate of biogenic dimethylated sulfur compounds in the Yellow Sea and Bohai Sea during spring. *J. Geophys. Res. C* 124, 5787–5800. <https://doi.org/10.1029/2019JC015085>.
- Xue, L., Kieber, D.J., 2021. Photochemical production and photolysis of acrylate in seawater. *Environ. Sci. Technol.* 55, 7135–7144. <https://doi.org/10.1021/acs.est.1c00327>.
- Yamashita, Y., Tanoue, E., 2008. Production of bio-refractory fluorescent dissolved organic matter in the ocean interior. *Nat. Geosci.* 1, 579–582. <https://doi.org/10.1038/ngeo279>.
- Yamashita, Y., Tsukasaki, A., Nishida, T., Tanoue, E., 2007. Vertical and horizontal distribution of fluorescent dissolved organic matter in the Southern Ocean. *Mar. Chem.* 106, 498–509. <https://doi.org/10.1016/j.marchem.2007.05.004>.

- Yamashita, N., Taniyasu, S., Petrick, G., Wei, S., Gamo, T., Lam, P.K.S., Kannan, K., 2008. Perfluorinated acids as novel chemical tracers of global circulation of ocean waters. *Chemosphere* 70, 1247–1255. <https://doi.org/10.1016/j.chemosphere.2007.07.079>.
- Yan, S., Song, W., 2014. Photo-transformation of pharmaceutically active compounds in the aqueous environment: a review. *Environ. Sci.: Processes Impacts* 16, 697–720. <https://doi.org/10.1039/c3em00502j>.
- Yang, Y., Pignatello, J.J., 2017. Participation of the halogens in photochemical reactions in natural and treated waters. *Molecules* 22, 1684. <https://doi.org/10.3390/molecules22101684>.
- Yang, G.-P., Chengxuan, L., Jialin, Q., Lige, H., Haijun, H., 2007. Photochemical oxidation of dimethylsulfide in seawater. *Acta Oceanol. Sinica* 26, 34–42.
- Yang, F., Song, G., Massicotte, P., Wei, H., Xie, H., 2020. Depth-resolved photochemical lability of dissolved organic matter in the Western Tropical Pacific Ocean. *J. Geophys. Res. Biogeosci.* 125, e2019JG005425. <https://doi.org/10.1029/2019JG005425>.
- Yang, Y., Sun, P., Padhye, L.P., Zhang, R., 2021. Photo-ammonification in surface water samples: mechanism and influencing factors. *Sci. Total Environ.* 759, 143547. <https://doi.org/10.1016/j.scitotenv.2020.143547>.
- Yocis, B.H., Kieber, D.J., Mopper, K., 2000. Photochemical production of hydrogen peroxide in Antarctic waters. *Deep Sea Res. I* 47, 1077–1099. [https://doi.org/10.1016/S0967-0637\(99\)00095-3](https://doi.org/10.1016/S0967-0637(99)00095-3).
- Zafiriou, O.C., 1974. Sources and reactions of OH and daughter radicals in seawater. *J. Geophys. Res.* 79, 4491–4497. <https://doi.org/10.1029/JC079i030p04491>.
- Zafiriou, O.C., 1977. Marine organic photochemistry previewed. *Mar. Chem.* 5, 497–522. [https://doi.org/10.1016/0304-4203\(77\)90037-8](https://doi.org/10.1016/0304-4203(77)90037-8).
- Zafiriou, O.C., 1986. Atmospheric, oceanic, and interfacial photochemistry as factors influencing air-sea exchange fluxes and processes. In: Buat-Ménard, P. (Ed.), *The Role of Air-Sea Exchange in Geochemical Cycling*, NATO ASI Series. Vol. 185. Springer, Dordrecht, pp. 185–207, https://doi.org/10.1007/978-94-009-4738-2_8.
- Zafiriou, O.C., 1996. Photochemistry and the sea-surface microlayer: Natural processes and potential as a technique. In: Burton, J.O., Brewer, P.G., Chesselet, R. (Eds.), *Dynamic Processes in the Chemistry of the Upper Ocean*. NATO Conference Series. Vol. 17. Springer, Boston, pp. 129–135, https://doi.org/10.1007/978-1-4684-5215-0_11.
- Zafiriou, O.C., Dister, B., 1991. Photochemical free radical production rates: Gulf of Maine and Woods Hole-Miami transect. *J. Geophys. Res. C* 96, 4939–4945. <https://doi.org/10.1029/90JC02444>.
- Zafiriou, O.C., McFarland, M., 1981. Nitric oxide from nitrite photolysis in the Central Equatorial Pacific. *J. Geophys. Res. C* 86, 3173–3182. <https://doi.org/10.1029/JC086iC04p03173>.
- Zafiriou, O.C., True, M.B., 1979a. Nitrite photolysis in seawater by sunlight. *Mar. Chem.* 8, 9–32. [https://doi.org/10.1016/0304-4203\(79\)90029-X](https://doi.org/10.1016/0304-4203(79)90029-X).
- Zafiriou, O.C., True, M.B., 1979b. Nitrate photolysis in seawater by sunlight. *Mar. Chem.* 8, 33–42. [https://doi.org/10.1016/0304-4203\(79\)90030-6](https://doi.org/10.1016/0304-4203(79)90030-6).
- Zafiriou, O.C., True, M.B., Hayon, E., 1987. Consequences of OH radical reaction in sea water: formation and decay of Br_2^- ion radical photochemistry of environmental aquatic systems. In: Zika, R.G., Cooper, W.J. (Eds.), *Photochemistry of Environmental Aquatic Systems*, ACS Symposium Series. Vol. 327. American Chemical Society, Washington, DC, pp. 89–105.
- Zafiriou, O.C., Blough, N.V., Micinski, E., Dister, B., Kieber, D.J., Moffett, J., 1990. Molecular probe systems for reactive transients in natural waters. *Mar. Chem.* 30, 45–70. [https://doi.org/10.1016/0304-4203\(90\)90061-G](https://doi.org/10.1016/0304-4203(90)90061-G).
- Zafiriou, O.C., Andrews, S.S., Wang, W., 2003. Concordant estimates of oceanic carbon monoxide source and sink processes in the Pacific yield a balanced global “blue-water” CO budget. *Global Biogeochem. Cycles* 17, 1015. <https://doi.org/10.1029/2001GB001638>.
- Zafiriou, O.C., Xie, H., Kieber, D.J., Wang, W., Song, G., Cohen, N., 2024. Cyanohydrin Equilibria implicate non-aromatic aldehydes in photochemical production of oceanic carbon monoxide, generating mechanistic prototypes. *Environ. Sci. Technol.* in review.
- Zepp, R.G., Andreae, M.O., 1994. Factors affecting the photochemical production of carbonyl sulfide in seawater. *Geophys. Res. Lett.* 21, 2813–2816. <https://doi.org/10.1029/94GL03083>.
- Zepp, R.G., Ritmiller, L.F., 1995. Photoreactions providing sinks and sources of halocarbons in aquatic environments. In: Huang, C.P., O’Meilia, C.R., Morgan, J.J. (Eds.), *Aquatic Chemistry*. Vol. 244. American Chemical Society, Washington, DC, pp. 253–278, <https://doi.org/10.1021/ba-1995-0244.ch013>.
- Zepp, R.G., Hoigne, J., Bader, H., 1987. Nitrate-induced photooxidation of trace organic chemicals in water. *Environ. Sci. Technol.* 21, 443–450. <https://doi.org/10.1021/es00159a004>.

- Zettler, E.R., Mincer, T.J., Amaral-Zettler, L.A., 2013. Life in the “plastisphere”: microbial communities on plastic marine debris. *Environ. Sci. Technol.* 47, 7137–7146. <https://doi.org/10.1021/es401288x>.
- Zhang, Y., Blough, N.V., 2016. Photoproduction of one-electron reducing intermediates by chromophoric dissolved organic matter (CDOM): relation to O_2^- and H_2O_2 photoproduction and CDOM photooxidation. *Environ. Sci. Technol.* 50, 11008–11015. <https://doi.org/10.1021/acs.est.6b02919>.
- Zhang, K., Parker, K.M., 2018. Halogen radical oxidants in natural and engineered aquatic systems. *Environ. Sci. Technol.* 52, 9579–9594. <https://doi.org/10.1021/acs.est.8b02219>.
- Zhang, Y., Xie, H., 2015. Photomineralization and photomethanification of dissolved organic matter in Saguenay River surface water. *Biogeoscience* 12, 6823–6836. <https://doi.org/10.5194/bg-12-6823-2015>.
- Zhang, Y., del Vecchio, R., Blough, N.V., 2012. Investigating the mechanism of hydrogen peroxide photoproduction by humic substances. *Environ. Sci. Technol.* 46, 11836–11843. <https://doi.org/10.1021/es3029582>.
- Zhang, Y., Simon, K.A., Andrew, A.A., del Vecchio, R., Blough, N.V., 2014. Enhanced photoproduction of hydrogen peroxide by humic substances in the presence of phenol electron donors. *Environ Sci Technol.* 48, 12679–12688. <https://doi.org/10.1021/es5035798>.
- Zhao, Z., Gonsior, M., Luek, J., Timko, S., Ianiri, H., Hertkorn, N., Schmitt-Kopplin, P., Fang, X., Zeng, Q., Jiao, N., Chen, F., 2017. Picocyanobacteria and deep-ocean fluorescent dissolved organic matter share similar optical properties. *Nat. Commun.* 8, 1–10. <https://doi.org/10.1038/ncomms15284>.
- Zhao, Z., Gonsior, M., Schmitt-Kopplin, P., Zhan, Y., Zhang, R., Jiao, N., Chen, F., 2019. Microbial transformation of virus-induced dissolved organic matter from picocyanobacteria: coupling of bacterial diversity and DOM chemodiversity. *ISME J.* 13, 2551–2565. <https://doi.org/10.1038/s41396-019-0449-1>.
- Zhou, C., Chen, J., Xie, H., Zhang, Y., Li, Y., Wang, Y., Xie, Q., Zhang, S., 2018. Modeling photodegradation kinetics of organic micropollutants in water bodies: a case of the Yellow River estuary. *J. Hazard. Mater.* 349, 60–67. <https://doi.org/10.1016/j.jhazmat.2018.01.051>.
- Zhu, Y., Kieber, D.J., 2018. Wavelength and temperature-dependent apparent quantum yields for photochemical production of carbonyl compounds in the North Pacific Ocean. *Environ. Sci. Technol.* 52, 1929–1939. <https://doi.org/10.1021/acs.est.7b05462>.
- Zhu, Y., Kieber, D.J., 2019. Concentrations and photochemistry of acetaldehyde, glyoxal, and methylglyoxal in the Northwest Atlantic Ocean. *Environ. Sci. Technol.* 53, 9512–9521. <https://doi.org/10.1021/acs.est.9b01631>.
- Zhu, Y., Kieber, D.J., 2020. Global model for depth-dependent carbonyl photochemical production rates in seawater. *Global Biogeochem. Cycles* 34, e2019GB006431. <https://doi.org/10.1029/2019GB006431>.
- Zhu, L., Zhao, S., Bittar, T.B., Stubbins, A., Li, D., 2020a. Photochemical dissolution of buoyant microplastics to dissolved organic carbon: rates and microbial impacts. *J. Hazard. Mater.* 383, 121065. <https://doi.org/10.1016/j.jhazmat.2019.121065>.
- Zhu, X., Miller, W.L., Fichot, C.G., 2020b. Simple method to determine the apparent quantum yield matrix of CDOM photobleaching in natural waters. *Environ. Sci. Technol.* 54, 14096–14106. <https://doi.org/10.1021/acs.est.0c03605>.
- Zhu, Y., Powers, L.C., Kieber, D.J., Miller, W.L., 2022. Depth-resolved photochemical production of hydrogen peroxide in the global ocean using remotely sensed ocean color. *Front. Remote Sens.* 3, 1009398. <https://doi.org/10.3389/frsen.2022.1009398>.
- Zika, R.G., 1981. Marine organic photochemistry. In: Duursma, E.K., Dawson, R. (Eds.), *Marine Organic Chemistry: Evolution, Composition, Interactions and Chemistry of Organic Matter in Seawater*. Elsevier, Amsterdam, pp. 299–325. [https://doi.org/10.1016/S0422-9894\(08\)70332-5](https://doi.org/10.1016/S0422-9894(08)70332-5).
- Ziolkowski, L.A., Miller, W.L., 2007. Variability of the apparent quantum efficiency of CO photoproduction in the Gulf of Maine and Northwest Atlantic. *Mar. Chem.* 105, 258–270. <https://doi.org/10.1016/j.marchem.2007.02.004>.
- Zito, P., Podgorski, D.C., Bartges, T., Guillemette, F., Roebuck, J.A., Spencer, R.G.M., Rodgers, R.P., Tarr, M.A., 2020. Sunlight-induced molecular progression of oil into oxidized oil soluble species, interfacial material, and dissolved organic matter. *Energy Fuels* 34, 4721–4726. <https://doi.org/10.1021/acs.energyfuels.9b04408>.
- Zuo, Y.T., Wu, J., Cheng, S., Cai, M.H., Han, Y.Z., Ji, W.X., Li, Y., Huo, Z.L., Korshin, G., Li, W.T., Li, A.M., 2022. Identification of pterins as characteristic humic-like fluorophores released from cyanobacteria and their behavior and fate in natural and engineered water systems. *Chem. Eng. J.* 428, 131154. <https://doi.org/10.1016/j.cej.2021.131154>.

Biogeochemistry of Marine Dissolved Organic Matter

Edited by Dennis A. Hansell and Craig A. Carlson

Biogeochemistry of Marine Dissolved Organic Matter, third edition, is the most up-to-date revision of the fundamental, all-encompassing reference for the biogeochemistry of marine dissolved organic matter. A necessary guide edited by the most distinguished experts in the field, this book is addressed to graduate students, marine scientists, as well as professionals interested in advancing their knowledge of the field.

Key Features

- Up-to-date knowledge on DOM, including eight new chapters
- The only published work to synthesize recent research on dissolved organic carbon in the South China Sea, a region receiving a great deal of attention in recent decades
- Offers contributions by world-class research leaders

About the Editors

Dennis A. Hansell

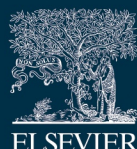
Professor of Ocean Sciences, Department of Ocean Sciences, Rosenstiel School of Marine, Atmospheric and Earth Science, University of Miami, Miami, FL, United States.

Dennis Hansell has conducted research on the biogeochemistry of major elements in the ocean for more than 30 years. His analyses have largely focused on data collected in the conduct of international projects addressing hydrographic and biogeochemical surveys of the global ocean. Questions of particular interest revolve around the role of dissolved organic matter (DOM) in the cycling of marine carbon, such as the accumulation of DOM in the surface ocean, its export to great depth with overturning circulation, its fate upon export, and its introduction to the deep ocean via sinking biogenic particles. This work has been done in all the major ocean basins; thus, the research products lend themselves to furthering understanding of the ocean as a global system. Hansell served as coeditor of the first two editions of this book.

Craig A. Carlson

Distinguished Professor of Marine Science, Department of Ecology, Evolution, and Marine Biology, University of California, Santa Barbara, Santa Barbara, CA, United States.

Craig Carlson's research interests for the past three decades have been shaped by an interdisciplinary blend of organic biogeochemistry and marine microbial ecology. His research contributions include assessing the dissolved organic matter (DOM) production, removal, and transformation processes in marine systems, providing accurate measurements of DOM inventories, and determining the role of DOM export in the biological carbon pump and its fate after export within the dark ocean. The overall goal of these research efforts is to make quantitative links between microbial community dynamics and DOM biogeochemistry in the open sea. Carlson served as coeditor of the first two editions of this book.



ACADEMIC PRESS

An imprint of Elsevier

elsevier.com/books-and-journals

Third Edition

ISBN 978-0-443-13858-4



9 780443 138584